

TN 8218

**Safety Report**

Transport cask TN 7-2  
for irradiated fuel assemblies

Author: W. Bergmann  
Division Manager: R. Christ

Edition 0  
May 1982

		<u>Page</u>
1.	Introduction	1-1
2.	Fuel assemblies	2.1-1
2.1	Description of fuel assemblies	2.1-2
2.2	Nuclear technology relevant data	2.2-2
2.3	Thermal power	2.3-1
2.4	Activity	2.4-1
2.5	Source intensity	2.5-1
2.6	Literature	2.6-1
3.	Description of the TN 7-2 cask	3.1-1
3.1	Total description	3.1-1
3.2	Description of components	3.2-1
3.2.1	Cask body	3.2-1
3.2.2	Lid	3.2-3
3.2.3	Shock absorbers	3.2-4
3.2.4	Tight enclosure	3.2-6
3.2.5	Integrated fixtures	3.2-6
3.2.6	Volume contents in the cask	3.2-10
3.3	Construction materials	3.3-1
3.3.1	Overview	3.3-1
3.3.2	Characteristics of materials	3.3-1
3.4	Literature	3.4-1
4.	Solidity under normal and accidental conditions	4.1-1
4.1	Calculation bases	4.1-1
4.1.1	Load assumptions	4.1-1
4.1.1.1	Design conditions	4.1-1
4.1.1.2	Handling and transport	4.1-2
4.1.1.3	Accident	4.1-2

4.1.2	Calculation methods	4.1-2
4.1.3	Characteristic values of materials	4.1-2
4.2	Cask body and lid system under design conditions	4.2-1
4.2.1	Design data	4.2-1
4.2.2	Admissible stresses	4.2-1
4.2.3	Thickness of the interior shell	4.2-1
4.2.4	Thickness of the interior bottom	4.2-4
4.2.5	Lid	4.2-5
4.2.5.1	Thickness of lid	4.2-5
4.2.5.2	Lid flange	4.2-5
4.2.6	Lid screws	4.2-8
4.2.7	Protective lid screws	4.2-18
4.2.8	Summary of results	4.2-14
4.2.9	Literature	4.2-15
4.3	Interior cladding under handling and transport conditions	4.3-1
4.3.1	Stresses	4.3-1
4.3.2	Stress criteria	4.3-1
4.3.3	Geometry	4.3-2
4.3.4	Stress on interior cladding and welding seams due to self weight, fuel assemblies, insert basket and pond water	4.3-3
4.3.4.1	Stresses in the shell and the welding seams	4.3-3
4.3.4.2	Stresses in the bottom	4.3-4
4.3.5	Handling conditions	4.3-5
4.3.6	Transport conditions	4.3-5
4.3.6.1	Stresses due to shock	4.3-5
4.3.6.2	Stresses due to continuous vibrations	4.3-8
4.3.7	Literature	4.3-9
4.4	Solidity of the trunnions	4.4-1
4.4.1	Load assumptions	4.4-1
4.4.2	Geometry	4.4-1
4.4.3	Dimensions, resistance momenta and section surfaces	4.4-2
4.4.4	Load on trunnions during transport and handling	4.4-3
4.4.4.1	Shock stresses due to transport incidents	4.4-3
4.4.4.2	Stresses during handling of cask	4.4-4

4.4.4.3	Stresses on trunnion and trunnion holding piece	4.4-4
4.4.4.4	Trunnion calculation according to KTA 3902 (handling)	4.4-8
4.4.4.5	Continuous trunnion and trunnion holding piece stress due to vibrations during transport	4.4-8
4.4.5	Stresses in trunnions screws	4.4-11
4.4.5.1	Maximum stress on screws during handling	4.4-11
4.4.5.2	Tightening torque for handling conditions	4.4-14
4.4.6	Literature	4.4-15
4.5	Solidity behaviour under accident conditions	4.5-1
4.5.1	Drop test with a 1:3 cask scale model	4.5-1
4.5.2	Literature	4.5-8
4.6	Verification of solidity for contents	4.6-1
4.6.1	DIDO and MERLIN insert baskets	4.6-1
4.6.1.1	Handling and transport conditions	4.6-1
4.6.1.1.1	Stresses due to thermal dilatation	4.6-1
4.6.1.1.2	Mechanical stresses	4.6-2
4.6.1.2	Accidental conditions	4.6-3
4.6.1.2.1	Horizontal drop from 9 m height	4.6-3
4.6.1.2.2	Vertical drop from 9 m height	4.6-6
4.6.1.2.3	Drop from 1 m height onto a gudgeon	4.6-7
4.6.2	RHF insert basket	4.6-7
4.6.2.1	Handling and transport conditions	4.6-8
4.6.2.1.1	Stresses due to thermal dilatation	4.6-8
4.6.2.1.2	Mechanical stresses	4.6-9
4.6.1.2	Accidental conditions	4.6-9
4.6.2.2.1	Horizontal drop from 9 m height	4.6-9
4.6.2.2.2	Vertical drop from 9 m height	4.6-17
4.6.2.3	Handling conditions	4.6-21
4.6.3	Literature	4.6-23
5.	Temperature distribution inside the cask	5.1-1
5.1	Generalities	5.1-1
5.2	Stationary temperature distribution inside the cask	5.2-1
5.2.1	Calculation model	5.2-1
5.2.2	Initial data	5.2-1
5.2.2.1	Thermal powers	5.2-1

5.2.2.2	Geometry	5.2.2
5.2.2.3	Compilation of initial data	5.2.2
5.2.3	Calculation of temperature distributions	5.2-3
5.3	Temperature distribution in the cask under accidental conditions	5.3-1
5.3.1	Description of the calculating program	5.3-1
5.3.2	Calculation model	5.3-1
5.3.3	Initial data and characteristic material data	5.3-3
5.3.3.1	Heat sources	5.3-3
5.3.3.2	Characteristic material data	5.3-3
5.3.3.3	Thermal transitions	5.3-6
5.3.3.4	Results of non stationary thermal calculations	5.3-8
5.4	Fire test on a TN 7-2 1/3 model	5.4-1
5.5	Literature	5.5-1
6.	Tightness of cask	6.1-1
6.1	Initial data for verification	6.1-1
6.2	Verification methods	6.2-1
6.3	Composition of fission product gas	6.3-1
6.4	Tightness under normal conditions	6.4-1
6.5	Tightness under accidental conditions	6.5-1
6.6	Literature	6.6-1
7.	Dose rate at cask surface	7.1-1
7.1	Structure of shielding	7.1-1
7.2	Source intensities	7.2-1
7.3	Calculation methodology	7.3-1
7.4	Initial data	7.4-1
7.4.1	Cross section for gamma radiation	7.4-1
7.4.2	Build-up factor	7.4-1
7.4.3	Conversion factor	7.4-1
7.5	Calculation and results	7.5.1
7.5.1	Dose rates under normal transport conditions	7.5.1

7.5.5.1	Dose rate at the lateral surface	7.5-1
7.5.1.2	Dose rate at the lid	7.5-5
7.5.1.3	Dose rate at the bottom	7.5-9
7.5.2	Dose rates under accidental conditions	7.5-13
7.5.2.1	Dose rate at the lateral surface	7.5-13
7.5.2.2	Dose rate at the lid	7.5-13
7.5.2.3	Dose rate at the bottom	7.5-15
7.6	Summary of results	7.6-1
7.7	Literature	7.7-1
8.	Criticality safety	8.1-1
8.1	Basic facts	8.1-1
8.2	Verification method	8.2-1
8.3	Results	8.3-1
8.4	Literature	8.4-1
	Appendix 8.1 Criticality safety of DIDO and MERLIN fuel assemblies in the TN 7 cask	
	Appendix 8.2 Criticality safety of irradiated RHF fuel assemblies in the TN 7 cask	
9.	Quality assurance	9.1-1
9.1	Quality assurance manual	9.1-1
9.2	Fabrication and inspection	9.2-1
9.2.1	Generalities	9.2-1
9.2.2	Selection of manufacturer	9.2-1
9.2.3	TN specification TN 7-2	9.2-4
9.2.4	Preliminary inspection documents	9.2-5
9.2.4.1	Specification TN 7-2	9.2-5
9.2.4.2	Construction materials data sheets	9.2-5
9.2.4.3	Fabrication follow-up plan	9.2-6
9.2.4.4	Welding plan	9.2-6
9.2.4.5	Fabrication and welding blueprints	9.2-7
9.2.4.6	Changes of the quality assurance plan	9.2-7

9.2.5	Special working and inspection instructions	9.2-8
9.2.6	Destructive and non destructive tests	9.2-8
9.2.7	Acceptance	9.2-9
9.3	Integrated fixtures	9.3-1
9.4	TN 7-2 transport cask - 1/3 scale model	9.4-1
9.5	Literature	9.5-1
10.	Handling and periodic inspections	10.1-1
10.1	Loading of cask	10.1-1
10.1.1	Preparations for loading	10.1-1
10.1.2	Loading	10.1-2
10.1.3	Preparation for removal transport	10.1-3
10.2	Unloading of cask	10.2-1
10.2.1	Preparations for unloading	10.2-1
10.2.2	Unloading	10.2-1
10.2.3	Preparations for removal transport	10.2-2
10.3	Periodic inspections	10.3-1
	Appendix 10.1 Periodic inspection plan	
11.	Drawings	11.1-1

## 1. Introduction

The TN 7-2 cask is a transport cask for spent fuel assemblies.

Heat is removed by natural convection over the cask surface.

The package is transported as closed cargo.

In the safety analysis report presented here it will be demonstrated that the cask fulfils the requirements set by the Road Traffic Act for

type B(U) package designs  
of nuclear safety class II  
(admissible number = 6)

as regards the following contents:

- A. a maximum of 62 irradiated DIDO and MERLIN fuel assemblies in up to four insert baskets
- B. a maximum of 2 irradiated fuel assemblies of the RHF reactor at Grenoble/France.

A separate safety analysis report will be compiled in the possible case of an extension of the cask licence to other cask contents, this report being based on the elaborations of the safety analysis report presented here.



## 2. Fuel assemblies

The TN 7-2 cask will be used for the transport of irradiated fuel assemblies from nuclear reactors. In the safety analysis report presented here a loading of different contents will be considered.

- A. A maximum of 62 irradiated fuel assemblies of the DIDO and MERLIN types, with the composition of the load and the condition of the fuel assemblies being specified in more detail below.
- B. A maximum of 2 irradiated fuel assemblies of the RHF reactor at Grenoble/France.

The technical data of the fuel assemblies, their irradiation history and the resulting residual heat and source intensity will be described below.

## 2.1 Description of the fuel assemblies

### A. DIDO and MERLIN fuel assemblies

#### a) DIDO fuel assemblies

Each fuel assembly is made up by four concentric fuel cylinders (U-Al alloy with an aluminum coating) surrounded by an aluminum cylinder and fixated by a top and a bottom plate. Fuel contents amount to a maximum of 185 g uranium 235 per fuel assembly.

Prior to transport, the fuel assemblies are cut up and only the centre parts (approx. 630 mm) of the four fuel cylinders, which contain the entire fuel, are transported. For reasons of handling the four cylinders are held together by a longitudinal tape (cf. Fig. 2-1).

Table 2-1: Dimensions of the fuel cylinders of the DIDO type

Exterior diameter:	93.2 - 83.4 - 73.6 - 63.8 mm
Wall thickness:	1.51 mm
Active length:	600 mm
Thickness of fuel:	0.66 mm

#### b) MERLIN fuel assemblies

These are rectangular MTR fuel assemblies and consist of 22 fuel plates, 2 aluminum plates as well as top and base plate.

Prior to transport, the fuel assemblies are cut up and only the centre part (approx. 638 mm), which contains the entire fuel, is transported.

The fuel plates consist of a U-Al alloy with an aluminum coating (the fuel contents per fuel assembly amount to a maximum of 270 g U-235).

Table 2-2: Dimensions of MERLIN type fuel plates

Active length:	600	mm
Wall thickness:	1.51	mm
Thickness of fuel:	0.51	mm

## c) Composition of the load

Up to four insert baskets are transported in the TN 7-2 cask, each basket containing:

either: a maximum of 15 irradiated cylindrical MTR fuel assemblies (of the DIDO type) with a maximum uranium 235 content of 185 g each and a burn up of approx. 80 to 93 %

or: a maximum of 16 irradiated rectangular MTR fuel assemblies (of the MERLIN type) with a maximum uranium 235 content of 270 g each and a burn up of approx. 80 to 93 %

The TN 7-2 transport cask may contain:

- 4 insert baskets with DIDO fuel assemblies  
(a maximum of 60 fuel assemblies altogether)
- 3 insert baskets with DIDO fuel assemblies and 1 insert basket with MERLIN fuel assemblies  
(a maximum of 61 fuel assemblies altogether)
- 2 insert baskets with DIDO fuel assemblies and 2 insert baskets with MERLIN fuel assemblies  
(a maximum of 62 fuel assemblies altogether)

## B. RHF fuel assemblies

The core of the RHF reactor at Grenoble consists of one fuel assembly. The outer dimensions of the fuel assembly can be seen in Table 2-3 and Fig. 2-2.

The active zone of the fuel assembly comprises 280 plates which are arranged radially between the outer and the inner aluminum cylinder. Inside the plates there is a core made of a U-Al alloy with a length of approx. 900 mm.

Prior to transport, the front structural parts are removed, so that the transport weight of the fuel assembly amounts to about 109 kg. The length of the fuel assembly thus amounts to 977 mm including the hand-ling equipment.

A maximum of 2 of these fuel assemblies may be transported in the TN 7-2 transport cask. The two fuel assemblies will then be stacked on top of each other.

Table 2-3: Main dimensions of the RHF fuel assembly

Exterior diameter:	413.6 mm
Interior diameter:	approx. 260 mm
Total length:	877 mm
Active length:	approx. 900 mm

## 2.2 Nuclear technology relevant data

The main nuclear data of all three types of fuel assembly are listed in Table 2-4.

Table 2-4: Nuclear technology relevant data of the fuel assemblies

	DIDO	MERLIN	RHF
Mass of U-235 (g)	185	270	8.67
Enrichment (%)	93	93	93
Power (MW)	1	0.25	57.5
In core time (d) approx.	70	220	44
Cooling time (d) minim.	160	170	310

## 2.3 Thermal power

### A. DIDO and MERLIN fuel assemblies

The maximum thermal power of the DIDO and MERLIN fuel assemblies is limited to 125 W per fuel assemblies for transport. This corresponds roughly to a minimum decay time of 160 d (DIDO) and 170 d (MERLIN) respectively (cf. /2-1/).

In addition a maximum thermal power of 1,125 W per insert basket has been defined, so that a complete basket load has to be composed in such a way that only some fuel assemblies may be loaded following their minimum decay time, whilst the remainder must be subject to a longer decay time.

Fuel elements with a thermal power of 125 W will only be set into the exterior basket positions.

Overall thermal power in the transport cask is limited to a maximum of  $4 \times 1,125 \text{ W} = 4,500 \text{ W}$ .

### B. RHF fuel assemblies

According to /2-2/, the residual thermal power of a RHF fuel assembly will be 2,250 W after a decay time of 310 d. This will result in an overall thermal power in a cask with 2 fuel assemblies of  $2 \times 2,250 \text{ W} = 4,500 \text{ W}$

## 2.4 Activity

### A. DIDO and MERLIN assemblies

According to /2-3/ the following maximum activity per fuel assembly can be found (corresponding to the minimum decay periods):

- DIDO: 40 kCi
- MERLIN: 20 kCi

The overall activity in the cask amounts to a maximum of  $2.1 \cdot 10^6$  Ci.

### B. RHF fuel assembly

After a decay period of 310 d, an irradiated RHF fuel assembly has an activity of  $1 \cdot 10^6$  Ci /2-2/. This will result in an overall activity of  $2 \times 1 \cdot 10^6$  Ci =  $2 \cdot 10^6$  Ci per transport cask.

## 2.5 Source intensity

### A. DIDO and MERLIN fuel assemblies

For shielding purposes, the fuel assemblies may be considered to be pure gamma emitters. Neutron emission is negligibly low.

The source intensity is identical for the different load compositions listed in chapter 2.1, i. e. the source intensity of a completely loaded DIDO in-sert basket corresponds to that of a completely loaded MERLIN basket.

Inside the cask, the following gamma source intensity is found for a load of 4 DIDO insert baskets (fuel assembly power  $1,0 \text{ MW}_{\text{th}}$ , irradiation period 70 d, decay period 231 d) according to /2-1/:

Table 2-5: Gamma source intensity for a load of DIDO fuel assemblies

Energy group (MeV)	Source intensity (1/sec)
1 - 1.7	$1.32 \cdot 10^{14}$
> 1.7	$5.28 \cdot 10^{13}$

A decay period of 231 d corresponds to the average decay period of the fuel assemblies per insert basket with regard to keeping within the 1,125 W limit (cf. also /2-3/).



## B. RHF fuel assemblies

According to /2-1/ the following source intensity is found (cf. also /2-2/):

Table 2-6: Gamma source intensity for a load of RHF fuel assemblies

Energy group (MeV)	Source intensity (1/sec)	Total source intensity (2 fuel ass.) (1/sec)
1 - 1.7	$6.4 \cdot 10^{14}$	$1.28 \cdot 10^{14}$
> 1.7	$9.5 \cdot 10^{12}$	$1.9 \cdot 10^{13}$

Gamma rays with a power of less than 1 MeV merely contribute to less than 1.5 % to the overall dose rate and are therefore neglected. Neutron emission is negligibly low.

2.6 Literature

- /2-1/ I.O. Blomeke/M.F. Todd  
U-235 Fission Product Production as a Function of Thermal Neutron Flux,  
Irradiation Time and Decay Time,  
ORNL 2127, Oak Ridge
- /2-2/ Safety Analysis Report, Transport of two Irradiated Fuel Assemblies in the  
TN 7 cask, TN 8021
- /2-3/ TN 7/MTR Package Design, Safety Report,  
TN 7701

### 3. Description of the TN 7-2 cask

The TN 7-2 transport cask (see Fig. 3-1) is used for the dry transport of spent fuel assemblies from nuclear reactors. The cask is laid out in such a way as to fulfil the national and international regulations for the transport of nuclear material (for example IAEA regulations, ADR).

The following chapter presents a description of the cask, its components and the types of material used.

#### 3.1 Total description

An overall view of the TN 7-2 cask is given in drawing 0-150-050-04-00 (cf. appendix). It essentially consists of the following main components:

- cask body with bottom, both composed of several layers
- 4 trunnions with trunnion holders made of stainless steel (1.4541); the trunnions are attached in pairs to the cask body with 12 screws each (M16x40) at the top and base
- 2 base plates made of 1.4541 stainless steel which are each welded on with an offset of 90 ° in relation to the trunnions
- a stainless steel (1.4541) lid with an integrated layer of lead for shielding purposes; the lid is attached to the cask body with 18 screws (M36)
- lid shock absorbers made of 37/2 structural steel and 1,4301 stainless steel with a balsa wood filling, attached to the side of the cask with 3 screws (M36)
- base shock absorbers (analogous to the lid shock absorbers)

- interior cask fittings such as insert baskets and spacers for the baskets.

All these components are summarised in the list of components (cf. Table 3-1) with the pertinent drawing number and material information.

Table 3-1: Components list for the TN 7-2 transport cask

Part no.	Designation	Drawing no.	Material
1	interior mantle	0-150-050-05-00	1.4541
2	lead casting	0-150-050-05-00	Pb 99.9
3	thermal insulation	0-150-050-05-00	cement
4	exterior mantle	0-150-050-05-00	1.4541
5	lid flange	0-150-050-05-00	1.4541
6	lid flange on lid	0-150-050-06-00	1.4541
7	trunnion holding piece	0-150-050-05-00	1.4541
8	trunnion	0-150-050-05-00	1.4541
9	base plate	0-150-050-05-00	1.4541
10	coupling insert	0-150-050-05-00	1.4541
11	drain pipe	0-150-050-05-00	1.4541
12	water inlet pipe	0-150-050-05-00	1.4541
13	protective lid for couplings	0-150-050-05-00/ -06-00	1.4541
14	fast coupling Hansen company, with viton ring gaskets	0-150-050-05-00/ -06-00	1.4305 viton
15	closing screw with gasket	0-150-050-05-00/ -06-00	1.4541 EPDM
16	safety fuse	0-150-050-05-00	polyamide
17	cylindrical screw M36 x 80	0-150-050-06-00	1.4057 or 1.6580
cadm.			
18	spring washer	0-150-050-06-00	1.541

Part no.	Designation	Drawing no.	Material
19	cylindrical screw M12 x 16	0-150-050-05-00/ -06-00	1.4057 or 1.6580 cadm.
20	cylindrical screw M16 x 40	0-150-050-05-00	1.4057 or 1.6580 cadm.
21	O-ring	0-150-050-05-00	EPDM or viton
22	O-ring	0-150-050-05-00	EPDM or viton
23	O-ring	0-150-050-05-00	EPDM or viton
24	O-ring	0-150-050-05-00	EPDM or viton
25	fin	0-150-050-05-00	1.4541
26	ring gasket	0-150-050-05-00	EPDM or viton
27	head piece	0-150-050-05-00	1.4541
28, 29	do not apply		
30	interior bottom	0-150-050-05-00	1.4541
31	water inlet piece	0-150-050-05-00	1.4541
32	bottom steel plate	0-150-050-05-00	1.4541
33	centring pin	0-150-050-05-00	1.4541
34	cylindrical screw M6 x 16	0-150-050-05-00/ -06-00	1.4057 or 1.6580 cadm.
35	spring washer	0-150-050-05-00/ -06-00	1.4541 or
36	closing flange M12 x 16	0-150-050-05-00/ -06-00	1.4541
37	O-ring	0-150-050-05-00/ -06-00	EPDM or viton
38	stopping block	0-150-050-05-00	1.4541
39	insert	0-150-050-06-00	1.4541
40	mantle	0-150-050-06-00	1.4541
41	supplementary shielding	0-150-050-05-00/ -06-00	U-metal
42	lid bottom	0-150-050-06-00	1.4541
43	lead casting	0-150-050-06-00	Pb 99.9
44	water inlet piece	0-150-050-06-00	1.4541
45	centring bolt	0-150-050-05-00	1.4541
46	O-ring	0-150-050-06-00	EPDM or viton

The main characteristics of the cask are summarised below.

Dimensions:

- diameter including shock absorbers	1660 mm
- diameter excluding shock absorbers and trunnions	1030 mm
- length including shock absorbers	3926 mm
- length excluding shock absorbers	3126 mm
- useful interior length	2675 mm
- useful interior diameter	540 mm

Weights:

- overall weight including shock absorbers (no load)	20720 kg
- weight of the shock absorbers	1560 kg
- weight of the lid	760 kg
- maximum allowed payload	3550 kg

Heat:

- maximum removable over cask surface	4.5 kW
---------------------------------------	--------

### 3.2 Description of components

#### 3.2.1 Cask body

The cask body (drawing no. 0-150-050-05-00 in the appendix) consists of a thickly walled basic body the walls and base of which are composed of several layers and which is smooth on the outside.

A stainless steel casing with a thickness of 10 mm and a welded-on base, which is 15 mm thick and displays a slight slope towards the centre, provides the inner containment. This is covered by a layer of lead with a thickness of 185 mm at the wall and 170 mm at the base, which serves as radiation shielding. A stainless steel wall and base with a thickness of 25 mm provide the outer solidity. A concrete layer with a thickness of approx. 20 to 25 mm is inserted between the lead covering and the outer steel wall. This concrete layer is used to prevent an inadmissible high temperature inside the cask in case of fire.

The entire main cask body is 3071 mm long and has a diameter of 1030 mm (without trunnions).

The inside of the cask has a diameter of 540 mm and is 2675 mm long.

The inner and outer wall each consist of two plates welded together. The individual cylinder plates are welded together from rolled sheet metal. The lead coating is cast, using a special technique, in a mould which consists of the inner lining and a lost outer mould. The concrete layer is inserted between the lead shielding and the outer lining using an established technique. The base plates of the inner and outer lining are each welded to the cylinders. The main cask body is closed at the lid between the outer and the inner lining with the lid flange, which is 60 mm thick. This is welded tight.

### 3.2-2

The cask has a water outlet at the base which also serves as flushing and drying connection. The inlet is welded to the centre of the base plate. A stain-less steel tube with an inner diameter of 15 mm is connected to this inlet and leads to the outer base plate through the lead shielding, taking due notice of radiation protection aspects. The tube is welded to a coupling element made of stainless steel which, in turn, is connected to the base plate and contains the screwed-in Hansen coupling. The opening of the coupling is closed with a lid which is tightened against the coupling connection with two O-ring gaskets which can be inspected.

A uranium plate is attached above the coupling element in order to compen-sate for the weakening of the lead shielding at this point.

Two stainless steel trunnion holders each, set off by 180 °, are welded to the outer cover. The trunnions used for cask handling are screwed on to these holders (12 M16 screws). During transport, the cask will rest on the two rear trunnion ledges and the front stainless steel base plate.

In order to attach the two front shock absorbers, 3 small locking devices each, set off by 180 °, are welded to the cask wall.

14 bore holes are drilled into the outer wall and closed with gaskets made of polyamide in order to prevent any inadmissible high generation of pressure in the concrete layer in case of a fire.

The main cask body is provided with a coat of paint on the outer wall which is easy to decontaminate.



Table 3-2: Dimensions of the main cask body

Length	l =	3071 mm
Diameter (with trunnions)	d =	1360 mm
Weight	G =	approx. 18400 kg

### 3.2.2 Lid

The upper frontal closure is assured by the lid. The lid consists of a massive stainless steel plate 70 mm thick and adjoining lead shielding, which is 165 mm thick and covered by a stainless steel casing 10 mm thick. The lid can be seen in drawing no. 0-150-050-06-00.

Table 3-3: Main dimensions of the lid

- Exterior diameter		
base plate	d <sub>1</sub> =	800 mm
shielding	d <sub>2</sub> =	588.5 mm
- Total height	h <sub>1</sub> =	245 mm
- Height of base plate	h <sub>F</sub> =	70 mm
- Weight	G =	approx. 760 kg

The lid is used for

shielding

sealing off the inside of the cask.

The lid is firmly attached to the cask body with 18 M36 screws and thus closes off the inside of the cask. Two grooves have been cut into the plate to accommodate two O-ring gaskets. A bore hole is provided between the two grooves which leads to a testing connection and is used for leak tests. This bore hole is closed by a stopper so as to be tight against gas leakage.

In addition, the lid is provided with a flushing and drying connection, similar to the base plate. A connector is welded to the centre of the lid's underside. A stainless steel tube with an interior diameter of 15 mm is connected to it which leads through the lead shielding and is welded to the lid plate. This tube is laid in such a way as give due consideration to radiation protection and leak tightness aspects. The orifice in the lid plate is closed by a Hansen coupling and an additional coupling lid. The coupling lid is tightened against the cask lid with two O-ring gaskets which can be inspected over a connector, similarly to the lid gaskets.

Five bore holes have been drilled into the lid plate to facilitate the handling of the lid.

During transport, the lid is protected by a shock absorber.

### 3.2.3 Shock absorbers

During transport, shock absorbers are attached to both ends of the cask. They cover the two ends of the cask completely; thus protecting the front sides and the edges against the effects of axial forces. The lid and the shock absorbers can be seen in drawing nos. 1-150-050-07-00 and 1-150-050-08-00. Both shock absorbers are identical in design, except for their height.

They consist of a welded steel sheet housing (37/2 and stainless steel), which is reinforced on the inside by fins. The space between the fins is filled with balsa wood for the purpose of shock absorption and heat insulation.

A lateral fish-plate is welded to the side of the shock absorber at its thrust point, in order to facilitate handling.

Ventilation bore holes are provided on the outer front sides which are closed by polyamide. These fuses melt at high temperatures (fire) and thus prevent any generation of pressure inside the housing.

The shock absorbers are attached with three screws each, which are placed askew on the side of the shock absorber. They are centred by means of the small stop blocks welded to the cask body and clamped tight.

Table 3-4: Main dimensions of the shock absorbers

max. diameter	d = 1660 mm
max. height	
lid shock absorber	$h_D = 720$ mm
bottom shock absorber	$h_B = 680$ mm
Weight	
lid shock absorber	= 780 kg
bottom shock absorber	= 780 kg

#### 3.2.4 Tight enclosure

The inner lining and the lid provide the tight enclosure of the cask required by the Road Traffic Act.

The lid is screwed tight with 18 M36 screws and sealed off with a double O-ring gasket. The efficiency of this gasket can be tested over the testing connection.

The safety casing is pierced in two places by the two flushing/drying connections in the base and lid. The two orifices are each sealed off by a coupling and a coupling lid with a double O-ring gasket and are gas-tight. The efficiency of these O-ring gaskets can also be checked over the testing connections. During transport the orifices are protected by the shock absorbers.

#### 3.2.5 Integrated fixtures

The insert baskets required for each load in particular are inside the cask.

The integrated fixtures required for the various types of cask contents, as set out in chapter 2, are described below.

These fixtures are used to ensure the safe installation and positioning of the fuel assemblies and guarantee criticality safety as well as sufficient heat removal from the fuel assemblies to the cask wall.

#### A. Insert basket for DIDO and MERLIN fuel assemblies

Different insert baskets are provided for DIDO and MERLIN fuel assemblies. Both types can be seen in drawing no. 1-150-025-17-00 and Fig 3-2 (cf. also /3-1/)

Four insert baskets are installed in the cask in the combinations described in chapter 2.1.

##### a) Insert basket for DIDO fuel assemblies

The basket for DIDO fuel assemblies consists of 15 cylinders made of 1.4541 stainless steel with an outer diameter of 108 mm and a wall thickness of 5 mm. These are welded onto a base plate (material: 1.4541 steel).

Reinforcement elements (material: 1.4541) are welded between the tubes, so that the basket provides a solid unit.

At the upper end of the insert basket, a lateral fish-plate is provided in the center, to facilitate handling of the basket.

Table 3-5: Main dimensions of the basket for DIDO fuel assemblies

Length	$l = 648 \text{ mm}$
Diameter	$d = 520 \text{ mm}$
Weight	$G = 145 \text{ kg}$

## b) Insert basket for MERLIN fuel assemblies

This insert basket consists of 16 rectangular shafts, 88 x 82 mm. The shafts are made up of stainless steel plates with a thickness of 14 mm and 7 mm (material: 1.4541), welded among themselves and to a base plate. Each shaft is surrounded by at least 7 mm of stainless steel. In the center, a full-length gap has a lateral fish-plate attached to the upper end to facilitate the handling of the basket.

Table 3-6: Main dimensions of the basket for MERLIN fuel assemblies

Length	$l = 676 \text{ mm}$
Diameter	$d = 520 \text{ mm}$
Weight	$G = 235 \text{ kg}$

## B. Insert basket for 2 RHF fuel assemblies

The insert basket is designed so as to fix the two fuel assemblies stacked on top of each other, radially and axially, in a central position related to the surrounding interior cavity limits. The basket fixtures consist are made of 1.4541 stainless steel and represented in drawing no. 1-150-025-21-00 and Fig. 3-3.

The fuel assemblies are supported from the outside by four vertical struts.

These struts are welded onto a base plate connected to each other by additional reinforcing metal sheets.

The entire interior installation has three parts: the two guide pieces for the fuel assemblies, as described above, and an upper spacer.

The two guide pieces with the fuel assemblies are stacked on top of each other. Any axial pushing together of the fuel assemblies is prevented by a base plate at the upper guide piece. The upper spacer is situated on the middle guide piece.

Loading of the basket is carried out according to the following sequence:

- lower part of the basket
- first fuel assembly
- upper part of the basket
- second fuel assembly
- upper spacer

Table 3-7: Main dimensions of the total RHF basket

Length	$l = 2655 \text{ mm}$
Diameter	$d = 536 \text{ mm}$
Weight	$G = 293 \text{ kg}$

## 3.2.6 Volume contents in the cask

The volume of an empty cask without internal fixtures is 0.613 m<sup>3</sup>.

The following free volumes result taking into account the internal fixtures and the fuel assemblies loaded.

## A. Loading with DIDO and MERLIN fuel assemblies

Table 3-8 lists the various volumes resulting from the loading of the cask.

Table 3-8: Summary of the various volumes resulting from the loading of DIDO and MERLIN fuel assemblies

- Interior cask cavity (empty)	0.613	m <sup>3</sup>
- 4 insert baskets		
a) 4 x DIDO	0.074	m <sup>3</sup>
b) 3 x DIDO + 1 x MERLIN	0.085	m <sup>3</sup>
c) 2 x DIDO + 2 x MERLIN	0.097	m <sup>3</sup>
- Fuel assemblies		
• DIDO (15 fuel assemblies)	0.014	m <sup>3</sup>
• MERLIN (16 fuel assemblies)	0.025	m <sup>3</sup>
- Free space inside the cask cavity		
with insert baskets, without fuel assemblies		
a)	0.539	m <sup>3</sup>
b)	0.528	m <sup>3</sup>
c)	0.516	m <sup>3</sup>
with insert baskets and fuel assemblies		
a)	0.483	m <sup>3</sup>
b)	0.461	m <sup>3</sup>
c)	0.438	m <sup>3</sup>



## B. RHF fuel assemblies

Table 3-9: Summary of the various volumes resulting from the loading of 2 RHF fuel assemblies

- Interior cask cavity (empty)	0.613	m <sup>3</sup>
- Insert basket for 2 RHF fuel assemblies	0.037	m <sup>3</sup>
- 2 RHF fuel assemblies	0.077	m <sup>3</sup>
- Free space inside the cask cavity		
with insert baskets, without fuel assemblies	0.576	m <sup>3</sup>
with insert baskets and 2 fuel assemblies	0.499	m <sup>3</sup>

### 3.3 Construction materials

#### 3.3.1 Overview

The various types of construction material used are listed in Table 3-1 in conjunction with the relevant components. This section will describe the properties of these types of construction materials. The cask consists of the following construction materials:

- stainless steel
- heat-treated steel for screws
- structural steel
- welding materials
- lead
- concrete
- EPDM and viton
- polyamide
- uranium metal
- balsa wood
- paint

The grades of steel used have been chosen taking into consideration pertinent regulations such as DIN standards, VdTÜV material forms, AD specifications and KTA regulations.

#### 3.3.2 Characteristics of materials

The materials are listed below including standard terms and characteristic data:

- X 10 CrNiTi 18 9  
material: 1.4541  
DIN 17440  
Tensile limit  $R_{0.2} = 205 \text{ N/mm}^2$  at room temperature

- X 22 CrNi 17

material: 1.4057

DIN 17440

Tensile limit  $R_{0.2} = 600 \text{ N/mm}^2$  at room temperature

- X 5 CrNi 18 9

material: 1.4301

DIN 17440

Tensile limit  $R_{0.2} = 190 \text{ N/mm}^2$  at room temperature

- St 37-2

material: 1.0114

DIN 17100

Tensile limit  $R_{0.2} = 240 \text{ N/mm}^2$  at room temperature

- 30 Cr Mo 4

material: 1.6580 heat-treated in accordance with strength requirement  
8.8

DIN 267

Tensile limit  $R_{0.2} = 640 \text{ N/mm}^2$  at room temperature

- welding additives

These must be suitable for the different types of weldings required for the cask and the shock absorbers and must conform to the guidelines of the AD specifications, HP series.

- Lead

Only lead with a degree of purity of at least 99.9 % is used. Therefore secondary lead or virgin lead may be used. The composition of the lead used can be found in the table below.

The density of the lead after casting is at least  $11.2 \text{ g/cm}^3$ .

Table 3-10: Chemical composition of the used lead

Chemical composition	Weight proportion %
Lead	99.9
Bismuth	0.09 (max.)
Antimony	0.002 (max.)
Silver	0.003 (max.)
Copper	0.005 (max.)
Zinc	traces
Iron	traces

- Cement

The gap between the outer lining and the lead shielding is filled up with cement containing aluminum, with an addition of 40 weight percent of water.

Type of cement: Fondu Lafarg

The chemical composition of the used cement is given in the table below.

Table 3-11: Chemical composition of the used cement

Chemical composition	Weight proportion %
SiO <sub>2</sub>	4.5
TiO <sub>2</sub>	2.5
Al <sub>2</sub> O <sub>3</sub>	39.0
Fe <sub>2</sub> O <sub>3</sub>	12.0
FeO	4.0
CaO	38.5
MgO	0.6
CO <sub>2</sub>	traces
SO <sub>3</sub>	0.15
K <sub>2</sub> O	0.15
Na <sub>2</sub> O	0.1

Table 3-12: Main physical properties of the used cement

• Density of cast cement (hydrated):	approx. 1.89 g/cm <sup>3</sup>
• Stable against pressure until:	40 N/mm <sup>2</sup>
• Thermal conductivity:	1.6 W/m·K
• Thermal expansion:	$6 \cdot 10^{-6}$ m/m·°C
• Shrinkage (after 60 days)	$225 \cdot 10^{-6}$ m/m

- 19357 viton gaskets

Some of the gaskets used consist of viton. Some typical characteristics of this material are listed below.

Table 3-13: Material characteristics of 19357 viton gaskets

- Shore hardness	70 - 80	
- Tensile strength	14	N/mm <sup>2</sup>
- Expansion	170	%
- Thermal expansion	$83 \cdot 10^{-6}$	
- Range of temperature for use	-30, +200	°C
- Maximum temperature (short term)	260	°C
- Minimum temperature (short term)	-40	°C
- Durability under radiation	$5 \cdot 10^7$	R

- 3457 EPDM gaskets

Table 3-14: Material characteristics of 3457 EPDM gaskets

- Shore hardness	70	
- Tensile strength	13	N/mm <sup>2</sup>
- Expansion	170	%
- Thermal expansion	$88 \cdot 10^{-6}$	
- Range of temperature for use	-60, +170	°C
- Maximum temperature (short term)	200	°C
- Durability under radiation	$10 \cdot 10^7$	R

Additional information can be found in the manufacturer's catalogs.

- Polyamide

Polyamide material used for safety fuses with the cask and the shock absorbers is heat-resistant up to a temperature of at least 100 °C and has a melting point of approx. 130 to 150 °C.

- Uranium

In order to compensate for the weakening of the lead shielding in the area of the connectors at the bottom and lid, uranium plates cast into the lead are placed so as to be in the main radiation direction. The plates consist of metallic uranium in a form which is not specified in particular.

- Balsa wood

Balsa wood is used as a filling for the shock absorbers. The wood is positioned in such a way that stresses are parallel to the direction of the grain.

Balsa wood grade A.

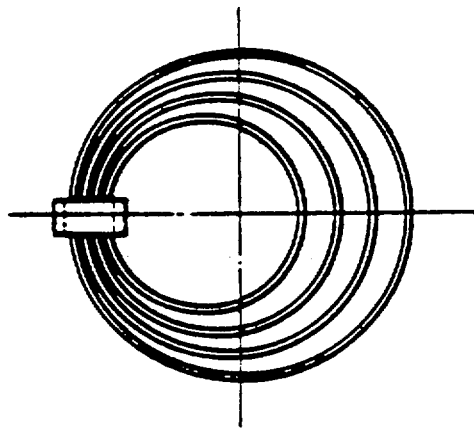
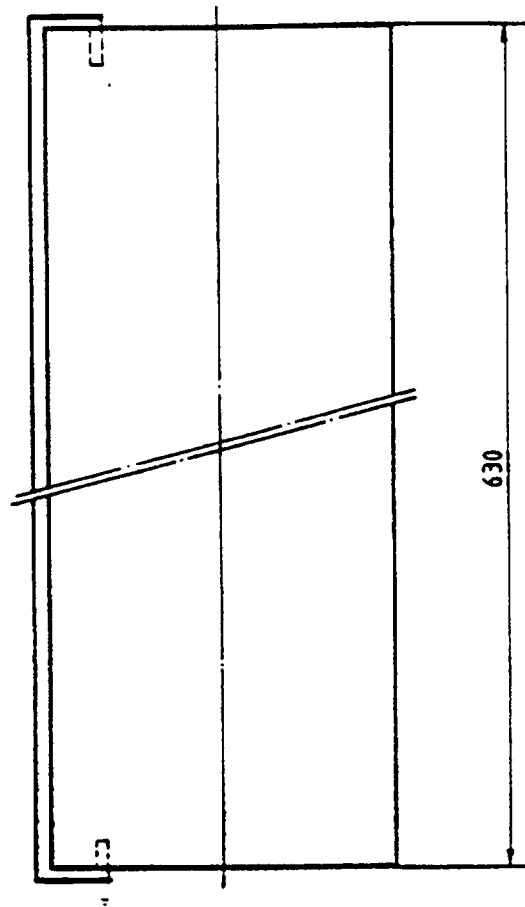
Density 0.13 - 0.185 g/cm<sup>3</sup>.

Maximum moisture 15 weight percent.

The dynamic behaviour of balsa wood under compression stress is described in /3-3/.

- Paint

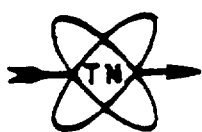
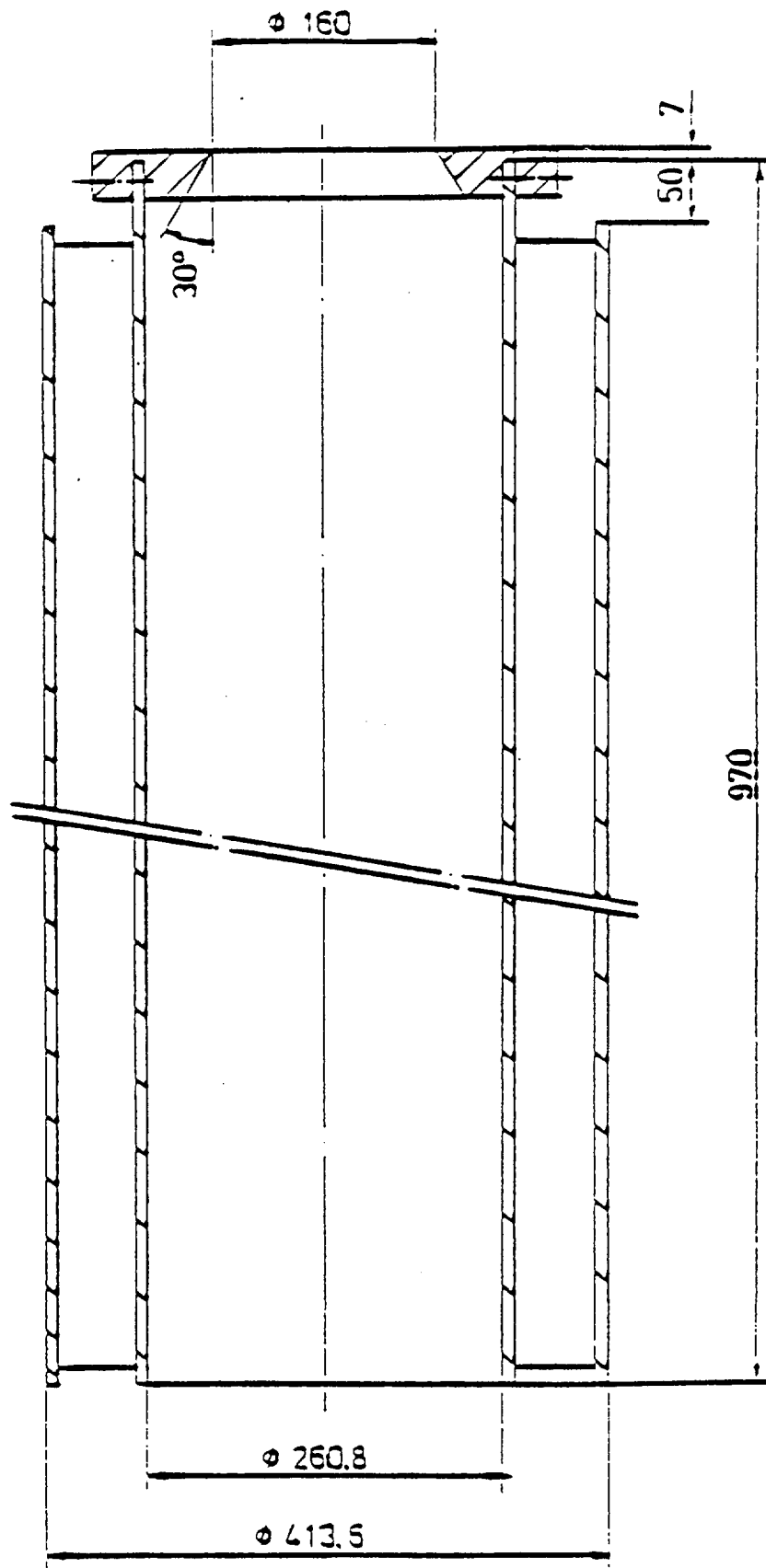
A paint is used which is easily decontaminated and radiation-resistant, in accordance with pertinent requirements.



DIDO fuel assembly under  
transport conditions

Fig. 2-1





RHF fuel assembly under  
transport conditions

Fig. 2-2

#### 4. Solidity under normal and accidental conditions

In the following, the construction of the cask is examined and it is verified that requirements for type B(U) packages are fulfilled.

##### 4.1 Calculation bases

###### 4.1.1.1 Load assumptions

For calculations, load assumptions are made for the following situations:

- design conditions
- handling and transport
- accident

###### 4.1.1.1 Design conditions

In the present case, design conditions are those for which a verification of solidity is carried out as under pressurized container conditions. As the cask is transported without interior overpressure, this verification merely has a formal significance.

Load assumptions are determined with:

pressure	7 bar
temperature	200 °C

#### 4.1.1.2 Handling and transport

Load assumptions for handling and transport during normal operating conditions comprise the following:

- pressure in the cask
- temperatures in the cask sides
- maximum accelerations
- loads due to vibrations during transport

They are summarized in table 4.1-1.

#### 4.1.1.3 Accident

Mechanical load assumptions for accidental cases are defined in transport regulations and comprise:

- free drop from 9 m height on an unyielding surface
- free drop from 1 m height on a gudgeon

Safety verification is carried out experimentally.

#### 4.1.2 Calculation methods

Calculations are based on the AD regulations. In case of stresses not considered in AD instruction sheets, the ASME code applies.

#### 4.1.3 Characteristic values of materials

Material data used for calculations are summarized in table 4.1-2.

Table 4.1-1: load assumptions for handling and transport

---

<u>Transport:</u>	
Interior pressure (bar)	0.6
Temperature (°C)	
max. cask mantle temperature	108
max. temperature of additional parts (lid, bottom, trunnions)	100
Acceleration values (g)	
- axial	10
- vertical	3
- lateral	5
Vibrations (g)	
- axial	1
- vertical	2
- lateral	1.5
<u>Handling:</u>	
Interior pressure (bar)	1.5
Temperature (°C)	
as for transport	
Acceleration values (g)	
- axial	1.5
- horizontal	3

---

Table 4.1-2: Characteristic data of materials

	Formula sign	Unit	Temperature °C	1.4541 according to DIN 17440	1.4057 according to DIN 17440	1.6580, 8.8 according to DIN 267	Remarks
0. 2% tensile limit	R <sub>0.2</sub> (K)	N/mm <sup>2</sup>	20	205	600	650	
			100	176	540	- <sup>1)</sup>	
			200	155	520	-	
Tensile strenght	R <sub>m</sub>	N/mm <sup>2</sup>	20	500	950	800-1000	
Modulus of elasticity	E	10 <sup>5</sup> N/mm <sup>2</sup>	20	2.0	2.16	2.0	
Poisson number				0.3	0.3	0.3	
Linear thermal expansion coefficient	$\alpha$	10 <sup>-6</sup> °C <sup>-1</sup>	20	-	-	-	
			20-150	16.5	10.0	11.0	
			20-100	17.0	10.5	11.0	
Yielding point	S <sub>y</sub>	N/mm <sup>2</sup>	20	205			
			100	-			
			200	155			
Tensile strength	S <sub>u</sub>	N/mm <sup>2</sup>	20	-			
			100	-			
			200	350			
Admissible tension	S <sub>m</sub>	N/mm <sup>2</sup>	20	-			
			100	-			
			200	87.5			

1) At temperatures above 100 °C, a decrease of the yielding poing must be expected.

## 4.2 Cask body and lid system under design conditions

Calculations are carried out for design pressure and temperature according to AD instruction sheets. Only the interior steel shell is used for design layout. The lead shielding and the exterior steel shell are not considered in the calculations.

### 4.2.1 Design data

Interior pressure	$p = 0.7 \text{ N/mm}^2$ (relative)
Temperature	$t = 200 \text{ } ^\circ\text{C}$

### 4.2.2 Admissible stresses

Table 4.1-2 summarizes solidity values. The tensile limit of the inner liner material is essential for solidity. This is made of 1.4541 stainless steel.

### 4.2.3 Thickness of the interior shell (cf. fig. 4.2-1)

Calculations are carried out according to AD instruction sheet B 1 /4.2-2/. It is valid for walls without significant temperature difference:

Required wall thickness  $S_e$ :

$$S_e = \frac{D_a + D_p}{23 \cdot \frac{K}{S} \cdot v + p} + C_1 + C_2$$

#### 4.2-2

- $p =$  7 bar interior pressure  
 $K =$  155 N/mm<sup>2</sup>  $\cong R_{0.2}$  stress at 200 °C  
 $S =$  1.5 safety coefficient according to /4.2-1/  
 $V =$  1  
 $C_1 =$  0  
 $C_2 =$  0

$$S_e = \frac{560 \cdot 7}{23 \cdot \frac{155}{1.5} \cdot 1 + 7} = 164 \text{ mm}$$

The implemented wall thickness of 10 mm is sufficient.

Reduced stress  $\sigma_v$  :

$$\begin{aligned}
 \sigma_{vi} &= \frac{p \cdot (D_a + S_e)}{23 S_e} = \frac{7 \cdot (560 + 10)}{23 \cdot 10} = \\
 &= 17.3 \text{ N/mm}^2 < \frac{155}{1.5} = 103 \text{ N/mm}^2 \\
 \sigma_{va} &= \frac{p \cdot (D_a - 3 S_e)}{23 S_e} = \frac{7 \cdot (560 - 3 \cdot 10)}{23 \cdot 10} = \\
 &= 16.1 \text{ N/mm}^2 < \frac{155}{1.5} = 103 \text{ N/mm}^2
 \end{aligned}$$

Values remain below the admissible stress K/S.

### - Stresses in the lead shielding

The lead shielding was not taken into account for the design of the pressure vessel. The maximum stress in the lead due to interior overpressure occurs at the junction between interior steel mantle and lead shielding.

Based on the ratio of the modules of elasticity, a conservative determination can be carried out approximately assuming equal expansion. The following assumptions apply:

$$\varepsilon_1 = \varepsilon_2$$

$$\frac{\sigma_1}{\sigma_2} = \frac{E_1}{E_2}$$

$$\sigma_1 = 16.1 \text{ N/mm}^2 = \text{stress at the exterior fibre of the steel liner}$$

$$E_1 (200^\circ\text{C}) = 2 \cdot 10^5 \text{ N/mm}^2 \text{ for steel}$$

$$E_2 (200^\circ\text{C}) \sim 1.4 \cdot 10^4 \text{ N/mm}^2 \text{ for lead}$$

$$\sigma_2 = \frac{\sigma_1 \cdot E_2}{E_1} = 1.2 \text{ N/mm}^2 < \sigma_{SPb} \approx 6 \text{ N/mm}^2 \text{ according to /4.2-6/}$$



4.2.4 Thickness of the interior bottom  
(cf. fig. 4.2-1)

Calculation is carried out according to /4.2-3/.

The required thickness of the bottom is calculated according to:

$$s = C \cdot D_1 \cdot \left( \frac{P \cdot S}{10K} \right) \cdot 0.5$$

$C = 0.35$  according to table 1, b

$D_1 \cong D_i = 540 \text{ mm}$

$P = 7 \text{ bar}$

$S = 1.5$

$K = 155 \text{ N/mm}^2 \cong R_{0.2}$  - stress at  $200^\circ\text{C}$

$$s = 15.5 \text{ mm}$$

The actual thickness of the bottom liner is between 20 and 15 mm. Its average thickness is 17.5 mm. The thickness of the bottom is thus sufficient.

## 4.2.5 Lid

## 4.2.5.1 Thickness of lid

Posterior calculations are carried out according to /4.2-3/. Required wall thickness is:

$$s = C \cdot D_1 \cdot \left( \frac{P \cdot S}{10K} \right) \cdot 0.5$$

C = 0.35 safety coefficient according to table 1, d

P = 7 bar

D<sub>1</sub> = 726 mm

K = 155 N/mm<sup>2</sup>  $\cong$  R<sub>0.2</sub> - stress at 200 °C

S = 1.5

$$s = 20.9 \text{ mm}$$

Neglecting the clad lead shielding, the bottom plate of the lid is 70 mm thick. This covers all losses of solidity due to drilled holes.

## 4.2.5.2 Lid flange

- Calculation and shearing due to interior pressure

Due to interior pressure, section A (cf. fig. 4.2-2) is submitted to shearing stresses.

$$\text{Section surface } A = 2 \cdot R_a \cdot \pi \cdot h_F = 2 \cdot 330 \cdot \pi \cdot 65$$

$$= 1.35 \cdot 10^5 \text{ mm}^2$$

Force due to interior pressure:

$$F_p = R_a^2 \cdot \pi \cdot p = 330^2 \cdot \pi \cdot 0.7 =$$

$$= 2.40 \cdot 10^5 \text{ N}$$

Shearing stress:

$$\tau_s = \frac{F_p}{A} = 1.8 \text{ N/mm}^2$$

$$\tau_{zu1} = \frac{0.4 \cdot 155}{1.5} = 413 \text{ N/mm}^2$$

- Calculation of flexion due to interior pressure and gasket stress forces

Calculations are carried out according to /4.2-5/.

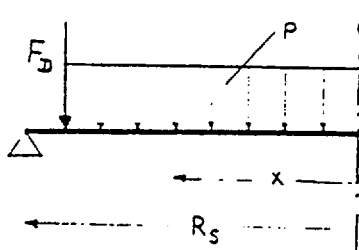
Momentum due to interior pressure:

$R_s = 363 \text{ mm}$  screw radius

$X \cong R_1 = 330 \text{ mm}$

$\nu = 0.3$

Mechanical model:



Momentum for  $x = R_1 = 330 \text{ mm}$

$$M_{r1} = \frac{p \cdot R_s^2}{16} \cdot (3 + \nu) \left(1 - \frac{R_1^2}{R_s^2}\right)$$

$$= \frac{0.7 \cdot 363^2}{16} \cdot (3 + 0.3) \left(1 - \frac{330^2}{363^2}\right)$$

$$= 3.30 \cdot 10^3 \text{ N/mm}$$

$$\begin{aligned}
 M_{t1} &= \frac{P \cdot R_S^2}{16} \cdot [(3+r) - (1+3\nu) \cdot \frac{R_1^2}{R_S^2}] \\
 &= \frac{0,7 \cdot 363^2}{16} \cdot [(3+0,3) - (1+0,9) \cdot \frac{330^2}{363^2}] \\
 &= 9,97 \cdot 10^3 \text{ Nmm/mm}
 \end{aligned}$$

Momenta due to tightening force:

$$F_D = 6,24 \cdot 10^5 \text{ N}$$

$$S \cong R_a = 330 \text{ mm}$$

$$R_S = 363 \text{ mm}$$

$$\begin{aligned}
 M_{r2} = M_{t2} &= \frac{F_D}{8 \cdot \pi} \cdot 2(1+\nu) \cdot \ln \frac{R_S}{R_a} + (1-\nu) \cdot \left(1 - \frac{R_a^2}{R_S^2}\right) \\
 &= \frac{6,24 \cdot 10^5}{8 \cdot \pi} \cdot 2(1+0,3) \cdot \ln \frac{363}{330} + (1-0,3) \cdot \left(1 - \frac{330^2}{363^2}\right)
 \end{aligned}$$

Momenta:

$$M_r = M_{r1} + M_{r2} = 9,45 \cdot 10^3 \text{ Nmm/mm}$$

$$M_t = M_{t1} + M_{t2} = 1,61 \cdot 10^4 \text{ Nmm/mm}$$

Stresses:

$$\sigma_r = \frac{6 \cdot M_t}{h_F^2} = \frac{6 \cdot 1,61 \cdot 10^4}{65^2} = 22,8 \text{ N/mm}^2$$

$$\sigma_t = \frac{6 \cdot M_r}{h_F^2} = \frac{6 \cdot 9,45 \cdot 10^3}{65^2} = 13,4 \text{ N/mm}^2$$

Reduced stress:

$$\begin{aligned} \sigma_v &= (\sigma_r^2 + \sigma_t^2 - \sigma_r \cdot \sigma_t)^{0,5} = (22,9^2 + 13,4^2 - 22,9 \cdot 13,4)^{0,5} \\ &= 20,3 \text{ N/mm}^2 \end{aligned}$$

$$\sigma_{zul} = \frac{R_{0,2}}{s} = \frac{155}{1,5} = 103 \text{ N/mm}^2$$

The reduced stress is smaller than the admissible stress.

#### 4.2.6 Lid screws

Posterior calculation of the lid screws is carried out according to /4.2-4/.

Minimum screwing force for operating conditions is:

$$F_{SB} = F_{RB} + F_{FB} + F_{DB}$$

with the individual components:

$$F_{RB} = \frac{P \cdot \pi \cdot d_i^2}{40} = \frac{7 \cdot \pi \cdot 590^2}{40} = 1,91 \cdot 10^5 \text{ N}$$

$$F_{FB} = \frac{P \cdot \pi \cdot (d_D^2 - d_i^2)}{40} = \frac{7 \cdot \pi \cdot (660^2 - 590^2)}{40} = 4,81 \cdot 10^4 \text{ N}$$

$$F_{DB} = \frac{P}{10} \cdot \pi \cdot d_D \cdot S_D \cdot K_1 = 0 \text{ für } K_1 = 0$$

$d_i$  = 540 mm interior flange diameter

$d_D$  = 660 mm average gasket diameter

$K_1$  = 0 mm gasket characteristic according to table 1 /4.2-4/

$$F_{SB} = 2,39 \cdot 10^5 \text{ N}$$

The minimum screwing force for installed components is calculated from:

$$F_{DV} = \pi \cdot d_D \cdot K_0 \cdot K_D$$

$K_0 \cdot K_D = 20 \text{ b}_d \approx 200 \text{ N/mm}$  deformation force for 2 gaskets

$$F_{DV} = \pi \cdot 660 \cdot 200$$

$$= 4.15 \cdot 10^5 \text{ N}$$

As  $F_{DV} > F_{SB}$ , the following applies:

$$\begin{aligned} F_{DV}^* &= 0.2 F_{DV} + 0.8 \sqrt{F_{SB} \cdot F_{DV}} \\ &= 3.35 \cdot 10^5 \text{ N} \end{aligned}$$

The required screw diameter is calculated as following for operating conditions:

$$d_k = Z \cdot \sqrt{\frac{F_{SB}}{K \cdot n}} + C_5$$

$$\begin{aligned} d_k &= 1.51 \cdot \sqrt{\frac{2.39 \cdot 10^5}{500 \cdot 18}} + 3 \\ &= 11.0 \text{ mm} \end{aligned}$$

$Z = 1.51$  auxiliary value according to table 3

$K = 500 \text{ N/mm}^2$  (according to table 4.1-2, solidity class 8.8)

$n = 18$  number of screws

$C_5 = 3 \text{ mm}$  supplement

The following applies for installed conditions:

$$d_k = Z \cdot \sqrt{\frac{F_{Dv}^*}{K_{20} \cdot n}}$$

$Z = 1.29$  according to table 3

$K_{20} = 600 \text{ N/mm}^2 \cong R_{0.2} \text{ at } 20^\circ \text{C}$

$$\begin{aligned} d_k &= 1.29 \cdot \sqrt{\frac{3.35 \cdot 10^5}{600 \cdot 18}} \\ &= 7.2 \text{ mm} \end{aligned}$$

Selected screws: M36 x 3 with  $d_k = 31.1 \text{ mm}$

- Calculation of the required tightening torque:

Calculation is carried out according to /4.2-5/.

Total torque:

$$M_G = F_V \cdot [0,5 d_m \cdot \operatorname{tg} (\alpha + \varrho) + r_A \cdot \mu_A]$$

$$d_m = 33,4 \text{ mm}; h = 3,0 \text{ mm}$$

$$\operatorname{tg} \alpha = \frac{h}{d_m \cdot \pi} = \frac{3}{33,4 \cdot \pi} \rightarrow \alpha = 1,64^\circ$$

$$\varrho = 6^\circ; \mu_A = 0,1$$

$$F_V = \frac{F_{DV}^*}{n} = \frac{3,35 \cdot 10^5}{18} = 1,9 \cdot 10^4 \text{ N}$$

$$r_A = \frac{54+36}{4} = 22,5 \text{ mm}$$

$$\begin{aligned} M_G &= 1,9 \cdot 10^4 \cdot [0,5 \cdot 33,4 \cdot \operatorname{tg} (1,64+6) + 22,5 \cdot 0,1] \\ &= 8,6 \cdot 10^4 \text{ Nmm} \end{aligned}$$

$$M_G = 86 \text{ Nm}$$

It is furthermore required that the preliminary tensing force must cover about 20 - 30 % of the tensile limit of the screw material.

$$F_V = R_{0,2} \cdot 0,21 \cdot A_3$$

$$= 500 \cdot 0,21 \cdot 817$$

$$= 8,38 \cdot 10^4 \text{ N}$$

One thus obtains the following tightening torque:



## 4.2.7 Protective lid screws

The protective lid screws are submitted to stress by the interior pressure of 7 bar.

According to /4.2-4/, the following is obtained for operating conditions:

$$\begin{aligned} F_{SB} &= F_{RB} + F_{FB} \\ &= \frac{P \cdot \pi \cdot d_B^2}{40} = 9872 \text{ N} \end{aligned}$$

$$d_B = 134 \text{ mm (maximum gasket diameter)}$$

The following applies for installed components:

$$F_{DV} = \pi \cdot d_D \cdot K_0 \cdot K_D$$

$$K_0 \cdot K_D = 20 \cdot b_d \approx 60 \text{ N/mm} = \text{deformation force for 2 gaskets}$$

$$F_{DV} = 2,53 \cdot 10^4 \text{ N}$$

As  $F_{DV} > F_{SB}$ , the following applies

$$\begin{aligned} F_{DV}^* &= 0,2 \cdot F_{DV} + 0,8 \cdot \sqrt{F_{SB} \cdot F_{DV}} \\ &= 1,77 \cdot 10^4 \text{ N} \end{aligned}$$

The required screw diameter is similar to chapter 2.6:

$$\begin{aligned}
 d_K &= Z \cdot \sqrt{\frac{F_{SB}}{K \cdot n}} + C_5 \\
 &= 1,51 \cdot \sqrt{\frac{9872}{500 \cdot 4}} + 3 \\
 &= 6,4 \text{ mm}
 \end{aligned}$$

The following applies for installed components:

$$\begin{aligned}
 d_K &= Z \cdot \sqrt{\frac{F_{DV}^*}{K_{20} \cdot n}} \\
 &= 1,51 \cdot \sqrt{\frac{1,77 \cdot 10^4}{600 \cdot 4}} \\
 &= 4,1 \text{ mm}
 \end{aligned}$$

Selected screws: M12 with  $d_K = 9.85 \text{ mm}$

- Calculation of the required tightening torque

Calculation is carried out according to /4.2-5/

$$M_G = F_V \cdot [0,5 d_m \cdot \operatorname{tg} (\alpha + \varphi) + r_A \cdot \mu_A]$$

$$d_m = 10,86 \text{ mm}$$

$$\alpha = 2,94^\circ$$

$$\varphi = 6^\circ$$

$$\mu_A = 0,1$$

$$r_A = 7,5 \text{ mm}$$

$$F_V = \frac{F_{DV}^*}{n} = \frac{1,77 \cdot 10^4}{4} = 4425 \text{ N}$$

$$M_G = 7.1 \text{ Nm}$$

The following must also be valid:

$$F_V = R_{0.2} \cdot 0.2 \cdot A_s$$

$$= 500 \cdot 0.2 \cdot 84.3$$

$$= 8430 \text{ N}$$

$$M_G = 13.5 \text{ Nm}$$

A tightening torque of 15 Nm is selected.

#### 4.2.8 Summary of results

Table 4.2-1 gives a summary of the main results.

Actual stresses are much lower than admissible values.

4.2.9 Literature

/4.2-1/ AD instruction sheet B0

/4.2-2/ AD instruction sheet B1

/4.2-3/ AD instruction sheet B5

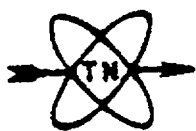
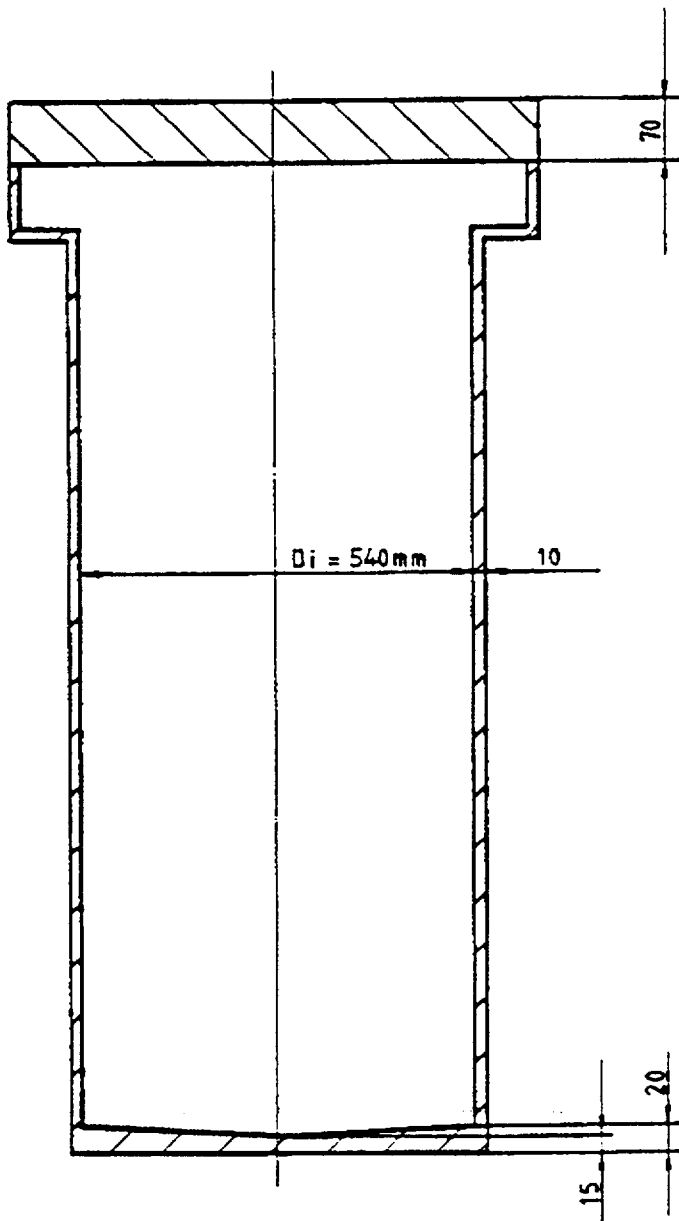
/4.2-4/ AD instruction sheet B7

/4.2-5/ Hütte I, 28th edition

/4.2-6/ Construction of chemical apparatuses with lead,  
Technical Working Sheets, Brochure 1,  
Bleiwerk Goslar KG, 1973

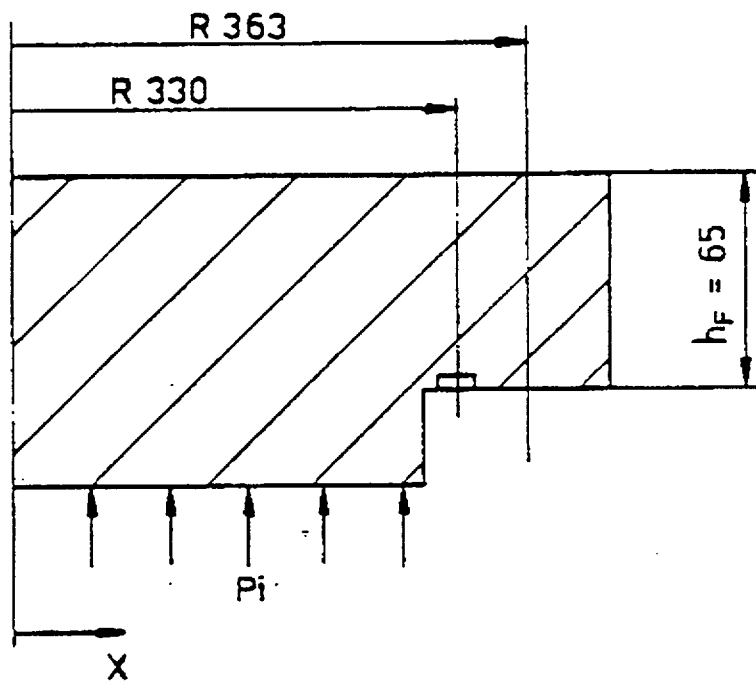
Table 4.2-1: Summary of results

Position	$\sigma_{zul} (\tau_{zul})$ N/mm <sup>2</sup>	$\sigma_{vorh} (\tau_{vorh})$ N/mm <sup>2</sup>
Interior shell of cask		
- interior fibre	103	17.3
- exterior fibre	103	16.1
Bottom of interior liner	103	< 103
Lid		
- Shear stress on flange	41.3	1.9
- Bending stress on flange	103	20.3
- Screws (operating conditions 200 °C)	min. 500	<< 500
- Screws (installed 20 °C)	min. 600	<< 600



Dimensions of tight enclosure

Fig. 4.2-1



Calculation model for lid

Fig. 4.2-2

### 4.3 Interior cladding under handling and transport conditions

#### 4.3.1 Stresses

Table 4.1-1 lists the requirements for handling and transport.

It is assumed that all interior forces act only on the interior cladding. The lead shielding is neglected for solidity calculations. Only the base plate is considered for the lid.

#### 4.3.2 Stress criteria

Both the interior cladding and the lid plate are made of stainless steel, material number 1.4541. Solidity values are listed in table 4.1-2.

The material for the tightening screws of the lid is 1.4057 or 1.6580, with the solidity values indicated in table 4.1-2.

For handling, admissible stresses are calculated according to the AD instruction sheets (safety factor  $S = 1.5$ ). For shock stresses during transport, design values are established against the tensile limits.



## 4.3.3 Geometry

The interior cladding geometry is represented in drawing no. 0-150-050-05-00. The following sketches show the main dimensions of shell and bottom.

$$d_a = 560 \text{ mm}$$

$$d_i = 540 \text{ mm}$$

$$s = 10 \text{ mm}$$

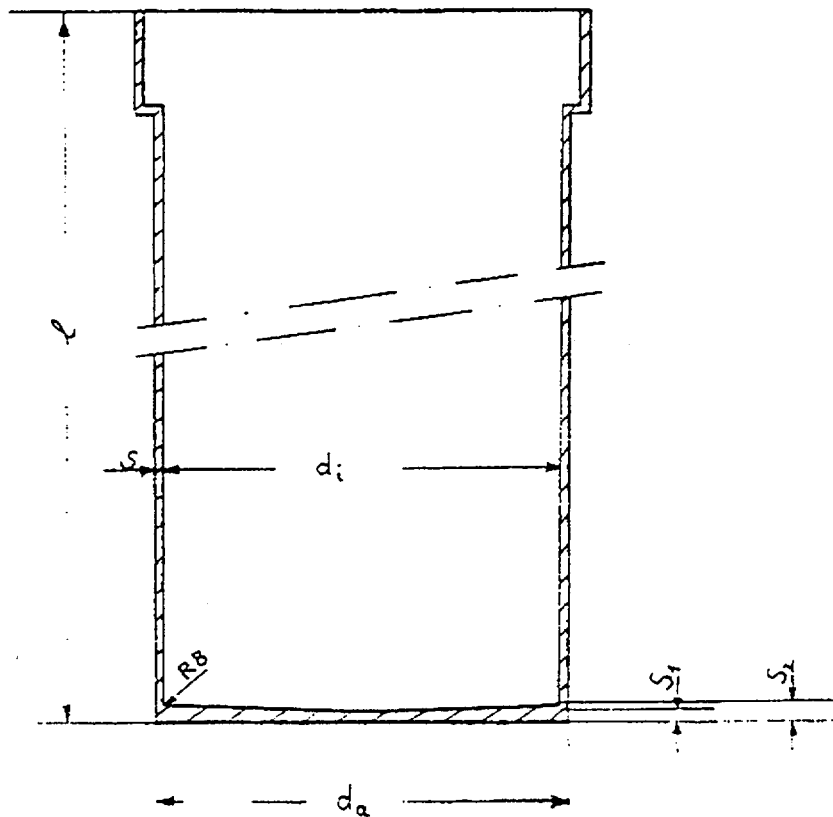
$$d_m = 550 \text{ mm}$$

$$l = 2800 \text{ mm}$$

$$s_1 = 15 \text{ mm}$$

$$s_2 = 20 \text{ mm}$$

$$s_m = 17,5 \text{ mm}$$



#### 4.3.4 Stress on interior cladding and welding seams due to self weight, fuel assemblies, insert basket and pond water

Assumptions:	temperature	40 °C
	weights:	
	fuel assemblies + interior parts	3550 kg
	interior cladding	approx. 500 kg

The weight of interior parts is assumed at this value in view of future extensions of the transport inventory.

Loading is carried out in approx. 10 m water depth (assumption):

$$P = \rho \cdot g \cdot h = 1000 \cdot 9.81 \cdot 10 = 1.0 \cdot 10^5 \text{ N/m}^2$$

$$\text{Bottom surface: } 0.54^2 \cdot \pi \cdot 0.25 = 0.229 \text{ m}^2$$

$$\text{Force exerted by water on the bottom: } 2.29 \cdot 10^4 \text{ N}$$

$$\text{Total force on the bottom: } 5.78 \cdot 10^4 \text{ N}$$

##### 4.3.4.1 Stresses in the shell and the welding seams

Stresses in the shell and in the welding seams are equal (weakening coefficient of the welding seams  $V = 1$ ).

$$\sigma = \frac{F}{A} = \frac{5.78 \cdot 10^4}{540 \cdot 10 \cdot \pi} = 3.4 \text{ N/mm}^2$$

Admissible stress for the interior cladding and the welding seams is:

$$\sigma_{zul} = \frac{R_{0.2}}{1.5} = \frac{205}{1.5} = 136.7 \text{ N/mm}^2$$

Actual stress is smaller than the admissible value.

## 4.3.4.2 Stresses in the bottom

Water pressure acts as a surface load on the bottom. For loads on the bottom due to fuel assemblies and inserts, it is assumed that these act as uniformly distributed surface loads over the whole bottom.

Calculations are carried out according to /4.3-2/.

Water, fuel assemblies and insert basket as uniformly distributed linear load:

$$p = \frac{F}{A} = \frac{5,78 \cdot 10^4}{540^2 \cdot \pi \cdot 0,25} = 0,253 \text{ N/mm}^2$$

$$M_r = \frac{p \cdot r_1^2}{16} \cdot [(1+\nu) - (3+\nu)] = -2301,0 \text{ Nmm/mm}$$

$$M_T = \frac{p \cdot r_1^2}{16} \cdot [(1+\nu) - (1+3\nu)] = -690,4 \text{ Nmm/mm}$$

$$\sigma_1 = \frac{6 \cdot M_r}{s_m^2} = \frac{-6 \cdot 2301,0}{17,5^2} = -45,1 \text{ N/mm}^2$$

$$\sigma_2 = \frac{6 \cdot M_T}{s_m^2} = -13,5 \text{ N/mm}^2$$

$$\sigma_v = \sigma_{\max} = |\sigma_1| = 45,1 \text{ N/mm}^2$$

Momentum at the middle of the plate

$$M_r = M_T = \frac{p \cdot r_1^2}{16} (1+\nu) = 1496 \text{ Nmm/mm}$$

$$\sigma_{1,2} = \frac{6 \cdot M}{s_m^2} = 29,3 \text{ N/mm}^2$$

$$\sigma_v = \sigma_1 = 29,3 \text{ N/mm}^2$$

#### 4.3.5 Handling conditions

During handling at the power plant, a supplementary load of 0.5 g must be assumed. Load assumptions for the weight due to load made in chapter 4.3.4 must be multiplied by a factor of 1.5 (DIN 15018 Lifting Load Coefficient  $\Psi = 1.5$ ).

- Mantle and welding seams:  
stresses remain below admissible values.

- Bottom:  
stresses remain below admissible values.

Stresses due to thermal dilatation may be neglected for the made assumptions ( $T = 40\text{ °C}$ ).

#### 4.3.6 Transport conditions

##### 4.3.6.1 Stresses due to shock

The following transport accelerations are assumed:

- axial                10 g
- vertical            3 g
- lateral             5 g

- Stresses in the mantle due to vertical and lateral shock

The resulting acceleration is:

$$a = (5^2 + 3^2)^{0.5} \text{ g} = 5.83 \text{ g}$$

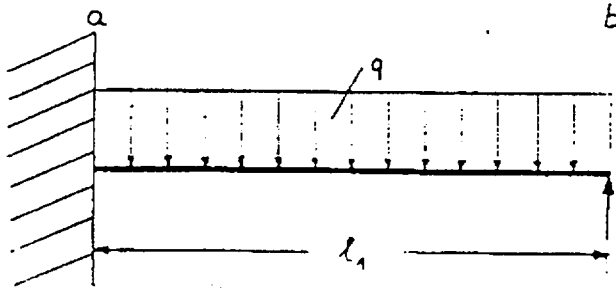
Weight (interior cladding, fuel assembly, insert basket):

$$G = 4050 \text{ kg}$$

Uniformly distributed linear load which acts on the interior cladding:

$$q = \frac{G \cdot 5,83 \text{ g}}{l_1} = \frac{4050 \cdot 5,83 \cdot 9,81}{2600} = 89,1 \text{ N/mm}$$

Calculation model (conservative simplification)



$$Q_a = \frac{3}{8} \cdot q \cdot l$$

$$M_{\max} = M_b = - \frac{q \cdot l_1^2}{8}$$

$$Q_b = \frac{5}{8} \cdot q \cdot l$$

$$Q_a = \frac{3}{8} \cdot 89,1 \cdot 2600 = 8,69 \cdot 10^4 \text{ N}$$

$$Q_b = \frac{5}{8} \cdot 89,1 \cdot 2600 = 1,45 \cdot 10^5 \text{ N}$$

$$M_b = - 7,53 \cdot 10^7 \text{ Nmm}$$

$$W_b \approx \pi \cdot s \cdot r^2 = \pi \cdot 10 \cdot 270^2 = 2,29 \cdot 10^6 \text{ mm}^3$$

Bending stress

$$\sigma_b = \frac{M_b}{W_b} = - 32,9 \text{ N/mm}^2$$

Shearing stress

$$\tau = \frac{Q_b}{A} = \frac{1,45 \cdot 10^5 \text{ N}}{540 \cdot \pi \cdot 10} = 8,5 \text{ N/mm}^2$$

Reduced stress:

$$\sigma_v = \sqrt{\sigma_b^2 + 3\tau^2} = 36.0 \text{ N/mm}^2$$

Admissible stress:

$$\sigma_{zul} = R_{0,2} (100 \text{ } ^\circ\text{C}) = 176 \text{ N/mm}^2$$

The reduced stress is smaller than the admissible stress.

- Stress in the mantle due to an axial shock

The accelerated weight of inserts causes a tensile stress in the mantle:

$$\tilde{\sigma}_Z = \frac{F}{A}$$

$$F = (G_{BE} + G_{Einb}) \cdot 10 \text{ g} = 3550 \cdot 10 \cdot 9,81 = 3,48 \cdot 10^5 \text{ N}$$

$$A = (560^2 - 540^2) \cdot \frac{\pi}{4} = 8,45 \cdot 10^4 \text{ mm}^2$$

$$\tilde{\sigma}_Z = 4,1 \text{ N/mm}^2$$

$$\tilde{\sigma}_Z < R_{0,2} (100^\circ\text{C}) = 176 \text{ N/mm}^2$$

## 4.3.6.2 Stresses due to continuous vibrations

The following transport accelerations are assumed:

- axial            1      g
- vertical        2      g
- lateral        1.5    g

Endurance is larger than  $10^6$ .

- Stresses in the mantle

Resulting acceleration:

$$a = \sqrt{2^2 + 1.5^2} = 2.5 \text{ g}$$

Reduced stress:

$$\sigma_{v_{vb}} = \sigma_v \cdot \frac{2.5}{5.83} = 15.4 \text{ N/mm}^2$$

$$\sigma_v < \sigma_{zul} = \frac{R_{0.2}}{1.5} (100 \text{ °C}) = 117 \text{ N/mm}^2$$

4.3.7 Literature

/4.2-1/ R.J. Roark, N.C. Young  
Formulas for Stress and Stress, New York (1975)

/4.3-2/ Physik Hütte, Vol. 1, 29. edition  
Hütte Ges. mbH, Berlin 1971



#### 4.4 Solidity of the trunnions

It will now be proved that the trunnions can withstand normal loads during transport and handling as well as stresses due to shock during transport accidents.

##### 4.4.1 Load assumptions

Cask weights:

Transport weight when loaded (horizontal) 25 000 kg <sup>1)</sup>

Handling (vertical): 24 000 kg <sup>2)</sup>

Accelerations:

- stresses due to shock

transport	axial	10 g
	vertical	3 g
	lateral	5 g
- handling	vertical	1.5 g

##### 4.4.2 Geometry

The geometry of the trunnions with their holding system is represented in fig. 4.4-1.

## 4.4.3 Dimensions, resistance momenta and section surfaces

The following table gives the dimensions, resistance momenta and section surfaces of the corresponding calculation levels.

Table 4.4-1: Dimensions, resistance momenta and section surfaces of the trunnions in the calculation levels

Section	A	B	C	D
Dimensions (mm)	Ø 100/40	Ø 130/40	Ø 255/130	□ 480 x 620 450 x 590 <sup>1)</sup>
Resistance value (mm <sup>3</sup> )	$9.56 \cdot 10^4$	$2.13 \cdot 10^5$	$1.52 \cdot 10^6$	$W_x: 5.91 \cdot 10^6$ $W_y: 5.14 \cdot 10^6$
Surface (mm <sup>2</sup> )	$6.59 \cdot 10^3$	$1.20 \cdot 10^4$	$3.78 \cdot 10^4$	$3.21 \cdot 10^4$
Moment of inertia (mm <sup>4</sup> )	$4.78 \cdot 10^6$	$1.39 \cdot 10^7$	$1.94 \cdot 10^8$	$I_x: 1.83 \cdot 10^9$ $I_y: 1.23 \cdot 10^9$
Static momentum (mm <sup>3</sup> )	$7.80 \cdot 10^4$	$1.77 \cdot 10^5$	$1.20 \cdot 10^6$	-

Transition radii were not taken into account.

- 1) The arched surface of the welding seam is projected into the calculation plane. Welding seam thickness  $a = 15$  mm.

## 4.4.4 Load on trunnions during transport and handling

## 4.4.4.1 Shock stresses due to transport incidents

- axial and vertical stresses.

Vertical and horizontal forces are absorbed uniformly by 2 trunnions. The fastening of the cask to the transport rack over the foot plate only absorbs vertical forces partially.

Maximal stresses have the following components:

$b_a = 10 \text{ g}$  in axial direction

$b_v = 3 \text{ g}$  in vertical direction

The maximum resulting acceleration per trunnion thus is:

$$b_{\max} = \sqrt{\left(\frac{10}{2}\right)^2 + \left(\frac{3}{4}\right)^2} = 5.056 \text{ g}$$

The accelerating force thus amounts to:

$$\begin{aligned} F_T &= 5.056 \cdot 9.81 \cdot 25000 = \\ &= 1.24 \cdot 10^6 \text{ N} \end{aligned}$$

- lateral stress

The lateral stress is absorbed by one trunnions. The function of the foot plate fastening is neglected.

Trunnion stress in the direction of the trunnions axis:

$$P = 5 \cdot 9.81 \cdot 25000 = 1.23 \cdot 10^6 \text{ N}$$

## 4.4.4.2 Stresses during handling of casks

It is assumed that the cask is lifted by two trunnions during handling in a nuclear facility. The handling weight is:

$$G_H \approx 24\,000 \text{ kg}$$

Considering an acceleration of 1.5 g during handling, one obtains the following stresses per trunnion:

$$\begin{aligned} F_H &= \frac{1.5}{2} \cdot 9.81 \cdot 24000 \\ &= 1.77 \cdot 10^5 \text{ N} \end{aligned}$$

## 4.4.4.3 Stresses on trunnion and trunnion holding piece

Calculated stresses during transport and handling are summarized in tables 4.4-3 and 4.4-4.

The main stress limits for trunnion and trunnion holding piece material no. 1.4541 at 100 °C are summarized in table 4.4-2.

Table 4.4-2: Stress limits for trunnion and trunnion holding piece materials

Trunnion holding piece	
Tensile limit (N/mm <sup>2</sup> )	176
Tensile strength (N/mm <sup>2</sup> )	350

Based on TÜV-decision no. 28/4.4-1/, the following stresses are admissible for components according to table 1:

Tensile and compression stresses, type of stress -H-

$$\sigma_{b\ zul} = 0.67 \cdot R_{0.2}$$

Shear stresses

$$\tau_{zul} = 0.4 \cdot R_{0.2}$$

Reduced stress

$$\sigma_v = 0.75 \cdot R_{0.2}$$

The tensile limit at 100 °C for M16 screws of the selected materials is:

$$R_{0.2} \geq 500 \text{ N/mm}^2$$

Based on the above mentioned decision, the following stresses are admissible for connecting parts according to table 1:

Tensile stresses, type of stress -H-

$$\sigma_{zul} = 0.42 R_{0.2}$$

These admissible stresses are used for cask handling.

Maximal stress in the trunnion flange mounting (according to /4.4-5/)  
during handling:

$$\sigma_{\max} = \frac{\beta \cdot M}{a \cdot t^2}$$

$$M = 1.10 \cdot 10^7 \text{ Nmm}$$

$$a = 200 \text{ mm (cf. fig. 4.4-2)}$$

$$t = 30 \text{ mm (cf. fig. 4.4-2)}$$

$$b = 100 \text{ mm (cf. fig. 4.4-2)}$$

$$\beta = 1.146 \text{ (according to table 1, /4.4-5/)}$$

b/a	0.5	0.6	0.633	0.7
$\beta$	1.146	0.749	0.708	0.467

$$\sigma_{\max} = 64.3 \text{ N/mm}^2$$

$$\sigma_{\max} < \sigma_{\text{zul}} = 176 \cdot 0.67 = 118 \text{ N/mm}^2$$

Table 4.4-3: Stresses on trunnion under transport conditions

Section	A	B	C	D
Force (N)	-	-	$1.24 \cdot 10^6$	$1.24 \cdot 10^6$
Torque (Nmm)	-	-	$3.72 \cdot 10^7$	$6.82 \cdot 10^7$
Bending stress (N/mm <sup>2</sup> )	-	-	24.5	11.5
Pressure stress (N/mm <sup>2</sup> )	-	-	32.8	38.6
Shear stress (N/mm <sup>2</sup> )	-	-	65.6	77.3
Reduced stress (N/mm <sup>2</sup> ) <sup>2)</sup>	-	-	143.2	162.5
Admissible stress (N/mm <sup>2</sup> )	-	-	176	176

Table 4.4-4: Stresses on trunnion under handling conditions

Section	A	B	C	D
Force (N)	$1.77 \cdot 10^5$	$1.77 \cdot 10^5$	$1.77 \cdot 10^5$	$1.77 \cdot 10^5$
Torque (Nmm)	$4.4 \cdot 10^6$	$9.72 \cdot 10^6$	$1.94 \cdot 10^7$	$2.30 \cdot 10^7$
Bending stress (N/mm <sup>2</sup> )	46.0	45.7	12.8	4.5
Pressure stress (N/mm <sup>2</sup> )	-	-	4.7	5.5
Shear stress (N/mm <sup>2</sup> )	48.2	25.1	8.8	11.0
Reduced stress (N/mm <sup>2</sup> ) <sup>2)</sup>	95.2	63.0	23.2	21.5
Admissible reduced stress (N/mm <sup>2</sup> )	132	132	132	132

$$2) \sigma_v = \sqrt{(\sigma_b + \sigma_d)^2 + 3\tau^2}$$

#### 4.4.4.4 Trunnion calculation according to KTA 3902 (handling)

According to KTA 3902 /4.4-2/, crane systems in nuclear facilities must be classified for maximum operating loads according to § 7.2.1 at least in lifting class H 4 and at least in load group B 4 (DIN 15018).

According to VDÜ sheet 1751 /4.4-3/, heavy duty crane systems must be classified at least in lifting class 4 and load group 5. Calculations are thus carried out for condition H 4 - B 5. The number of loading operations on the handling organs is significantly lower than 20000. According to DIN 15018 /4.4-4/, this means that only a general stress verification is required.

Table 2 of /4.4-4/ indicates a lifting load coefficient  $\Psi = 1.5$  for a lifting speed  $V_H \approx 11$  m/min.

As the lifting load coefficient coincides with the value used in 4.4.4.2 for acceleration during handling, this mode of calculation must yield the same results as those obtained in 4.4.4.3.

#### 4.4.4.5 Continuous trunnion and trunnion holding piece stress due to vibrations during transport

- Initial data

Table 4.4.5: Accelerations and forces due to transport vibrations

	max. acceleration	force acting on
axial vibration	1 g	2 trunnion holding pieces
vertical vibration	2 g	foot plate + 2 trunnion holding pieces
lateral vibration	1.5 g	1 trunnion holding piece



Endurance is  $> 10^6$ .

Fatigue limit is  $176 \text{ N/mm}^2$  at  $100^\circ \text{C}$ .

- Stress calculation

Half the vertical acceleration is endured by the foot plate. The resulting maximum acceleration is:

$$b_{\max} = \sqrt{\left(\frac{1}{2}\right)^2 + \left(\frac{2}{4}\right)^2} = 0.707 \text{ g}$$

Acceleration acts in a direction  $45^\circ$  against horizontal.

Force resulting from acceleration:

$$\begin{aligned} F_N &= 25000 \cdot 9.81 \cdot 0.707 \\ &= 1.73 \cdot 10^5 \text{ N} \end{aligned}$$

The force acting on the trunnion due to lateral acceleration is:

$$\begin{aligned} P &= 1.5 \cdot 9.81 \cdot 25000 \\ &= 3.68 \cdot 10^5 \text{ N} \end{aligned}$$

Sections C and D are submitted to the strongest stresses.

Stresses are directly proportional to the applying load.

$$\sigma_{b \text{ vib}} = \sigma_{b \text{ shock}} \cdot \frac{F_{\text{vib}}}{F_{\text{shock}}}$$

$$\tau_{b \text{ vib}} = \tau_{b \text{ shock}} \cdot \frac{F_{\text{vib}}}{F_{\text{shock}}}$$

Table 4.4-6: Stress on the trunnions due to transport vibrations

Section	C	D
$F_{\text{vib}} \text{ (N)}$	$1.67 \cdot 10^5$	$1.67 \cdot 10^5$
$F_{\text{shock}} \text{ (N)}$	$1.24 \cdot 10^6$	$1.24 \cdot 10^6$
$\sigma_{\text{b shock}} \text{ (N/mm}^2\text{)}$	24.5	11.5
$\tau_{\text{b shock}} \text{ (N/mm}^2\text{)}$	65.6	77.3
$\sigma_{\text{b vib}} \text{ (N/mm}^2\text{)}$	3.4	1.6
$\tau_{\text{b vib}} \text{ (N/mm}^2\text{)}$	9.2	10.8
$\sigma_{\text{d vib}} \text{ (N/mm}^2\text{)}$	9.8	11.5
$\sigma_{\text{v}} \text{ (N/mm}^2\text{)}$	20.7	22.8

$$\sigma_{\text{v}} = \sqrt{(\sigma_{\text{b}} + \sigma_{\text{d}})^2 + 3\tau^2}$$

$$\sigma_{\text{zul}} = \frac{R_{0.2}}{\nu}, \text{ assuming } \nu = 2$$

$$= 88 \text{ N/mm}^2$$

## 4.4.5 Stresses in trunnion screws

The largest strains occur during handling. Trunnion screw calculations are based on these strains.

$$F = 1.77 \cdot 10^5 \text{ N}$$

## 4.4.5.1 Maximum stress on screws during handling

$$M_{\max} = 1.77 \cdot 10^5 \text{ N} \cdot 55 \text{ mm} = 9.74 \cdot 10^6 \text{ Nmm}$$

The geometric position of the screws is shown in fig. 4.4-3. The flange is fastened to the cask by means of 12 screws M16.

Maximal stress on screws is due to all torques acting around point  $M_0$ .

According to /4.4-6/ the following holds:

$$F_{\text{scr}} = \frac{M_{\max}}{\frac{\sum y^2}{1}} = F_B$$

$$F_B = \frac{9.74 \cdot 10^6 \text{ Nmm} \cdot 227.5}{2.55 \cdot 10^5}$$

$$F_B = 8.69 \cdot 10^3 \text{ N}$$

Preliminary tightening force should reach to 20 - 30 % of the tensile limit /4.4-6/. The preliminary tightening force is thus:

$$F_V = R_{0.2} \cdot 0.3 \cdot A$$

$$F_V = 500 \cdot 0.3 \cdot 141$$

$$F_V = 2.1 \cdot 10^4 \text{ N}$$

The stress diagram is determined for the screws submitted to the most severe stress (exterior border).

Rigidity of the trunnion flange:

$$C_F = \frac{E \cdot A_F}{L}$$

$$E = 2,0 \cdot 10^5 \text{ N/mm}^2 \quad (t = 100^\circ\text{C})$$

$$A_F = \frac{\pi}{4} \cdot (30^2 - 18^2) = 453 \text{ mm}^2 \quad (\text{cf. fig. 4.4-4})$$

$$L = 15 \text{ mm}$$

$$C_F = 6,03 \cdot 10^6 \text{ N/mm}$$

Rigidity of the screw:

$$C_S = \frac{E \cdot A_S}{L_S}$$

$$E = 2,0 \cdot 10^5 \text{ N/mm}^2$$

$$A_S = 141 \text{ mm}^2$$

$$L_S = 15 \text{ mm}$$

$$C_S = 1,88 \cdot 10^6 \text{ Nmm}$$

Elongation of the screw due to preliminary tightening force:

$$\Delta L_S = \frac{F_V}{C_S} = 0,011 \text{ mm}$$

Compression of the flange due to preliminary tightening force:

$$\Delta L_F = \frac{F_V}{C_F} = 0,004 \text{ mm}$$

The resiliency of the screw head is neglected, which means that the more disadvantageous case is used for calculation.

The distortion diagram shows that the in presence of the average stress, deflection stress values remain below the admissible values.

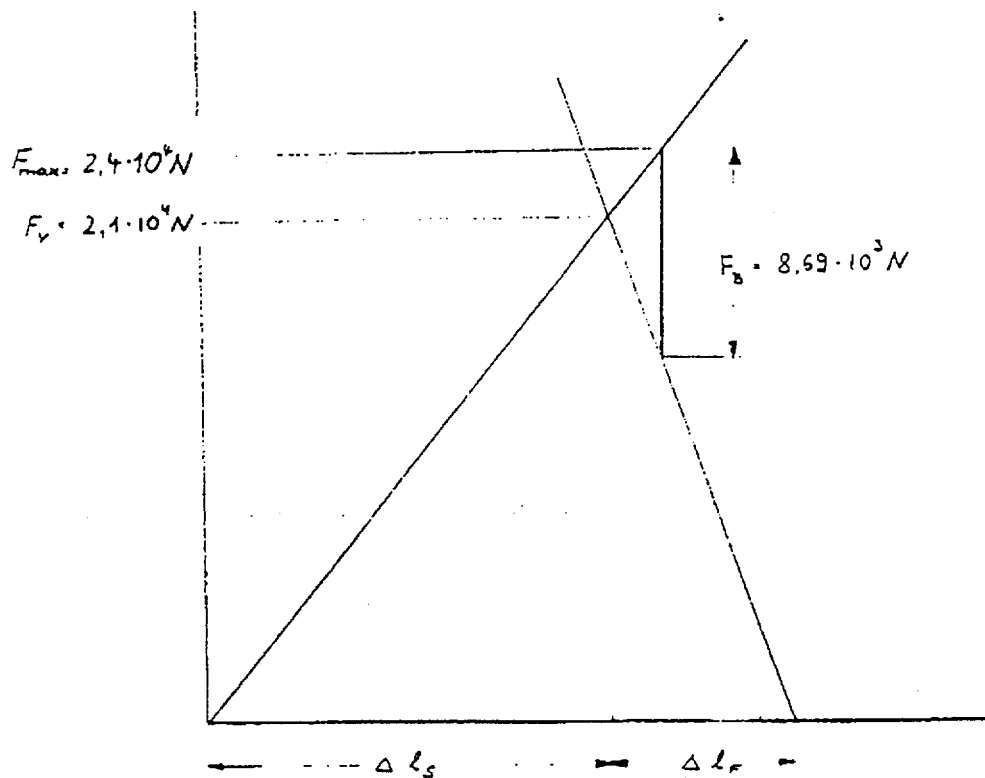
The following result is obtained:

$$F_{\max} = 2,4 \cdot 10^4 \text{ N}$$

$$\sigma_{\max} = \frac{2,4 \cdot 10^4 \text{ N}}{141 \text{ mm}^2} = 170 \text{ N/mm}^2$$

$$\sigma_{\max} < R_{0,2} \cdot 0,42 = 210 \text{ N/mm}^2$$

Distortion diagram of the screw submitted to the largest stress under normal transport conditions:



Deflection strain:

$$F_a = \frac{1}{2} (2,4 \cdot 10^4 - 2,1 \cdot 10^4) = 1,5 \cdot 10^3 \text{ N}$$

## 4.4.5.2 Tightening torque for handling conditions

Calculation is carried out according to /4.4-5/.

$$\text{Total torque: } M_G = F_V \cdot (r \cdot \tan (\alpha + \varphi) + r_A \cdot \mu_A)$$

$$F_V = 2,1 \cdot 10^4 \text{ N}$$

$$r = 7,2 \text{ mm}$$

$$\alpha = 2,5^\circ$$

$$\varphi = 7,97^\circ$$

$$r_A = 11,2 \text{ mm}$$

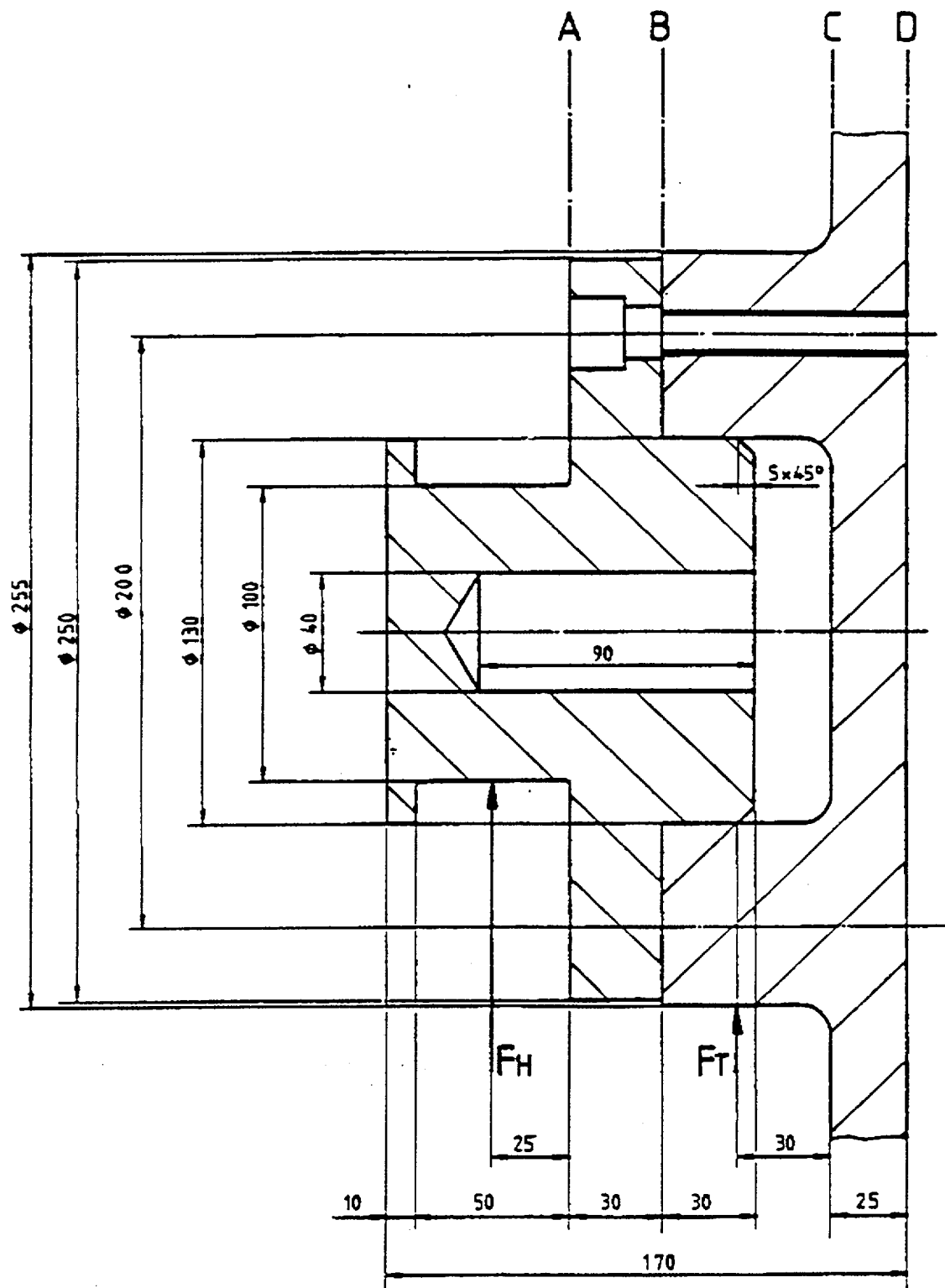
$$\mu_A = 0,14$$

$$M_G = 6,09 \cdot 10^4 \text{ Nmm} = 60,9 \text{ Nm}$$

Selected value 61 Nm

4.4.6 Literature

- /4.4-1/ VdTÜV Decision ordinance no. 28
- /4.4-2/ KTA 3902
- /4.4-3/ VdTÜV sheet 1751
- /4.4-4/ DIN 15018
- /4.4-5/ R.J. Rork / W.G. Young  
Formulas for Stress and Strains  
Mc-Graw-Hill, New York
- /4.4-6/ Niemann, Maschinenelemente, Vol 1, 1961  
Springer Verlag, Heidelberg



TN 7 - 2 trunnion

Fig. 4.4-1



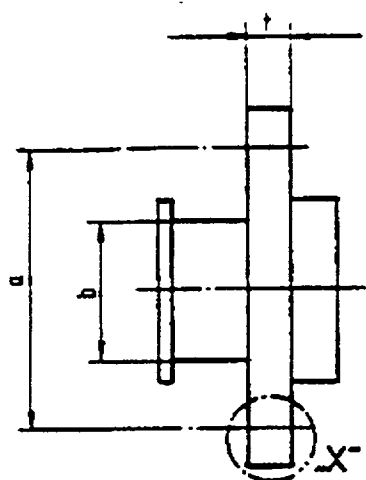


Fig. 4.4-2

Detail "X"

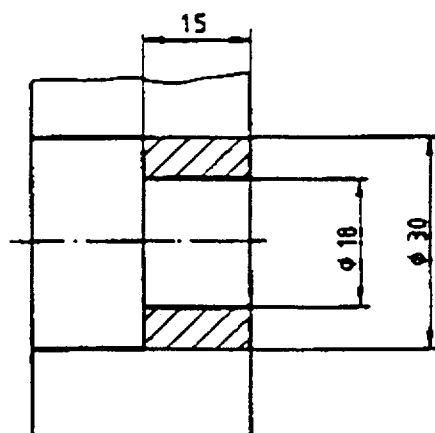


Fig. 4.4-4

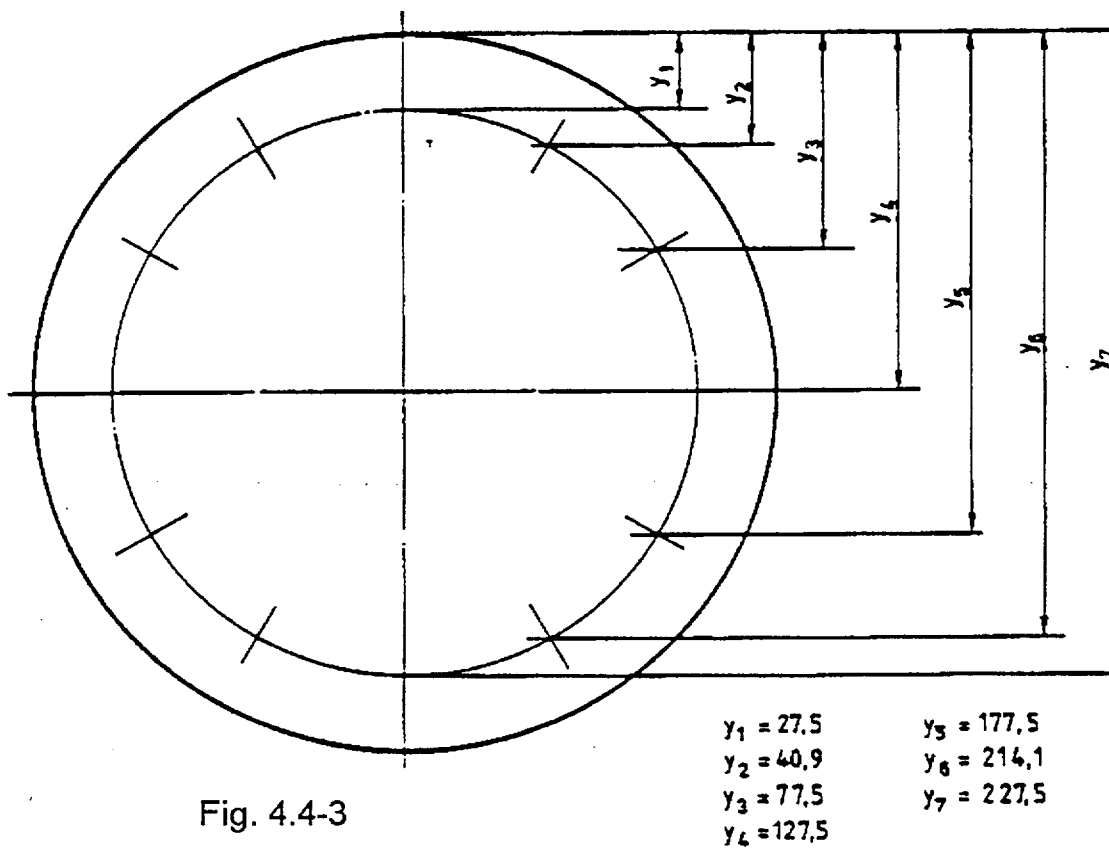


Fig. 4.4-3



## 4.5 Solidity behaviour under accidental conditions

### 4.5.1 Drop test with a 1:3 cask test model

The safety of the cask under accidental conditions was investigated by means of fall tests performed on a 1:3 scale model, as foreseen by IAEA /4.5-1/. The model was used to carry out the following tests at room temperature (about 20 °C):

- 9 m drop on the edge of the lid with lid shock-absorber  
(vertical inclination of the cask axis:  $\theta = 18.5^\circ$ )
- 9 m drop on the edge of the bottom with bottom shock-absorber  
(same inclination as above)
- 9 m drop on cask mantle with lid and bottom shock-absorbers
- Gudgeon drop test, drop from 1 m, on lid with shock-absorber
- Gudgeon drop test, drop from 1 m, on bottom with shock-absorber
- Gudgeon drop test, drop from 1 m, on cask mantle

The tests were concluded with the main results summarized in table 4.5-1. An extensive description of the tests is found in /4.5-2/.

After the 9 m drop onto the cask mantle, both shock absorbers were no longer firmly fastened to the cask. As this was however required for the following fire test, the test was repeated with a modified shock-absorber. It was verified that the connection between cask and shock-absorber remains intact with the new shock-absorber design. With the new shock-absorber design, maximum acceleration was lower as with the old one, so that this value was used for calculations. Furthermore, aluminum disks were integrated in such a way in the bottom area of the initial shock-absorbers, that coupling lids had better protection against damages caused by a gudgeon.

The main result of the solidity behaviour of the cask under mechanical accidental conditions can be summarized as follows:

- the tight enclosure of the cask always remained intact. The leak rate remained below  $10^{-4}$  torr · l/s, which corresponds to  $1.33 \cdot 10^{-4}$  mbar · l/s.
- Maximum accelerations calculated for the original cask, based on values obtained for the model, are:
  - drop in vertical position: 60 g
  - drop in horizontal position: 67 g
- The shielding of a cask is not impaired by an accident.

After the following fire test, during which the cask was submitted for 10 minutes to a fire at 800 °C, no modification of the cask was detected (cf. also chapter 5.3).

Maximum acceleration values determined on the 1/3 scale model can be converted over the model scale to the original cask by following calculation:

$$b_{\text{ORIG.}} = b_{\text{MOD.}} \cdot \frac{1}{3}$$

Table 4.5-1: Summary of the main drop test results

No.	Drop position	Mechanical behaviour	Leak rate display after the test (sum over the 3 interior tightness points) (mbar · l · sec <sup>-1</sup> )	maximum accelerations	
				1:3 model	original cask
1	9 m drop on edge of lid	slight deformation of the unprotected cask bottom, no effect on tight enclosure	$7.2 \cdot 10^{-6}$	150 g	50 g
2	9 m drop on edge of bottom	no damage to cask	$7.0 \cdot 10^{-6}$	170 g	57 g
3	9 m drop on cask mantle	no damage to cask; shock absorbers no longer firmly attached to cask	$6.7 \cdot 10^{-6}$	300 g	100 g
4	Gudgeon drop on lid	slight deformation of the coupling lid; no effects	-	110 g	37 g
5	Gudgeon drop on bottom	slight deformation of the coupling lid, cracks in the welding seam connecting the coupling to the bottom; no effects on tight enclosure	-	110 g	37 g
6	Gudgeon drop on mantle	dent in the mantle caused by gudgeon. Integrity of exterior mantle is maintained	$2.3 \cdot 10^{-6}$	90 g	30 g
7	9 m drop on the cask mantle (new shock absorber design on the lid side)	no damages to cask; shock absorber remains firmly attached to cask	no measurement	200 g	67 g

4.5.2 Literature

- /4.5-1/ IAEA Regulations for the Safe Transport of Radioactive Materials, Vienna, 1973
- /4.5-2/ Instrumented drop and fire tests with a transport cask for fuel assemblies of the TN 7-2 type, experimental report 2041, Federal Agency for Testing of Materials, Berlin, May 19, 1982.

## 4.6 Verification of solidity for contents

In this chapter, calculation of the mechanical behaviour of the fuel assembly insert baskets are carried out under normal transport and accidental conditions. Calculations are carried out separately for the foreseen contents. The corresponding geometry of the insert basket is found in chapter 3.2.5 and in the drawings.

### 4.6.1 DIDO and MERLIN insert baskets

#### 4.6.1.1 Handling and transport conditions

DIDO and MERLIN insert baskets have been used quite often in the TN 7 cask, which is very similar to this one. No damages or alterations of the insert baskets occurred during handling or transport. A formal verification of solidity is nonetheless carried out here.

Insert basket geometry can be seen from drawing no. 1-150-025-17-00. The basket is made of 1.4541 stainless steel. Solidity values are found in table 4.1-2.

##### 4.6.1.1.1 Stresses due to thermal dilatation

It is verified that the insert baskets can expand in all directions without hindrance, which assures that no thermal stresses occur if uniform temperature of the insert basket is assumed. The geometrically most unfavourable case is considered, which consists in loading with 2 DIDO and 2 MERLIN fuel assemblies.

axial:

$$\Delta l = \alpha \cdot l \cdot (t_2 - t_1)$$

$$= 18 \cdot 10^{-6} \cdot 2648 \cdot 380 = 18.1 \text{ mm}$$

$$\alpha = 18 \cdot 10^{-6} \text{ (for 1.4541 steel, temperature range 20 - 400 °C)}$$

$$l = 2648 \text{ mm (total length of the 4 insert baskets)}$$

$$t_1 = 20 \text{ °C}$$

$$t_2 = 400 \text{ °C (conservative assumption for insert basket temperature)}$$

Conservative calculations yield 18.1 mm for longitudinal expansion  $\Delta l$ . At ambient temperature, the gap is 27 mm.

radial:

$$\Delta d = \alpha \cdot d \cdot (t_2 - t_1)$$

$$= 18 \cdot 10^{-6} \cdot 520 \cdot (400 - 20)$$

$$= 3.56 \text{ mm}$$

Under conservative considerations, radial expansion is 3.56 mm. At ambient temperature, a 20 mm gap is found.

#### 4.6.1.1.2 Mechanical stresses

Mechanical stresses are due to shocks and vibrations during transport. They are noticeably smaller than those which may occur under accidental conditions, e. g. a drop from 9 m onto an unyielding surface. It is thus sufficient if it is verified in the next chapter that stresses remain below the admissible limit values even under accidental conditions.

## 4.6.1.2 Accidental conditions

The following situations are considered:

- Horizontal drop from 9 m height onto an unyielding surface.
- Vertical drop from 9 m height onto an unyielding surface.
- Drop from 1 m height onto a gudgeon.

This is done under the following assumptions:

- Acceleration of the insert basket upon impact is the same as for the cask.
- During horizontal drop, acceleration forces act as a uniformly distributed linear load on each insert basket.
- During vertical drop, the lowest insert basket is submitted to the largest stress.

## 4.6.1.2.1 Horizontal drop from 9 m height

The acceleration determined by means of model experiments (cf. chapter 4.5) acts on every insert basket:

$$b = 67 \text{ g}$$

Applying the following equation:

$$F = m \cdot a$$

the following accelerating forces are found:

DIDO insert basket with 15 fuel assemblies

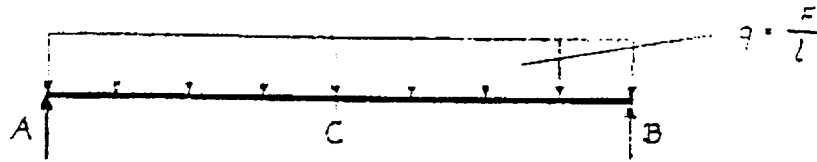
$$(m_i = 186 \text{ kg}) \quad : F = 1.23 \cdot 10^5 \text{ N}$$

MERLIN insert basket with 16 fuel assemblies

$$(m = 307 \text{ kg}) \quad : F = 2.02 \cdot 10^5 \text{ N}$$



The considered stress is calculated in a simplified way according to the model of a beam supported at both ends, according to /4.6-1/, p. 390, case 13:



The highest stress is found in the middle of the insert basket.

Maximum torque  $M_c$  :

$$M_c = \frac{F \cdot l}{8}$$

The maximum bending stress on the insert basket is thus:

$$\sigma_b = \frac{M_c}{W_{bc}}$$

The transverse force is:

$$\tau = \frac{F}{A}$$

All calculated values and initial data are listed in table 4.6-1 for both insert baskets.

Table 4.6-1: Results of solidity calculations for the horizontal 9 m drop

Insert basket	DIDO	MERLIN
Accelerating force F (N)	$1.23 \cdot 10^5$	$2.02 \cdot 10^5$
Uniformly distributed linear load q (N/mm)	$1.90 \cdot 10^2$	$2.99 \cdot 10^2$
max. torque $M_c$ (Nmm)	$9.92 \cdot 10^6$	$1.70 \cdot 10^7$
insert basket surface (mm <sup>2</sup> )	$2.42 \cdot 10^4$	$4.1 \cdot 10^4$
section modulus $W_c$ (mm <sup>3</sup> ) <sup>1)</sup>	$3.26 \cdot 10^6$	$4.26 \cdot 10^6$
moment of inertia $I_c$ (mm <sup>4</sup> )	$4.15 \cdot 10^8$	$6.46 \cdot 10^8$
max. bending stress $\sigma_b$ (N/mm <sup>2</sup> )	3.1	4.0
shearing stress $\tau$ (N/mm <sup>2</sup> )	5.1	4.9
reduced stress $\sigma_v$ (N/mm <sup>2</sup> )	9.4	9.4
admissible stress $\sigma_{zul}$ (N/mm <sup>2</sup> )	125	125

1) The section modulus is approximately the same for both insert baskets for all bending axes, so that any axis may be selected. Calculations are carried out applying Steiner's law according to /4.6-1/.

2) In this case, the admissible stress under accidental conditions is the tensile limit of the material. Assuming an insert basket temperature of 400 °C, this is:

$$R_{0.2} (400 \text{ °C}) = 125 \text{ N/mm}^2 \text{ for 1.4541 steel}$$

$$3) \sigma_v = \sqrt{\sigma_b^2 + 3\tau^2}$$

## 4.6.1.2.2 Vertical drop from 9 m height

The complete stress with the maximum acceleration determined by means of the model experiment (cf. chapter 4.5) acts on the lower insert basket:

$$b = 60 \text{ g}$$

This yields a maximum accelerating force

$$\begin{aligned} F_{\max} &= m_{\max} \cdot b \\ &= 986 \cdot 9.81 \cdot 60 = 5.8 \cdot 10^5 \text{ N} \end{aligned}$$

$$\text{with } m_{\max} = 2 \cdot 186 \text{ kg} + 2 \cdot 307 \text{ kg} = 986 \text{ kg}$$

It is verified that the DIDO insert basket, and thus also the MERLIN insert basket, is not buckled under this stress.

Slenderness ratio  $\lambda$  (according to /4.6-1/):

$$\lambda = s/i = 1296/131 = 9.89$$

$$\begin{aligned} \text{with } s &= \text{free buckling length} = 2 l = 2 \cdot 648 \\ &= 1296 \text{ mm} \end{aligned}$$

$$i = \sqrt{I/A} = \sqrt{4.15 \cdot 10^8 / 2.42 \cdot 10^4} = 1.31 \cdot 10^2$$

As  $\lambda \ll \lambda_0$ , inelastic buckling occurs.

According to Tetmajer, the following applies:

$$4700 - 23.0 \cdot \lambda = \sigma_K = \text{buckling stress (kp/cm}^2\text{)}$$

$$\sigma_K = 4472 \text{ kp/cm}^2 = 439 \text{ N/mm}^2$$

In order to obtain this buckling stress, the following buckling force is required:

$$F_K = \sigma_K \cdot A = 439 \cdot 2.42 \cdot 10^4$$

$$= 1.06 \cdot 10^7 \text{ N}$$

As  $F_{\max} = 5.8 \cdot 10^5 \text{ N}$ , no buckling occurs.

#### 4.6.1.2.3 Drop from 1 m height onto a gudgeon

Accelerations during a drop from 1 m height onto a gudgeon are smaller as for a 9 m drop (cf. chapter 4.5). The verification of solidity for the insert baskets carried out for the 9 m drop thus also covers the 1 m drop.

#### 4.6.2 RHF insert basket

The geometry of the insert basket is shown by drawing 1-150-025-21-00 "C". The insert basket is made of stainless steel 1.4541. A verification of solidity was carried out for this insert basket as a component of the TN 7 transport cask (/4.6-2/).

This is taken over here.

## 4.6.2.1 Handling and transport conditions

## 4.6.2.1.1 Stresses due to thermal dilatation

It is verified, that the insert basket can expand in all directions without hindrance. Assuming relatively constant temperature in the insert basket, thermal stresses are negligible.

axial:

$$\begin{aligned}\Delta l &= \alpha \cdot l \cdot (t_2 - t_1) \\ &= 18 \cdot 10^{-6} \cdot 2655 \cdot (350 - 20) \\ &= 16.6 \text{ mm}\end{aligned}$$

where  $\alpha = 18 \cdot 10^{-6}$  (cf. chapter 4.6.1.1.1)  
 $l = 2655 \text{ mm}$  (insert basket length)  
 $t_1 = 20 \text{ }^{\circ}\text{C}$   
 $t_2 = 350 \text{ }^{\circ}\text{C}$

The following gap remains in the cask:

$$s = 2675 - (16.6 + 2655) = 3.4 \text{ mm}$$

radial:

$$\begin{aligned}\Delta d &= \alpha \cdot d \cdot (t_2 - t_1) \\ &= 18 \cdot 10^{-6} \cdot 536 \cdot (350 - 20) \\ &= 3.18 \text{ mm}\end{aligned}$$

The following gap remains in the cask:

$$s = 540 - (536 + 3.18) = 0.82 \text{ mm}$$

#### 4.6.2.1.2 Mechanical stresses

Mechanical stresses are assessed under accidental conditions. Cf. also chapter 4.6.1.1.2.

#### 4.6.2.2 Accidental conditions

Assumptions made under 4.6.1.2 apply. Calculations are carried out for the horizontal 9 m drop according to /4.6-2/, with a modified acceleration value.

##### 4.6.2.2.1 Horizontal drop from 9 m height

Supplementary assumptions:

- both fuel assemblies act as a uniformly distributed linear load
- every integrated component is considered separately
- the insert basket is not supported over its whole length by the side of the cask

Fig. 3.3 is a sketch of the principle of the insert basket.

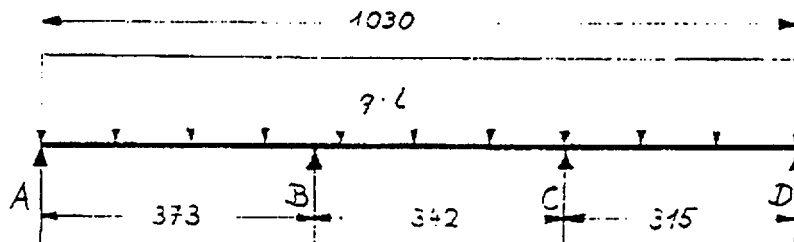
Initial data:

b	=	67 g	$G_{AH}$	=	57 kg
$G_{BE}$	=	109 kg	$G_{strut}$	=	5.3 kg
$G_{basket}$	=	126 kg	t	=	400 °C
$G_{basket2}$	=	110 kg			

- lower insert basket

Calculations are only carried out for the length submitted to the load of the fuel assembly. The following conservative substitution system is selected:

- a) Load on a longitudinal beam under its own load and the load for a fuel assembly



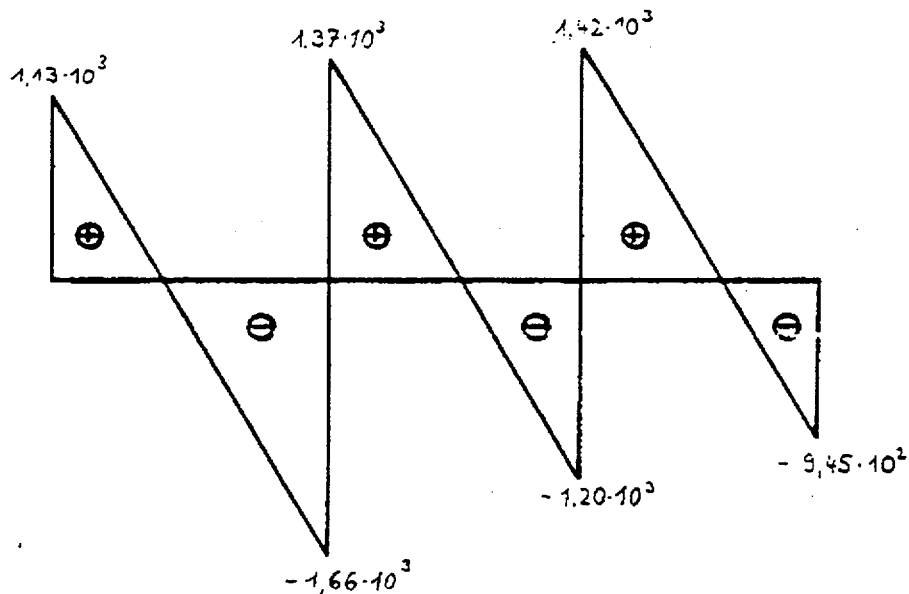
$$q \cdot l = F = (G_{BE} + G_{Str}) \cdot b = 115 \text{ kg} \cdot 67 \text{ g}$$

$$F = 7,57 \cdot 10^4 \text{ N}$$

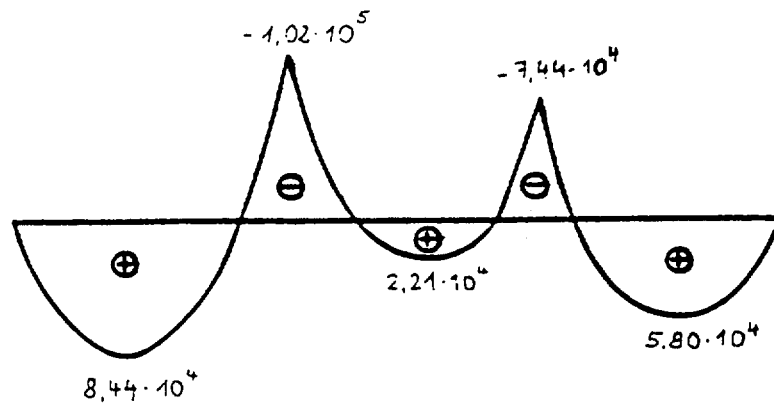
The system is subject to double static indetermination.

The following diagram is found for momenta and transverse forces.

Q-diagram (N):



Course of M (Nmm) :



The maximum load is found in point B.

Stress calculation:

Bending stress:

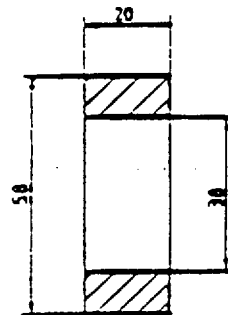
$$\sigma_b = \frac{M_b}{W_b}$$

$$M_b(B) = 1.02 \cdot 10^5 \text{ Nmm}$$

$$W_{b \min} = \frac{b \cdot (H^3 - h^3)}{6 \cdot H} = \frac{20 \cdot (58^3 - 38^3)}{6 \cdot 58}$$

$$= 8060 \text{ mm}^3$$

$$(B) \sigma_b = \frac{1.02 \cdot 10^5}{8060} = 12.7 \text{ N/mm}^2$$





Shearing stress:

$$\tau = \frac{F}{A}$$

$$(B)F = 3,03 \cdot 10^3 \text{ N}$$

$$A = 20 \cdot 2 \cdot 10 = 400 \text{ mm}^2$$

$$\tau = \frac{3,03 \cdot 10^3}{400} = 7,6 \text{ N/mm}^2$$

Reduced stress:

$$\sigma_v = \sqrt{\sigma_b^2 + 3\tau^2} = 18,3 \text{ N/mm}^2$$

$$\sigma_{zul} = R_{0,2} (1.4541 \text{ für } 400^\circ\text{C}) = 125 \text{ N/mm}^2 > \sigma_v$$

Tensile stresses in the supporting struts:

$$\sigma_Z = \frac{F}{A}$$

$$A = 40 \cdot 15 = 600 \text{ mm}^2$$

$$F = 3,03 \cdot 10^3 \text{ N (in B)}$$

$$F = 2,62 \cdot 10^3 \text{ N (in C)}$$

$$\sigma_Z = 5,03 \text{ N/mm}^2 \text{ (in B)}$$

$$\sigma_Z = 4,35 \text{ N/mm}^2 \text{ (in C)}$$

Stress in the upper supporting ring:

$$\sigma_Z = \frac{F}{A}$$

$$A = 20 \cdot 20 = 400 \text{ mm}^2$$

$$F = 1,13 \cdot 10^3 \text{ N (in A)}$$

$$\sigma_Z = 2,8 \text{ N/mm}^2$$

Stresses in the bottom steel plate:

$$F = 9.45 \cdot 10^2 \text{ N}$$

No revision of stress calculations is carried out, as the actual stress is lower than in the upper supporting ring.

b) Revision of calculations for the transmitting rib in the longitudinal struts.

Assumption: surface load on strut due to fuel assembly load

$$(b = 67 \text{ g})$$

$$F = 109 \text{ kg} \cdot 67 \text{ g} = 7.17 \cdot 10^4 \text{ N}$$

$$\sigma_D = \frac{F}{A}$$

In order to take into account the notch effect due to existing slots, the following selection is made:

$$\sigma_D = \sigma_{zul} = \frac{R_{0.2}}{15} = \frac{125}{1.5} = 83 \text{ N/mm}^2$$

If the actual rib width is  $s = 20 \text{ mm}$ , the required transmission length is:

$$l = \frac{A}{s} = \frac{F}{\sigma_D \cdot s} = \frac{7.17 \cdot 10^4}{83 \cdot 20} \\ = 43.2 \text{ mm}$$

The existing transmitting total length is

$$l = 240 \text{ mm}$$

One thus obtains:

$$\begin{aligned}\sigma_D &= \frac{F}{A_{\text{vorh}}} = \frac{7.17 \cdot 10^4}{240 \cdot 20} \\ &= 14.9 \text{ N/mm}^2\end{aligned}$$

c) Surface pressing against the cask wall

$$p = \frac{F}{A}$$

$$F = (G_1 + G_2) \cdot b = 1.44 \cdot 10^5 \text{ N}$$

$$G_1 = \text{weight of a fuel assembly} = 109 \text{ kg}$$

$$\begin{aligned}G_2 &= \text{maximum insert basket weight over the calculated length} \\ &= 110 \text{ kg}\end{aligned}$$

Surface lying against the cask wall:

$$A = 1030 \cdot 20 = 2.06 \cdot 10^4 \text{ mm}^2$$

$$p = 9.4 \text{ N/mm}^2$$

$$p < p_{\text{zul}} = R_{0.2} = 125 \text{ N/mm}^2$$

d) Surface pressing between fuel assembly and longitudinal strut

- strut

$$p = \frac{F}{A}$$

$$F = G_{BE} \cdot b = 109 \text{ kg} \cdot 67 \text{ g} = 7.2 \cdot 10^4 \text{ N}$$

$$A = 1 \cdot b = 920 \cdot 9.16 = 8427 \text{ mm}^2$$

$$p = 8.5 \text{ N/mm}^2$$

$$p < p_{\text{zul}} = R_{0.2} (1.4541) = 125 \text{ N/mm}^2$$

- fuel assembly

Calculations are revised according to /4.6-3/.

The following is valid:

$$p_{\max} = \frac{2 \cdot P}{\pi \cdot b \cdot l}$$

with:

$$b = \frac{8 \cdot P \cdot r (1 - \nu^2)}{\pi \cdot E \cdot l} = 5,33 \text{ mm}$$

$$\nu = 0,3$$

$$E = 7000 \text{ N/mm}^2 \text{ (aluminum alloy)}$$

$$l = 920 \text{ mm (length of fuel assembly tube)}$$

$$r = 413,6/2 = 206,8 \text{ mm (radius of exterior fuel assembly tube)}$$

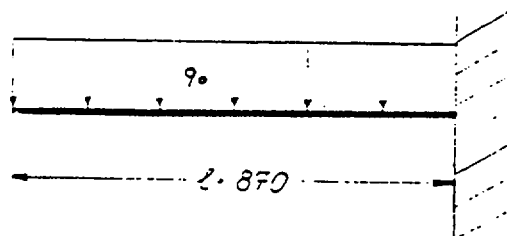
$$P = 7,2 \cdot 10^4 \text{ N}$$

$$p_{\max} = 6,2 \text{ N/mm}^2$$

$$p_{\max} < R_{0,2} \text{ (Al alloy at } 380^\circ\text{C)} = 17 \text{ N/mm}^2 \text{ (according to /4.6-4/)}$$

e) Interior tube and self weight

The interior tube has no supporting function. The load is due to the accelerated self weight. The tube is fastened on one end. The following substitution system is selected.



$$F = q_0 \cdot l = G_{\text{tube}} \cdot b = 41,5 \text{ kg} \cdot 67 \cdot 9,81 = 2,8 \cdot 10^4 \text{ N}$$

The maximum stress occurs at the fastening point. The following is valid:

- Bending stress

$$M_{\max} = \frac{F \cdot l}{2} = \frac{2,8 \cdot 10^4 \cdot 870}{2} = 1,22 \cdot 10^7 \text{ Nmm}$$

$$W_b = \frac{\pi}{32} \cdot \left( \frac{D^4 - d^4}{D} \right) = \frac{\pi}{32} \cdot \left( \frac{240^4 - 224^4}{240} \right) = 3,27 \cdot 10^5 \text{ mm}^3$$

$$\sigma_b \cdot \frac{M}{W_b} = \frac{1,22 \cdot 10^7}{3,27 \cdot 10^5} = 37,2 \text{ N/mm}^2$$

- Transverse stress

$$F_{\max} = 2,8 \cdot 10^4 \text{ N}$$

$$A = \frac{\pi}{4} \cdot (240^2 - 224^2) = 5830 \text{ mm}^2$$

$$\tau = \frac{F}{A} = \frac{2,8 \cdot 10^4}{5830} = 4,8 \text{ N/mm}^2$$

- Reduced stress

$$\sigma_v = \sqrt{\sigma_b^2 + 3\tau^2} = 38,1 \text{ N/mm}^2$$

$$\sigma_v < \sigma_{zul} = R_{0,2} (1.4541) = 125 \text{ N/mm}^2$$

- Upper insert basket

The upper insert basket corresponds to the calculated part of the lower one. Stresses found for the latter are also valid here.

## 4.6.2.2.2 Vertical drop from 9 m height

$$b = 60 \text{ g}$$

- Lower insert basket

a) Surface pressing against the cask bottom

$$p = \frac{F}{A}$$

$$\begin{aligned} F &= (2 \cdot G_{BE} + G_{Körbe}) \cdot 60 \text{ g} = \\ &= (2 \cdot 109 + 126 + 110 + 57) \cdot 60 \text{ g} \\ &= 3,0 \cdot 10^5 \text{ N} \end{aligned}$$

$$A = (540^2 - 400^2) \cdot \frac{\pi}{4} = 1,03 \cdot 10^5 \text{ mm}^2$$

$$p = 2,9 \text{ N/mm}^2$$

$$p < p_{zul} = R_{0,2} (1.4541) = 125 \text{ N/mm}^2$$

b) Buckling safety of the struts in the fuel assembly zone

During a vertical drop, the whole lower insert basket is submitted to a stress by the upper basket with fuel assemblies and the spacers.

$$\begin{aligned} F_K &= (G_{BE} + G_{K_2} + G_{AH}) \cdot 60 \text{ g} \\ &= 276 \text{ kg} \cdot 60 \text{ g} = 1,63 \cdot 10^5 \text{ N} \end{aligned}$$

Buckling force per strut:

$$F_{KS} = \frac{F_K}{4} = 4,07 \cdot 10^4 \text{ N}$$

Calculation is carried out according to /4.6-1/. The part wherein the fuel assembly is located,  $l = 1030$ , is taken as length of the insert basket. The radial supporting struts are conservatively neglected.

$$\text{Free buckling length} \quad s = 0,7 \cdot l = 721 \text{ mm}$$

$$\text{Inertial radius} \quad i = \sqrt{I/S}$$

$$\text{Slenderness ratio} \quad \lambda = s/i$$

$$\lambda > \lambda_0 = 96 \rightarrow \text{elastic buckling.}$$

The critical buckling force according to Euler thus is:

$$K = \frac{\pi^2 \cdot E \cdot I}{s^2} = \frac{\pi^2 \cdot 2 \cdot 10^5 \cdot 1,33 \cdot 10^4}{721^2}$$

$$= 5,05 \cdot 10^4 \text{ N}$$

$$F_{KS} < K \rightarrow \text{no buckling occurs}$$

and tension in the struts amounts to

$$\sigma_d = \frac{F_{KS}}{A} = \frac{4,07 \cdot 10^4}{400}$$

$$= 101,8 \text{ N/mm}^2$$

$$\sigma_d < \sigma_{zul} = R_{0,2} (1.4541) = 125 \text{ N/mm}^2$$

c) Buckling of the lower part of the insert basket (spacer part)

$$\begin{aligned} F_K &= (2 \cdot G_{BE} + G_{K1} + G_{K2} + G_{AH}) \cdot 60 \text{ g} \\ &= 3,0 \cdot 10^5 \text{ N} \end{aligned}$$

$$F_{KS} = F_K/4 = 7,52 \cdot 10^4 \text{ N (buckling force per strut)}$$

$$l = (1320 - 1030) = 290 \text{ mm}$$

$$s = 0,7 \cdot l = 203 \text{ mm}$$

$$I_{\min} = h \cdot b^3/12 = 58 \cdot 20^3/12 = 3,87 \cdot 10^4 \text{ mm}^4$$

$$A = S = b \cdot h = 58 \cdot 20 = 1160 \text{ mm}^2$$

$$i = \sqrt{I/S} = 5,78$$

$$\lambda = s/i = 203/5,78 = 35,1$$

$$\lambda > \lambda_0 = 96 \rightarrow \text{inelastic buckling.}$$

According to Tetmajer, critical buckling stress is:

$$\begin{aligned} \sigma_K &= 3030 - 12,9 \cdot \lambda \quad (\text{kp/cm}^2) \\ &= 252,7 \text{ N/mm}^2 \end{aligned}$$

and critical buckling force is:

$$\begin{aligned} K &= \sigma_K \cdot S = 252,7 \cdot 1160 \\ &= 2,93 \cdot 10^5 \end{aligned}$$

$$F_{KS} < K \rightarrow \text{no buckling occurs.}$$



Stress in the strut:

$$\sigma_d = \frac{F_{KS}}{A}$$

$$= 64,8 \text{ N/mm}^2$$

$$\sigma_d < \sigma_{zul} = R_{0,2} (1.4541) = 125 \text{ N/mm}^2$$

d) Surface pressing between upper and lower insert basket

$$F = (G_{BE} + G_{K2} + G_{AH}) \cdot 60 \text{ g}$$

$$= 1,62 \cdot 10^5 \text{ N}$$

$$A = (516^2 - 486^2) - \frac{\pi}{4} = 2,36 \cdot 10^4 \text{ mm}^2$$

$$\sigma_d = \frac{F}{A} = 6,9 \text{ N/mm}^2$$

$$\sigma_d < \sigma_{zul} = R_{0,2} (1.4541) = 125 \text{ N/mm}^2$$

- Upper insert basket

The load on the upper insert basket due to the lower one during a 9 m drop on the lid is:

$$F_K = (G_{BE} + G_{K1}) \cdot 60 \text{ g} = 1,38 \cdot 10^5$$

It is thus smaller than in the opposite case. This means that the upper insert basket does not buckle.

- Upper spacer

The force acting on the upper spacer during a 9 m drop on the lid is:

$$\begin{aligned} F_K &= (2 \cdot G_{BE} + G_{K1} + G_{K2}) \cdot 60 \text{ g} \\ &= 2,68 \cdot 10^5 \text{ N} \\ F_{KS} &= F_K/4 = 6,68 \cdot 10^4 \text{ N} \end{aligned}$$

The stress is smaller than that acting on the spacer part of the lower insert basket. As the buckling length ( $l = 275 \text{ mm}$ ) is smaller than for the lower spacer, no buckling occurs.

$$\begin{aligned} \sigma_d &= \frac{F_{KS}}{A} = \frac{6,68 \cdot 10^4}{1160} \\ &= 57,6 \text{ N/mm}^2 \end{aligned}$$

$$\sigma_d < \sigma_{zu1} = R_{0,2} (1.4541) = 125 \text{ N/mm}^2$$

#### 4.6.2.3 Handling conditions

Maximal stress occurs when the insert baskets are lifted with the facility crane. This stress is much smaller than that occurring under accidental conditions, so that no verification is required for normal handling.

Merely the solidity of the lifting shackles is demonstrated in the following. They are only used to handle the empty insert basket.

Maximum force during lifting (acceleration = 1.5 g)

$$F = m \cdot b = 126 \text{ kg} \cdot 1.5 \text{ g}$$

$$= 1855 \text{ N}$$

Stress in the lifting shackles:

each lifting shackle is welded on both sides to the interior tube (that is, fastened by clamping). Maximum stress occurs in the middle of the shackle.

$$M_{\max} = \frac{F \cdot l}{8} = \frac{1855 \cdot 224}{8} = 5,2 \cdot 10^4 \text{ Nmm}$$

$$W_b = \frac{\pi}{32} \cdot D^3 = \frac{\pi}{32} \cdot 25^3 = 1534 \text{ mm}^3$$

$$\sigma_b = \frac{M}{W_b} = 33,9 \text{ N/mm}^2$$

$$\tau = \frac{F}{A} = 3,8 \text{ N/mm}^2$$

$$\sigma_v = \sqrt{\sigma_b^2 + 3\tau^2} = 34,5 \text{ N/mm}^2$$

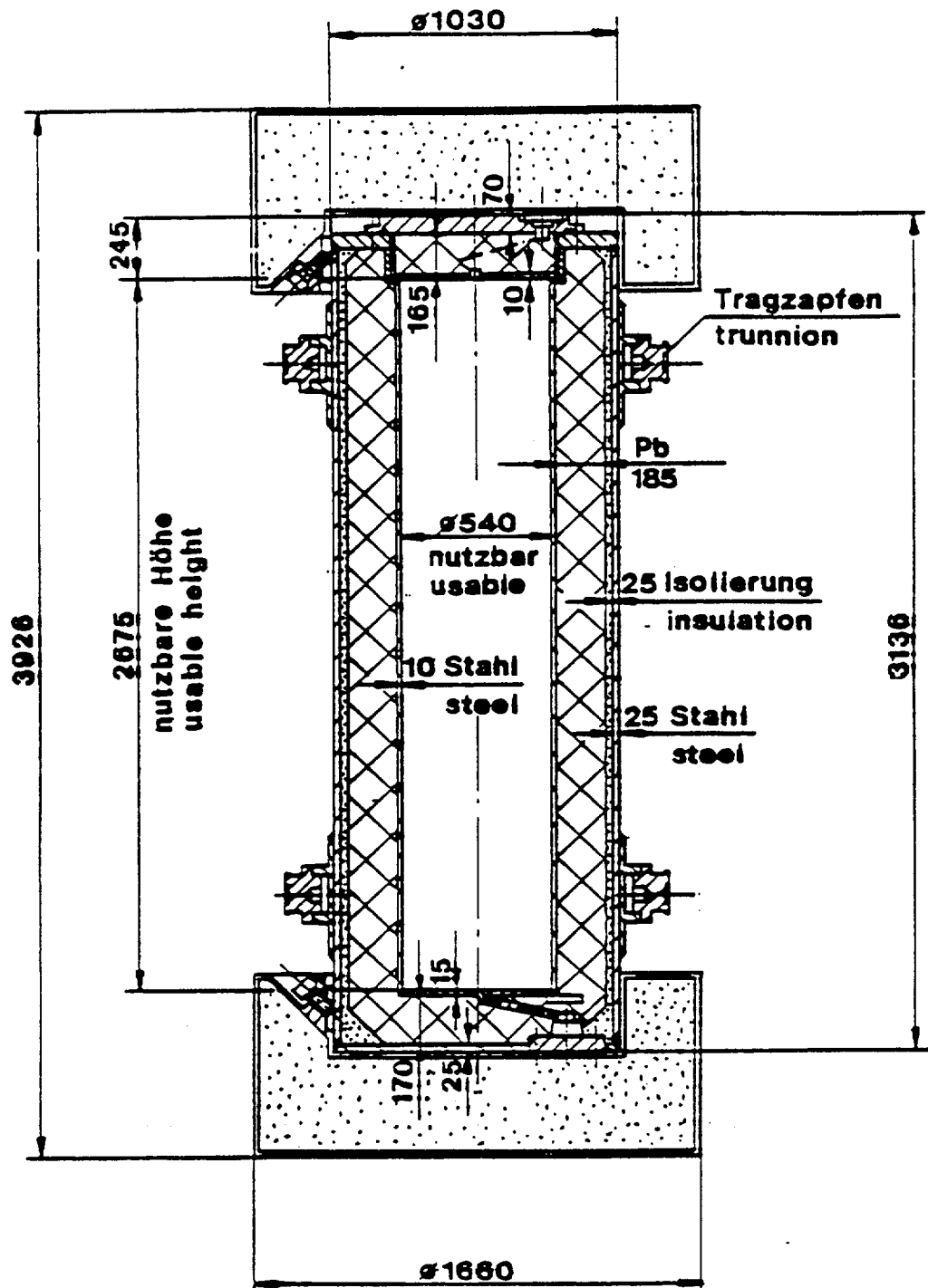
$$\sigma_v < \sigma_{zul} = R_{0,2} (1.4541) \cdot 0,4 = 50 \text{ N/mm}^2$$

The solidity of the lifting shackles is sufficient.

Stresses in the interior tube (240 x 8) are very small.

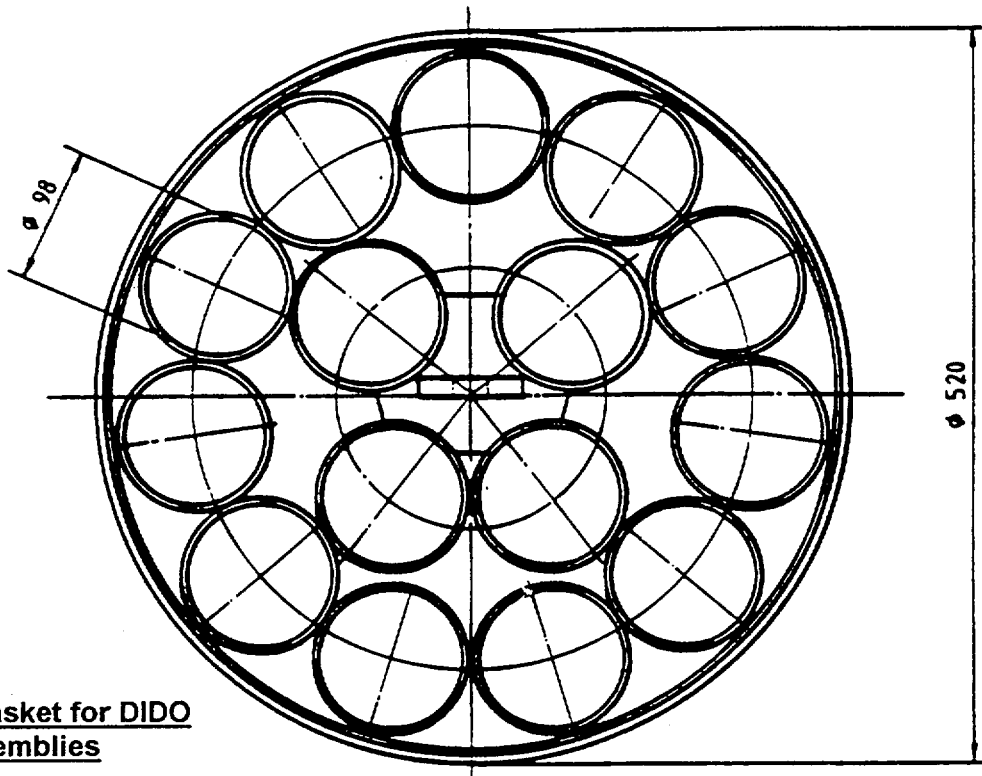
4.6.3 Literature

- /4.6-1/ Dubbel, Taschenbuch für den Maschinenbau,  
Springer-Verlag Berlin, 1970
- /4.6-2/ Safety report, transport of two irradiated RHF fuel assemblies in the TN 7  
cask,  
TN report 8021, rev. 2
- /4.6-3/ Hütte I, 28. edition
- /4.6-4/ Altenpohl, Aluminium und Aluminiumlegierungen,  
Springer Verlag Berlin, 1965

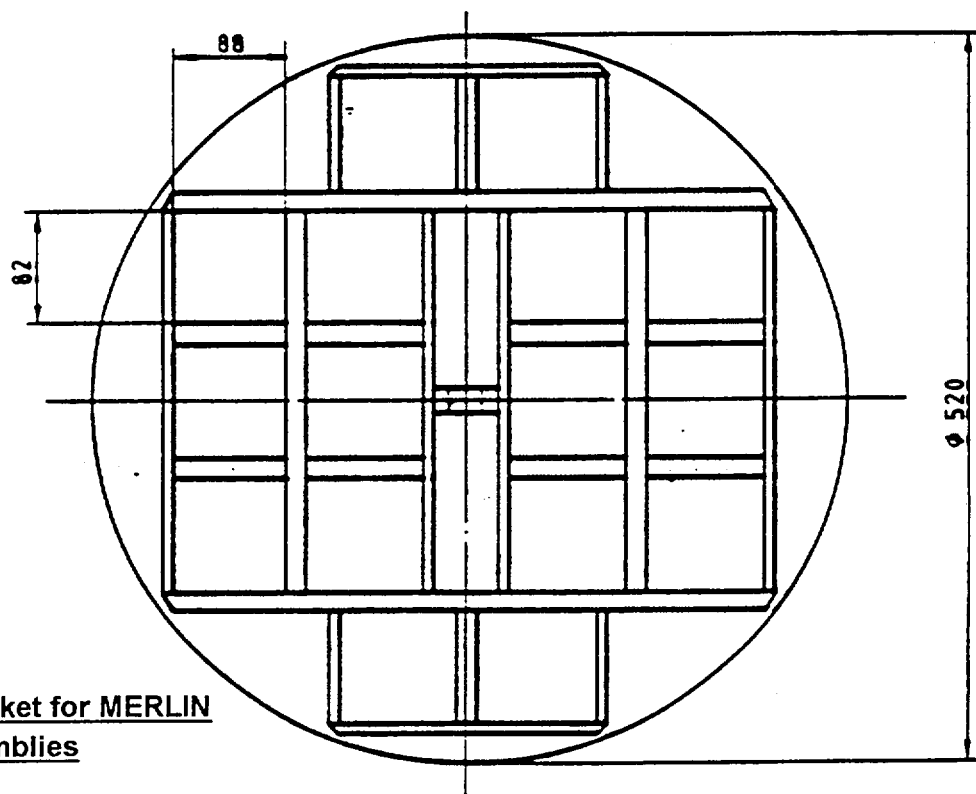


Weights: total	20720 kg
shock absorber (head)	780 kg
lid	760 kg
shock absorber (foot)	780 kg





Insert basket for DIDO  
fuel assemblies

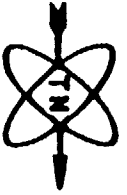


Insert basket for MERLIN  
fuel assemblies



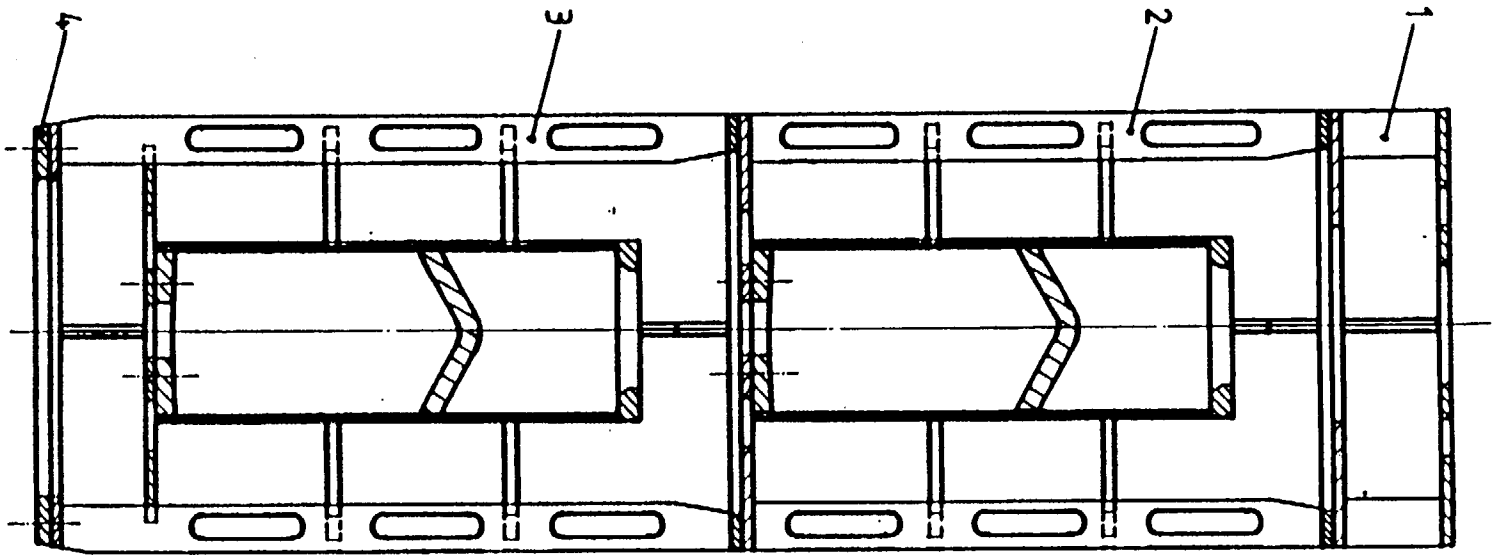
Insert baskets for DIDO and  
MERLIN fuel assemblies

Fig. 3-2



Insert basket for 2 RHF fuel assemblies

Fig. 3-3



- 1 = upper spacer
- 2 = upper fuel assembly insert basket
- 3 = lower fuel assembly with lower spacer
- 4 = spacer

## 5. Temperature distribution inside the cask

In this chapter, stationary temperature situations under normal operation and non stationary temperature situations expected in case of fire are calculated for the TN 7-2 cask. Non stationary thermal calculations are carried out using the HEATING 5 program /5-1/.

### 5.1 Generalities

The cask is designed in such a way that it assures tight enclosure of the contents under the most different conditions. Heat is removed over the surface of the cask by natural convection and released to the environment.

Maximum decay heat released by the loaded fuel assemblies is found in chapter 2.3

Calculation of stationary temperature distribution is carried out separately for the different types of load. Non stationary heat calculations in an accidental fire are based on a representative model which covers all individual cases.



## 5.2 Stationary temperature distribution inside the cask

Calculations were carried out similarly to /5-2/ and /5-3/.

### 5.2.1 Calculation model

Temperature calculations are carried out for the horizontal central plane of the cask. The model is based on the following assumptions and simplifications:

1. The cask lies horizontally.
2. Transport is carried out dry.
3. Calculations are carried out in one dimension.
4. For calculation of the cask wall temperatures, heat sources inside the cask cavity are homogenised.
5. Gaps which may occur between the lead shielding and the surrounding layers disappear under operating conditions due to thermal expansion.
6. Thermal transfer from the exterior cask mantle occurs through convection and radiant heat transfer.

### 5.2.2 Initial data

#### 5.2.2.1 Thermal powers

Thermal powers are also shown in chapter 2.3

#### A. DIDO and MERLIN fuel assemblies

Maximum thermal power per insert basket is 1125 W. There are four insert baskets in the cask. Maximum thermal power within the cask is 4500 W.

## B. RHF fuel assemblies

Thermal power per fuel assembly: 2250 W at the utmost.

Maximum thermal power within the cask is 4500 W.

## 5.2.2.2 Geometry

Radial cask geometry in the central plane is shown in Fig. 5-1. Geometry of the insert baskets may be taken from the corresponding drawings.

## 5.2.2.3 Compilation of initial data

Table 5-1: Compilation of initial data for the assessment of cask body temperature

Index	Position	Material	Interior	$\alpha \left[ \frac{\text{W}}{\text{m}^2 \text{K}} \right]$	$\lambda \left[ \frac{\text{W}}{\text{m K}} \right]$	$\varepsilon [-]$
(Place)			diameter [m]			
$\infty$	environment	air	-	-	0.0189	-
W	surface	steel/paint	1.03	3.66	-	0.9
1	exterior cladding	steel/paint	0.98	-	15	-
2	insulation	cement	0.938	-	1.6	-
3	shielding	lead	0.563	-	35	-
4	interior cladding	steel	0.54	-	15	0.55

## 5.2.3 Calculation of temperature distributions

## A. DIDO and MERLIN fuel assemblies

The results of calculations are listed in table 5-3. Calculations are carried out according to the VDI-heat distribution chart /5-4/:

a) Temperature  $t_w$  at the surface of the cask

$$\dot{Q} = \varepsilon \cdot C_S \cdot A \cdot \left[ \left( \frac{T_w}{100} \right)^4 - \left( \frac{T_\infty}{100} \right)^4 \right] + \alpha_K \cdot A \cdot (t_w - t_\infty)$$

where  $\varepsilon$  = 0.90 (radiation coefficient of paint)

$C_S$  = 5.77 (Stefan-Boltzmann constant)

$A$  = 9.16 m<sup>2</sup> (total heat releasing surface between the two shock absorbers)

$T_w$  = wall temperature in K

$T_\infty$  = ambient temperature in K = 311 K (according to /5-5/)

$\alpha_K$  = heat transfer coefficient for a horizontal cylinder =  $f(\text{Nu}, \text{Gr}, \text{Pr}, \lambda)$

$$\text{Gr} = \frac{g \cdot h \cdot \rho^2 \cdot \beta \cdot (t_w - t_\infty)}{\nu^2} = 9,84 \cdot 10^9$$

$$l' = \frac{\pi}{2} \cdot d_a = 1,62 \text{ m}$$

$$h = d_a$$

$\text{Pr}, \beta$  and  $\nu$  related to  $t_m = 60^\circ\text{C}$

$$\text{Gr} \cdot \text{Pr} = 9,84 \cdot 10^9 \cdot 0,69 = 6,79 \cdot 10^9$$

according to Fig. 1, Fa2 /5-4/, central curve according to Krischer:

$$\text{Nu}_{l'} = 205$$

$$\alpha_K = \frac{\text{Nu}_{l'} \cdot \lambda_m}{l'} = 3,66 \frac{\text{W}}{\text{m}^2\text{K}}$$

$t_w, t_\infty$  = temperatures in  $^\circ\text{C}$

Surface temperature  $t_w = 82^\circ\text{C}$

Thus, surface temperature remains below the admissible limit according to /5-5/.

b) Temperature at cask surface with solar irradiation  $t_1$

According to /5-5/, thermal flow due to solar irradiation over 24 h on the effective cask surface is:

$$\varnothing = 193.5 \text{ W/m}^2$$

This yields the following thermal power:

$$\begin{aligned}\dot{Q}_S &= A \cdot \varepsilon \cdot \varnothing = 9,16 \cdot 0,3 \cdot 193,5 \\ &= 531,8 \text{ W}\end{aligned}$$

Temperature  $t_1$  is now calculated as follows:

$$\begin{aligned}t_1 &= t_\infty + \frac{\dot{Q} + \dot{Q}_S}{\dot{Q}} \cdot (t_w - t_\infty) \\ &= 38 + \frac{4500 + 531,8}{4500} \cdot (82 - 38) \\ &= 88^\circ\text{C}\end{aligned}$$

c) Heat penetration through the basic body - temperature of interior cask wall  $t_4$

$$\Delta t = \frac{\dot{Q}}{2 \pi \cdot l} \cdot \left( \frac{\ln \frac{d_w}{d_1}}{\lambda_1} + \frac{\ln \frac{d_1}{d_2}}{\lambda_2} + \frac{\ln \frac{d_2}{d_3}}{\lambda_3} + \frac{\ln \frac{d_3}{d_4}}{\lambda_4} \right)$$

where:  $\Delta t$  = temperature gradient in cask wall

$$l = \text{average length} = \frac{l_a + l_i}{2} = 2,84 \text{ m}$$

$$Q = 4500 \text{ W}$$

Further values are found in table 5-1.

$$\Delta t = 12.1 \text{ }^{\circ}\text{C}$$

$$t_4 = t_1 + \Delta t = 99 \text{ }^{\circ}\text{C}$$

Maximum temperatures of:

- cement :  $t_2 = 94 \text{ }^{\circ}\text{C}$

- lead:  $t_3 = 98 \text{ }^{\circ}\text{C}$

Thus temperatures of these materials remain below the admissible limits.

#### d) Temperature of insert basket and fuel assemblies

Calculations are carried out as in /5-2/. It is shown in /5-2/ that the highest temperatures occur in the DIDO insert basket; temperature distribution is thus calculated for this case. Calculations are carried out according to the following procedure:

1. Heat transfer from the exterior surface of the insert basket to the interior lining of the cask occurs through radiation. The surface of the interior lining is considered as heat transfer surface.
2. Residual heat of the four interior tubes plus 50 % of the heat of the exterior row of tubes is transferred from the walls of the exterior tubes to 1/3 of the perimeter.
3. The four central tubes transfer their heat to the exterior row of tubes through radiation.

$$Q/\text{insert basket} = 1125$$

$$l_{\text{basket}} = 630 \text{ mm}$$

Only radiation is considered for the heat transfer from the cask wall to the exterior row of insert basket tubes (this is conservative). Exterior temperature of the exterior row of tubes is:

$$T_5^4 = T_4^4 + \frac{Q \cdot 10^8}{\varepsilon \cdot A \cdot C_s}$$

where:  $T_4 = 372.6 \text{ K}$  (temperature of the interior cask wall)

$$Q = 1125 \text{ W}$$

$$\varepsilon = 0.55 \text{ (radiation coefficient of stainless steel)}$$

$$A = d \cdot \pi \cdot l = 0.54 \cdot \pi \cdot 0.63 = 1.07 \text{ m}^2$$

(interior lining surface over the length of the basket)

$$C_s = 5.77$$

$$t_5 = 206 \text{ }^\circ\text{C}$$

Heat transfer in the exterior row of tubes due to conduction:

$$t_6 - t_5 = \frac{Q \cdot S}{\lambda \cdot A}$$

where:  $Q = 712/14 = 51 \text{ W}$

$$s = \text{tube perimeter} = 1/3 \cdot d \cdot \pi =$$

$$1/3 \cdot 0.108 \cdot \pi = 0.11 \text{ m}$$

$$A = 2 \cdot 0.005 \cdot 0.63 = 0.0063 \text{ m}^2$$

$$\lambda = 15 \text{ W/mK}$$

Temperature  $t_6$  of the side of the exterior row of tubes facing the centre of the basket is:

$$t_6 = 265 \text{ }^\circ\text{C}$$

The four central tubes radiate onto the exterior row of tubes. Temperature  $t_7$  of the side of the central tubes facing the exterior row of tubes is:

$$T_7^4 = T_6^4 + \frac{\dot{Q} \cdot 10^8}{\varepsilon \cdot A \cdot C_S}$$

$$= 8,377 \cdot 10^{10} + \frac{75 \cdot 10^8}{0,55 \cdot 0,068 \cdot 5,77}$$

$$t_7 = 314^\circ\text{C}$$

Thermal conductivity through the wall of the central tube. Temperature  $t_8$  of the interior wall:

$$t_8 - t_7 = \frac{Q \cdot S}{\lambda \cdot F} = \frac{75 \cdot 0,11}{2 \cdot 15 \cdot 0,0063}$$

$$t_8 = 358^\circ\text{C}$$

Average temperature  $t_9$  of the central basket tube:

$$t_9 = \frac{314 + 358}{2} = 336^\circ\text{C}$$

Further calculation of fuel assembly temperature is carried out on the base of this average temperature.

Maximum fuel assembly temperature:

The fuel assemblies, which consist of 4 concentric cylinders, stand in the insert basket tubes. Thermal transfer between the single cylinders and the insert basket is due to radiation and conductivity in air. The following is valid:

$$Q = \varepsilon \cdot C_S \cdot A \cdot \left[ \left( \frac{T_{10}}{100} \right)^4 - \left( \frac{T_9}{100} \right)^4 \right] + A \cdot \frac{\lambda}{S} (t_{10} - t_9)$$

This allows to calculate temperatures up to the innermost fuel assembly cylinder temperature  $t_{13}$ . This is done on the base of following data:

Table 5-2: Input data to assess temperatures in the central fuel assemblies

Position	Thermal power Q (W)	Transmitting surface A (m <sup>2</sup> )	Radiation number $\varepsilon$ (-)	Thermal conduct. $\lambda$ (W/mK)	Gap width S (m)
10/9	75	0.184	0.33	0.053	$2.4 \cdot 10^{-3}$
11/10	52	0.165	0.11	0.053	$3.4 \cdot 10^{-3}$
12/11	32	0.145	0.11	0.053	$3.4 \cdot 10^{-3}$
13/12	15	0.126	0.11	0.053	$3.4 \cdot 10^{-3}$

This yields the following results:

$$t_{10} = 351 \text{ }^{\circ}\text{C}$$

$$t_{11} = 370 \text{ }^{\circ}\text{C}$$

$$t_{12} = 383 \text{ }^{\circ}\text{C}$$

$$t_{13} = 390 \text{ }^{\circ}\text{C}$$

Temperature of a fuel assembly in an exterior row insert basket tube  
(Q = 125 W)

$$\text{Exterior tube temperature: } t_5 = 206 \text{ }^{\circ}\text{C}$$

$$\text{Interior tube temperature: } t_6 = 296 \text{ }^{\circ}\text{C}$$

$$\text{Average temperature: } t_m = 251 \text{ }^{\circ}\text{C}$$

The same pattern of calculation yields a temperature of less than 390 °C for the innermost fuel cylinder.



Table 5-3: Temperature distribution in a TN 7-2 cask loaded with DIDO and MERLIN fuel assemblies

Position	Temperature °C
Exterior cask wall	
- without solar irradiation $t_w$	82
- with solar irradiation $t_1$	88
Interior cask wall $t_4$	100
Central insert basket $t_8$	358
Interior fuel cylinder $t_{13}$	390

The results show that temperature distribution within the cask has no influence on the tight enclosure. Temperatures remain below the admissible values for the different materials.

#### B. RHF fuel assemblies

The main results of calculations are listed in table 5-4.

As the thermal power in the cask is the same ( $Q = 4500 \text{ W}$ ) and it may be surmised that the heat releasing cask surface is identical, the following values may be taken over from 5.2.3.A, a) and b):

$$t_w = 82 \text{ °C}$$

$$t_1 = 88 \text{ °C}$$

Further calculations are carried out similarly to /5-3/.

c) Heat transfer through the basic body - interior cask wall temperature  $t_4$

Assumption: heat propagates trapezoidally between the interior heat releasing length ( $l_i = 1.9$  m) and the exterior heat releasing length ( $l = 2.53$  m). The average diameter of the four cask layers is calculated according to:

$$d_m = \frac{d_a - d_i}{\ln \frac{d_a}{d_i}}$$

The length  $l_m$  obtained from this diameter is used to assess  $\Delta t$ .

Temperature differences are assessed according to:

$$t = \frac{Q}{2 \cdot \pi \cdot l_m} \cdot \frac{\ln \frac{d_a}{d_i}}{\lambda}$$

where:  $Q = 4500$  W

$l_{m1} = 2.50$  m

$l_{m2} = 2.44$  m

$l_{m3} = 2.15$  m

$l_{m4} = 1.91$  m

Further input data can be taken over from table 5-1.

$$\begin{aligned} t_4 &= t_1 + \Delta t \\ &= 88 + (1.0 + 8.0 + 4.9 + 1.0) \\ &= 103 \text{ } ^\circ\text{C} \end{aligned}$$

$t_2 = 97 \text{ } ^\circ\text{C}$  (maximum temperature of cement)

$t_3 = 102 \text{ } ^\circ\text{C}$  (maximum temperature of lead)

No inadmissible material temperatures occur.

d) Temperature of fuel assembly  $t_6$ ,  $t_7$  and of insert basket  $t_5$

Thermal transfer from the exterior cylinder of the RHF fuel assembly and the cask wall occurs through radiation and convection. Calculation is carried out according to equation:

$$Q = \varepsilon \cdot A_m \cdot C_{12} \cdot \left[ \left( \frac{T_5}{100} \right)^4 - \left( \frac{T_4}{100} \right)^4 \right] + \alpha_K \cdot A_m \cdot (t_5 - t_4)$$

with following initial data:

$$A_m = \left( \frac{d_a + d_i}{2} \right) \cdot \pi \cdot l_m$$

$$d_a = 0,54 \text{ m}$$

$$d_i = 0,414 \text{ m}$$

$$l_m = 1,98 \text{ m}$$

$$\varepsilon_a = 0,55$$

$$\varepsilon_i = 0,11$$

$$\dot{Q} = 4500 \text{ W}$$

$$t_a = 103^\circ\text{C}$$

$$\alpha_{LK} = f(\text{Pr}, \text{Gr}, \text{Nu}, \lambda)$$

The obtained result is:

$$t_6 = 335^\circ\text{C}$$

The temperature of the interior fuel assembly tube is calculated assuming that half the heat of the assembly is transferred to the interior over the 280 fuel/aluminum plates. Due to the high aluminum contents and to the good thermal conductivity of aluminum, temperature gradient is small.

The following applies:

$$\Delta t = \frac{Q \cdot S}{\lambda \cdot A}$$

$$Q = 2250/2 = 1125 \text{ W}$$

$$S = \frac{(d_a - d_i)}{2} = \frac{(0,41 - 0,26)}{2} = 0,075 \text{ m}$$

$$\lambda = 100 \text{ W/mK} \quad (\text{assumed thermal conductivity of the fuel/aluminum plates})$$

$$A = b \cdot l \cdot 280 = 0,00127 \cdot 0,9 \cdot 280 = 0,32 \text{ m}^2$$

$$\Delta t = \frac{1125 \cdot 0,075}{100 \cdot 0,32} = 2,7^\circ\text{C}$$

The temperature of the interior fuel assembly tube is:

$$t_7 = 338^\circ\text{C}$$

The temperature of the insert basket  $t_5$  is lower than that of the fuel assembly.

The solidity of all materials is sufficient for the calculated temperatures.

Table 5-4: Temperature distribution in a TN 7-2 cask loaded with 2 RHF fuel assemblies.

Position	Temperature °C
Exterior cask wall	
- without solar irradiation $t_w$	82
- with solar irradiation $t_1$	88
Interior cask wall $t_4$	103
Insert basket $t_5$	< 338
Fuel assembly $t_7$	338

### 5.3 Temperature distribution in the cask under accidental conditions

In accordance with IAEA regulations /5-5/, the cask will have to withstand half-hour accidental fires with a constant temperature of 800 °C. It will be demonstrated by way of non stationary calculation that even in case of an accidental fire, the admissible maximum temperature of the individual types of material will not be reached.

#### 5.3.1 Description of the calculating program

The non stationary temperature calculation is carried out by two dimensional temperature calculation using the HEATING 5 program /5-1/.

This program is capable of solving the surface-heat-transfer equations in Cartesian and cylindrical co-ordinates (one-, two- and three-dimensional). An implicit difference method is applied for this.

The general formulation of the program allows for the processing of temperature- and location-dependent material data, apart from a large variety of other boundary conditions (radiation, convection, etc.)

#### 5.3.2 Calculation model.

The model equivalent for temperature behaviour shown in Fig. 5-2 was compiled based on the geometry of the TN 7-2 transport cask according to drawing no. 1-150-050-04-00.

The model is based on following assumptions and simplifications:

1. The cask is lying horizontally.
2. Transport is carried out under dry conditions.
3. The calculation is carried out two-dimensionally.

4. The inside of the cask is homogenised. Conservatively, its heat capacity is taken into account. The heat source inside the cask is assumed so as to be representative for the different types of loading.
5. The shock absorbers are considered to be a homogeneous area. Deformations caused by a previous fall from a height of 9 m are taken into account with regard to the lid shock absorber.
6. Heat-surface-transfer on the outside of the cask takes place by convection and radiation.
7. The trunnions and the base plates are not taken into account in the calculation model.
8. Possible gaps within the cask body will disappear due to thermal expansion of the material.
9. Heat source density in the axial direction is assumed to be constant.
10. The heat-surface-transfer in the gap between the heat source and the inner lining is due to heat conduction and radiation.
11. It is conservatively assumed that the thermal conductivity of the cement will not decrease due to desiccation of the material during a fire. Evaporation heat required by evaporation of the water component of the cement is not taken into account. Two calculation runs are carried out as it is possible that the cement will not dry out completely, contrary to cask philosophy, and that thermal conductivity will thus decrease. The two runs will differ only by the thermal conductivity of the cement during the cooling phase.

Run 1:  $\lambda_{\text{cement}} = 1.6 \text{ W/mK}$

Run 2:  $\lambda_{\text{cement}} = 0.25 \text{ W/mK}$

### 5.3.3 Initial data and characteristic material data

#### 5.3.3.1 Heat sources

The non stationary temperature calculation should be as general as possible in order to cover all considered types of loading. The following is assumed in order to assure this:

- The heat source inside the cask is homogenised. The dimensions of the cylindrical heat source are being assumed as follows:

- diameter: 0.473 m
- height: 2.5 m
- distance from the cask bottom: 0.1 m
- distance from the cask lid: 0.07 m

The gap between the inner cask wall with a diameter of 0.54 m and the heat source is being chosen at a conservatively high value so that little heat will be transferred into the cask inside.

- The thermal power of the load is 4.5 kW.
- The heat source was conservatively not assigned any thermal capacity.

#### 5.3.3.2 Characteristic material data

The individual material data have been derived from the literature or manufacturer's information. Fig. 5-2 shows the various types of materials used for the calculation model.



Material 1: stainless steel

$$\lambda = 15 \frac{\text{W}}{\text{mk}}$$

$$\rho = 7880 \frac{\text{kg}}{\text{m}^3}$$

$$C_p = 500 \frac{\text{J}}{\text{kgK}}$$

Material 2: lead

$$\lambda = 35 \frac{\text{W}}{\text{mk}}$$

$$\rho = 11200 \frac{\text{kg}}{\text{m}^3}$$

$$C_p = 130 \frac{\text{J}}{\text{kgK}}$$

Material 3: thermal insulation (cement)

$$\lambda = 16 \frac{\text{W}}{\text{mk}} \quad (\text{hydrated cement})$$

$$\lambda = 0.25 \frac{\text{W}}{\text{mk}} \quad (\text{dehydrated cement})$$

$$\rho = 1890 \frac{\text{kg}}{\text{m}^3}$$

$$C_p = 3150 \frac{\text{J}}{\text{kgK}}$$

Desiccation of the cement starts at 100 °C and is completed at approximately 200 °C. For the purpose of calculation it is conservatively assumed that the heat conductivity and the specific thermal capacity do not change between these temperature values (i.e.  $\lambda$  is assumed to remain constant at 1.6 W/mK during a fire).

## Material 4: shock absorbers

The shock absorbers consist of balsa wood as well as of a metal sheet casing and steel rods. An effective value for  $\lambda$  is determined higher than the heat conductivity of balsa wood.

$$\lambda = 0.1 \frac{\text{W}}{\text{mk}}$$

$$\rho = 135 \frac{\text{kg}}{\text{m}^3}$$

$$C_p = 2721 \frac{\text{J}}{\text{kgK}}$$

## Material 5:

Material 5 is the homogenised area of insert basket components and fuel assemblies. The effective material values are conservatively estimated:

$$\lambda_{\text{eff}} = 4 \frac{\text{W}}{\text{mk}}$$

$$\rho_{\text{eff}} = 1460 \frac{\text{kg}}{\text{m}^3}$$

$$C_{p \text{ eff}} = 10 \frac{\text{J}}{\text{kgK}}$$

The thermal capacity of the homogenised inside area is conservatively set to 0.

## Material 6: air

Temperature dependence of the heat conductivity of air is taken into account. The values quoted in 20 °C steps in /5-4/ are interpolated linearly and  $C_p$  is assumed to be constant.

$$\rho = 1 \frac{\text{kg}}{\text{m}^3}$$

$$C_p = 1000 \frac{\text{J}}{\text{kgK}}$$

### 5.3.3.3 Thermal transitions

- The thermal transition between a fire and the cask body is assured by radiation and convection.

According to /5-7/, the thermal radiation transition coefficient  $\alpha_S$  is 90 % for a flame temperature of approximately 800 °C and the natural convection coefficient  $\alpha_K$  is 10 % of the total thermal transition coefficient  $\alpha_{Ges}$ .

The emission coefficient of flames is  $\varepsilon_F = 0.7 - 0.9$  according to literature. For calculations,  $\varepsilon_F = 1$  is assumed (conservatively).

The absorption coefficient  $\varepsilon$  of the surface is also set to 1 in order to take account of a change in the coefficient due to sooting.

The amount of heat assumed per unit area is determined by:

$$q'' = \alpha_K \cdot (T_F - T_0) + \alpha_S \cdot (T_F - T_0) \frac{W}{m^2}$$

where  $\alpha_S = \varepsilon \cdot \sigma \cdot (T_F^2 + T_0^2) (T_F - T_0)$

$$\alpha_K = \frac{0,1}{0,9} \cdot \alpha_S = 0,11 \alpha_S$$

$$\begin{aligned} q'' &= \varepsilon \cdot 1,1 \cdot \sigma \cdot (T_F^4 - T_0^4) = \\ &= 6,34 \cdot 10^{-8} \cdot (T_F^4 - T_0^4) \frac{W}{m^2} \end{aligned}$$

- During the cooling stage thermal transition to the environment takes place by radiation and convection over the cask mantle and the mantle and ends of the shock absorbers.

## 1. Radiation

$$\dot{q} = \bar{\varepsilon} \cdot (T_i^4 - T_a^4)$$

$\varepsilon = 0.9$  (radiation coefficient of the paint layers)

$\sigma$  = Stefan-Boltzmann constant

$$\bar{\varepsilon} = \varepsilon \cdot \sigma = 0.9 \cdot 5.77 \cdot 10^{-8}$$

$$= 5.2 \cdot 10^{-8} \frac{\text{W}}{\text{m}^2 \text{K}^4}$$

## 2. Convection

$$\dot{q} = \alpha_K \cdot (T_i - T_a) \text{ W/m}^2$$

The thermal transition factor  $\alpha_K$  is a function of the Grasshoff, Prandl and Nusselt numbers and of the heat conductivity  $\lambda$ .

$$\alpha_K = f(\text{Gr}, \text{Pr}, \text{Nu}, \lambda)$$

The Grasshoff number is derived from:

$\text{Nu} = f(\text{Gr}, \text{Pr})$  according to the average curve of 0.  
Krischer, from /5-4/.

and  $\alpha_K$  from:

$$\alpha_K = \frac{\text{Nu} \cdot \lambda}{\frac{\pi}{2} \cdot D} \quad (\text{mantle parts})$$

$$\alpha_K = \frac{\text{Nu} \cdot \lambda}{D/2} \quad (\text{front end})$$

- Thermal transition in the gap between the inner cask wall and the homogenised insert basket and fuel assembly area takes place by radiation and conduction.

The radiation coefficient for stainless steel is assumed to be  $\varepsilon_a = 0.55$ , the radiation coefficient for the homogenised source area to be  $\varepsilon = 0.55$ .

#### 5.3.4 Results of non stationary thermal calculations

The results of the non stationary calculations for the instants  $t = 0$  s (start of the fire), 1,800 s (end of the fire) and 12,600 s (end of calculations) are found in the computer printouts, Tables 5-5, 5-6 and 5-7.

Table 5-8 and fig. 5-3 show the time dependence of temperature for several key locations on the cask.

- During the fire, the temperature of the outer steel wall rises to a maximum of 642 °C at the centre of the cask and decreases again rapidly.
- The maximum temperature of lead, 285 °C, is reached during the cooling phase at  $t = 4,800$  s. There will thus be melting of lead.
- The maximum gasket temperature of 177.5 °C occurs during the cooling stage at the end of calculations, at  $t = 12,600$  s. At this point in time a slight increase in the gasket temperature can still be observed. The increase is, however, so slight that a temperature of less than 185 °C may be expected. The proper functioning of the gaskets will not be impaired.
- The temperature of the inner cask wall will reach a maximum of 286 °C at  $t = 4,800$  s.

A second calculation run will be carried out in addition to the first, with preliminary requirements changed in one respect. The heat conductivity of cement was no longer assumed to be constant at 1.6 W/mK, but a heat conductivity of the dehydrated cement of 0.25 W/mK was assumed for the cooling stage.

The results of this calculation run correspond to those of the preceding run until  $t = 1,800$  s (see Tables 5-5, 5-6). The results for  $t = 14,000$  s (end of calculations) are listed in Table 5-9. Table 5-10 and Fig. 5-4 show the time dependence of the temperature for several key points. It should be noted that under these conditions, which are obviously conservative, the corresponding temperatures are lower than or approximately equal to those observed during the first calculation run. The following maximum temperatures are obtained:

- cask surface:	641,6 °C
- lead shielding:	244,5 °C
- lid gasket:	169,6 °C
- inner cask wall:	244,5 °C

It should be noted here that the gasket temperatures reached their maximum value at the end of calculations and that a slight increase in temperature could be observed at that time. It may, however, be assumed that the temperature of less than 185 °C calculated during the first run will not be exceeded. The higher temperature of the inner wall determined during the first run is used as a base for calculating the temperature of the insert basket and of fuel assemblies during a fire.

Table 5-5: Temperature distribution at time  $t = 0$  s  
(Beginning of fire) First calculation run

TN 7/2 Non stationary temperature distribution in a 800 °C fire and during cooling

HEATING

GROSS GRID		TEMPERATURE DISTRIBUTION AFTER 0 TIME STEPS, TIME = 0.										
I	FINI GRID DISTANCE	1	2	3	4	5	6	7	8	9	10	11
		1	2	3	4	5	6	7	8	9	10	11
1	0.00	39.67	39.60	39.62	39.60	39.59	39.58	39.49	39.39	39.36	39.31	38.05
2	0.19	63.13	62.97	62.96	61.98	61.89	61.69	60.38	58.88	58.33	57.55	38.68
3	0.37	88.67	88.19	87.51	87.03	86.95	86.79	86.08	84.91	84.61	84.26	39.48
4	0.56	88.75	88.36	87.39	87.06	86.99	86.82	86.15	84.94	84.62	84.31	39.51
5	0.77	89.14	88.74	87.50	87.15	87.05	86.86	86.13	85.03	84.52	84.43	39.51
6	0.97	90.71	90.14	89.07	87.32	87.14	86.87	85.91	85.39	83.15	82.98	39.40
7	1.16	91.71	91.01	89.01	87.10	86.99	86.85	85.88	85.31	82.64	82.43	39.33
8	1.36	272.03	269.30	269.00	87.35	87.27	87.09	85.66	84.57	77.12	75.67	38.44
9	1.55	287.29	281.00	280.00	87.99	87.52	87.16	85.66	84.55	77.32	76.43	0.00
10	1.75	322.83	314.40	299.90	91.46	90.82	90.31	88.23	87.08	80.69	79.88	0.00
11	1.94	136.03	125.30	299.90	93.74	93.06	92.51	90.29	89.09	82.43	81.58	0.00
12	2.14	137.43	126.69	303.00	94.99	94.30	93.74	91.47	90.24	83.40	82.53	0.00
13	2.33	136.23	129.33	303.00	95.37	94.66	94.10	91.83	90.59	83.69	82.82	0.00
14	2.53	137.43	128.50	303.00	95.91	94.23	93.67	91.41	90.16	83.35	82.48	0.00
15	2.73	131.93	125.20	299.10	96.61	92.93	92.39	90.18	88.98	82.33	81.49	0.00
16	2.93	122.53	114.90	290.10	91.30	90.66	90.15	88.08	86.74	80.57	79.77	0.00
17	3.13	280.13	279.99	261.00	87.85	87.91	87.04	85.48	84.38	77.29	76.42	0.00
18	3.33	237.43	232.70	219.10	87.11	87.05	86.89	85.46	84.41	76.77	74.87	38.38
19	3.53	91.43	90.61	86.55	87.17	86.95	86.69	85.47	84.71	80.77	80.40	39.14
20	3.73	90.80	90.21	86.19	87.42	87.25	86.67	85.47	84.76	81.36	81.10	39.23
21	3.93	89.07	88.19	87.92	87.12	87.02	86.60	85.58	85.00	84.49	84.33	39.48
22	4.13	88.67	88.73	87.28	87.30	86.91	86.65	85.72	84.90	84.65	84.40	39.45
23	4.33	88.13	88.01	87.11	86.63	86.74	86.57	85.80	85.07	84.67	84.30	39.19
24	4.53	61.97	61.69	61.01	60.15	60.00	59.67	57.49	55.05	54.30	53.34	38.54
25	4.73	39.41	39.41	39.35	39.32	39.31	39.29	39.16	39.03	38.98	38.93	38.04

Table 5-6: Temperature distribution at time  $t = 1800$  s  
(End of fire) First calculation run

TN 7/2 Non stationary temperature distribution in a 800 °C fire and during cooling

# HEATING5

GROSS GRID	FINE GRID DISTANCE	TRANSIENT TEMPERATURE DISTRIBUTION AFTER 82 TIME STEPS, TIME = 1.800000E+03											
		1	2	3	4	5	6	7	8	9	10	11	12
1	0.00	798.75	798.74	798.74	798.74	798.74	798.74	798.74	798.74	798.74	798.75	800.00	
2	0.19	798.75	798.74	798.74	798.74	798.74	798.74	798.74	798.74	798.74	798.75	799.34	
3	0.37	798.75	798.74	798.74	798.74	798.74	798.74	798.74	798.74	798.74	798.75	799.35	
4	0.56	798.75	798.74	798.74	798.74	798.74	798.74	798.74	798.74	798.74	798.75	799.36	
5	0.75	798.75	798.74	798.74	798.74	798.74	798.74	798.74	798.74	798.74	798.75	799.41	
6	0.94	798.75	798.74	798.74	798.74	798.74	798.74	798.74	798.74	798.74	798.75	799.44	
7	1.13	798.75	798.74	798.74	798.74	798.74	798.74	798.74	798.74	798.74	798.75	799.98	
8	1.32	798.75	798.74	798.74	798.74	798.74	798.74	798.74	798.74	798.74	798.75	800.00	
9	1.51	798.75	798.74	798.74	798.74	798.74	798.74	798.74	798.74	798.74	798.75	800.00	
10	1.70	798.75	798.74	798.74	798.74	798.74	798.74	798.74	798.74	798.74	798.75	800.00	
11	1.89	798.75	798.74	798.74	798.74	798.74	798.74	798.74	798.74	798.74	798.75	800.00	
12	2.08	798.75	798.74	798.74	798.74	798.74	798.74	798.74	798.74	798.74	798.75	800.00	
13	2.27	798.75	798.74	798.74	798.74	798.74	798.74	798.74	798.74	798.74	798.75	800.00	
14	2.46	798.75	798.74	798.74	798.74	798.74	798.74	798.74	798.74	798.74	798.75	800.00	
15	2.65	798.75	798.74	798.74	798.74	798.74	798.74	798.74	798.74	798.74	798.75	800.00	
16	2.84	798.75	798.74	798.74	798.74	798.74	798.74	798.74	798.74	798.74	798.75	800.00	
17	3.03	798.75	798.74	798.74	798.74	798.74	798.74	798.74	798.74	798.74	798.75	800.00	
18	3.22	798.75	798.74	798.74	798.74	798.74	798.74	798.74	798.74	798.74	798.75	800.00	
19	3.41	798.75	798.74	798.74	798.74	798.74	798.74	798.74	798.74	798.74	798.75	800.00	
20	3.60	798.75	798.74	798.74	798.74	798.74	798.74	798.74	798.74	798.74	798.75	800.00	
21	3.79	798.75	798.74	798.74	798.74	798.74	798.74	798.74	798.74	798.74	798.75	800.00	
22	3.98	798.75	798.74	798.74	798.74	798.74	798.74	798.74	798.74	798.74	798.75	800.00	
23	4.17	798.75	798.74	798.74	798.74	798.74	798.74	798.74	798.74	798.74	798.75	800.00	
24	4.36	798.75	798.74	798.74	798.74	798.74	798.74	798.74	798.74	798.74	798.75	800.00	
25	4.55	798.75	798.74	798.74	798.74	798.74	798.74	798.74	798.74	798.74	798.75	800.00	



Table 5-7: Temperature distribution at time  $t = 12600$  s  
(3 h after end of fire) First calculation run

**TN 7/2** Non stationary temperature distribution in a 800 °C fire and during cooling

50114

GROSS GRID		TRANSFORMED DATA DISTRIBUTION AFTER 206 TIME STEPS, TIME = 1.26000E+04									
FINE GRID DISTANCE	I	I					I				
		1	3	4	5	6	7	8	9	10	
1	0.00	96.93	96.91	96.90	96.89	96.89	46.85	46.88	46.88	46.84	40.70
2	.19	97.12	97.10	97.10	97.12	97.12	80.51	81.67	82.41	83.35	58.99
3	.37	97.16	97.16	97.16	97.16	97.16	172.04	160.17	158.09	155.67	60.79
4	.56	97.23	97.23	97.23	97.23	97.23	172.82	160.22	158.52	157.90	60.87
5	.75	97.29	97.29	97.29	97.29	97.29	175.22	173.40	165.21	164.62	60.89
6	.94	97.33	97.33	97.33	97.33	97.33	177.05	175.54	167.48	166.89	59.14
7	1.13	97.36	97.36	97.36	97.36	97.36	177.39	175.78	166.54	165.79	57.88
8	1.32	97.37	97.37	97.37	97.37	97.37	180.10	176.87	160.59	145.04	41.25
9	1.51	97.37	97.37	97.37	97.37	97.37	180.40	177.11	151.77	148.36	0.00
10	1.70	97.37	97.37	97.37	97.37	97.37	202.44	199.57	177.29	173.68	0.00
11	1.89	97.37	97.37	97.37	97.37	97.37	218.66	215.46	190.18	186.08	0.00
12	2.08	97.37	97.37	97.37	97.37	97.37	226.65	223.16	195.79	191.42	0.00
13	2.27	97.37	97.37	97.37	97.37	97.37	228.85	225.25	197.22	192.79	0.00
14	2.46	97.37	97.37	97.37	97.37	97.37	226.50	223.01	195.67	191.32	0.00
15	2.65	97.37	97.37	97.37	97.37	97.37	218.39	215.19	189.44	185.84	0.00
16	2.84	97.37	97.37	97.37	97.37	97.37	202.34	199.44	177.08	173.48	0.00
17	3.03	97.37	97.37	97.37	97.37	97.37	181.47	178.23	153.23	149.86	0.00
18	3.22	97.37	97.37	97.37	97.37	97.37	180.89	177.83	150.77	143.41	41.68
19	3.41	97.37	97.37	97.37	97.37	97.37	179.58	177.65	165.13	163.92	54.85
20	3.60	97.37	97.37	97.37	97.37	97.37	177.95	176.75	167.16	166.35	56.51
21	3.79	97.37	97.37	97.37	97.37	97.37	177.95	176.75	175.33	174.90	60.84
22	3.98	97.37	97.37	97.37	97.37	97.37	177.95	176.75	175.01	174.06	61.08
23	4.17	97.37	97.37	97.37	97.37	97.37	177.95	176.75	175.01	174.06	60.01
24	4.36	97.37	97.37	97.37	97.37	97.37	177.95	176.75	175.01	174.06	57.18
25	4.55	97.37	97.37	97.37	97.37	97.37	177.95	176.75	175.01	174.06	40.43

Table 5-8: Time dependence of temperature in °C at some points on the cask. First calculation run

Place Time (s)	Cask surface (central plane)	Lead shielding (exterior radius)	Lid gasket	Protective lid gasket at the bottom	Interior cask wall (central plane)
0	82,8	90,6	86,7	86,9	95,4
10	99,0	90,6	86,7	86,9	95,4
20	113,5	90,6	86,7	86,9	95,4
40	138,1	90,7	86,7	86,9	95,4
80	175,8	91,0	86,7	86,9	95,4
160	229,0	92,8	86,7	86,9	95,4
320	308,4	100,5	86,7	86,9	95,8
640	432,1	125,3	86,7	87,3	100,5
1280	582,0	188,7	88,3	92,4	132,0
1800	641,6	240,9	92,3	101,2	173,1
1840	594,4	244,8	92,8	102,0	176,6
1880	566,4	248,3	93,2	102,8	180,1
1960	532,3	254,4	94,1	104,6	187,2
2220	465,1	267,2	97,6	110,6	209,7
2500	413,4	274,3	102,0	117,3	230,2
2800	372,1	279,3	107,2	124,2	248,2
3400	317,1	283,2	117,9	136,4	270,4
4000	283,9	283,3	128,0	146,0	280,9
4800	257,5	280,2	139,5	155,7	285,1
5800	238,9	273,9	150,8	164,0	282,7
7000	225,8	265,0	160,6	170,2	275,3
8000	218,1	257,3	166,5	173,3	267,9
9500	208,8	246,2	172,3	175,9	256,5
11000	200,7	235,7	175,7	176,9	245,5
12600	192,8	225,3	177,5	176,9	234,6

Table 5-9: Temperature distribution at time  $t = 14000$  s  
(3 h and 23 min. after end of fire) Second calculation run

TN 7/2 Non stationary temperature distribution in a 800 °C fire and during cooling

HEATING

GROSS GRID		TRANSIENT TEMPERATURE DISTRIBUTION AFTER 14 HRS 31.1PS, TIME = 1.40000E+04									
FIRE GRID	DISTANCE	1	3	4	5	6	7	8	9	10	11
		1.00	0.24	0.27	0.28	0.30	0.40	0.47	0.49	0.52	0.83
1	0.00	44.92	44.89	44.86	44.87	44.87	44.84	44.87	44.87	44.85	39.90
2	0.19	81.09	81.43	81.21	81.14	81.00	80.41	81.48	82.05	82.71	54.18
3	0.37	171.94	171.13	170.75	170.56	170.18	166.32	150.12	147.39	145.13	55.91
4	0.50	172.28	171.52	171.12	170.97	170.61	167.48	149.72	147.16	146.46	55.97
5	0.47	173.24	172.72	172.50	172.54	172.44	171.75	171.43	149.04	147.75	55.94
6	0.57	175.32	174.92	175.25	175.38	175.56	175.13	174.44	145.79	145.45	54.42
7	0.58	176.32	175.53	175.39	176.15	176.26	175.76	175.30	143.84	143.43	53.42
8	0.60	310.49	297.70	182.34	182.27	182.10	180.61	179.28	119.40	116.32	40.51
9	0.69	330.56	305.88	183.45	182.98	182.63	181.04	179.07	119.40	117.59	0.00
10	1.00	372.58	340.20	205.98	205.13	204.78	202.42	200.97	137.65	135.57	0.00
11	1.31	367.40	354.56	272.96	272.26	271.66	219.06	217.46	144.68	142.39	0.00
12	1.63	396.63	361.48	252.38	231.66	231.06	220.33	226.59	147.45	145.05	0.00
13	1.94	398.67	363.38	239.21	234.44	233.88	231.12	229.33	144.17	143.74	0.00
14	2.25	396.50	361.36	232.16	231.44	230.34	228.12	226.38	147.39	144.99	0.00
15	2.56	369.12	380.49	222.52	221.82	221.22	218.63	217.03	144.55	142.26	0.00
16	2.88	372.05	363.97	205.32	204.67	204.13	201.78	200.35	137.61	135.54	0.00
17	3.19	329.42	304.59	181.74	181.62	181.62	180.09	178.79	121.63	119.84	0.00
18	3.21	290.67	273.65	180.52	180.48	180.36	179.08	177.05	122.25	117.92	40.85
19	3.26	174.86	175.13	176.22	176.68	176.83	176.19	175.22	141.93	141.32	50.94
20	3.27	174.16	174.70	175.31	175.50	176.21	175.70	174.74	145.01	144.60	52.22
21	3.33	171.43	171.73	171.84	171.85	172.04	171.48	167.55	165.82	164.90	55.98
22	3.44	170.13	170.23	170.62	169.71	169.61	169.21	167.50	166.27	165.06	50.20
23	3.51	168.20	168.31	168.14	158.98	167.94	167.27	120.34	114.50	110.70	55.21
24	3.61	99.04	95.87	98.67	98.60	98.42	96.74	91.14	90.31	89.47	52.73
25	3.72	44.39	44.36	44.34	44.33	44.31	44.16	43.78	43.72	43.65	39.85

Table 5-10: Time dependence of temperature in °C at some points on the cask. Second calculation run

Place Time (s)	Cask surface (central plane)	Lead shielding (exterior radius)	Lid gasket	Protective lid gasket at the bottom	Interior cask wall (central plane)
1800	641,6	240,9	92,3	101,2	173,1
1850	588,3	236,1	92,9	102,2	177,4
2000	536,2	228,6	94,7	105,4	189,4
2500	459,9	224,9	101,5	115,1	211,9
3000	404,7	227,6	108,4	122,5	221,7
4000	328,7	238,4	120,4	133,5	232,2
5000	278,9	237,3	130,4	141,8	238,3
8000	199,5	240,2	151,3	158,0	244,5
10000	173,3	238,0	159,9	165,7	243,2
14000	145,7	229,3	169,6	172,4	235,2

### 5.3.5 Insert basket and fuel temperature during accidental fires

No non stationary calculations is carried out to determine the maximum temperature of the insert baskets and fuel assemblies. The temperature is calculated on the basis of the calculated maximum temperature of the interior wall during an accidental fire. Calculation is continued inwards in analogy to the determination of the temperature distribution under routine operating conditions (cf. also chapter 5.2).

The maximum temperature of the inner wall during an accidental fire is 286 °C.

#### A. DIDO and MERLIN fuel assemblies

Thermal calculations using the new initial temperature yield the temperature distribution shown below. Calculations are only carried out for DIDO fuel assemblies as higher temperatures are expected with them.

Table 5-11: Temperature distribution in the DIDO basket during an accidental fire

Position	Temperature °C
- Interior wall temperature $t_4$	286
- Temperature of exterior fuel shafts	
- exterior $t_5$	331
- interior $t_6$	390
- Temperature of the exterior wall of the central fuel shaft $t_7$	418
- Temperature of the interior wall of the central fuel shaft $t_8$	462
- Average temperature of the central fuel shaft $t_9$	440
- Temperature of the exterior fuel assembly tube $t_{10}$	452
- Temperature of the innermost fuel assembly tube $t_{13}$	479

The maximum temperature of the basket is approximately 462 °C.

Thus, sufficient solidity of the stainless steel can be guaranteed. The maximum temperature of the fuel assemblies is 479 °C, which is considerably lower than the melting point of the material of 600 °C.

#### B. RHF fuel assemblies

During an accidental fire the maximum temperature of a fuel assembly is  $t_7 = 440$  °C, whilst temperature  $t_4$  of the inner cask wall is 286 °C. The temperature limit of 600 °C will not be reached.

#### 5.4 Fire test on a TN 7-2 1/3 scale model

Apart from the non stationary thermal calculations, a fire test was carried out with a 1/3 scale model of the TN 7-2 in order to investigate the behaviour of the cask in an accidental fire.

The fire test was used to determine the heating-up graph of the cask and to investigate the vapour pressure behaviour of the cement.

According to model laws, a heating up period of approximately 3.5 min would suffice. As an exact determination of the duration of a fire for the 1/3 scale model, which would be representative for the 30 minute fire exposure of a full size cask, is not possible, the test was stopped when the melting point of lead was reached. Effects which would occur on account of a fire lasting too long were not taken into consideration.

The locations of the measurement points can be found in the enclosed measurement location plan.

The test was carried out in a closed furnace of the Federal Institute for Materials Testing. It was heated by oil burners.

The burners were switched off after 9 minutes and 57 seconds. At this point the melting point of lead was reached.

The temperature development during and after the fire can be seen in the enclosed figure. It appears that heating over the perimeter of the cask model is irregular (cf. comparison of measurement locations 2 and 5).

In spite of the fact that the melting point of lead was exceeded at several locations on the cask, the temperatures measured at the gaskets remained considerably below the admissible values which have to be withstood for short periods of time by the gasket material without impairing its specific functions

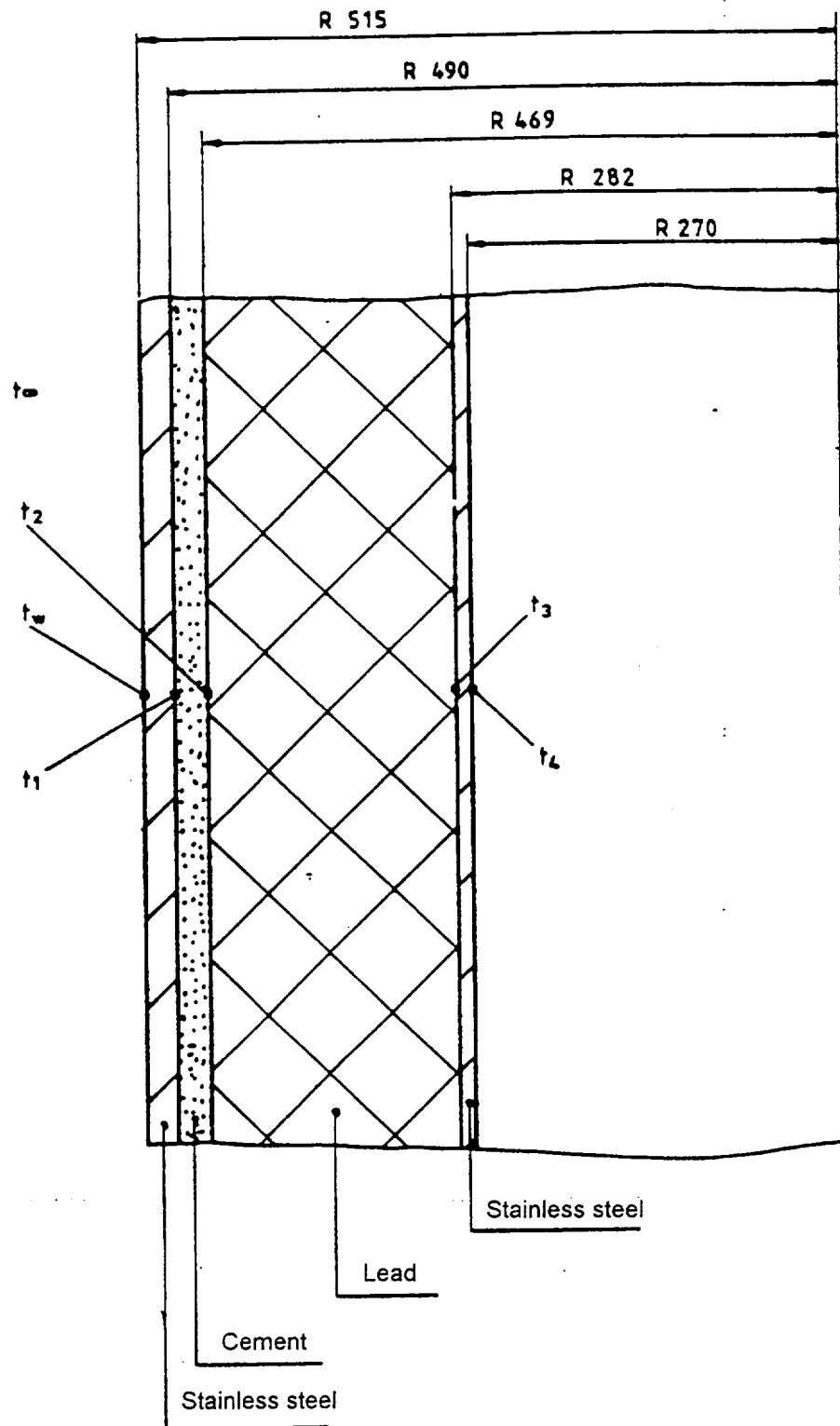
No changes of the cask due to melting of lead and building up of pressure in the cement layer were found.

A detailed description of the test can be found in /5-8/.



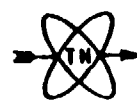
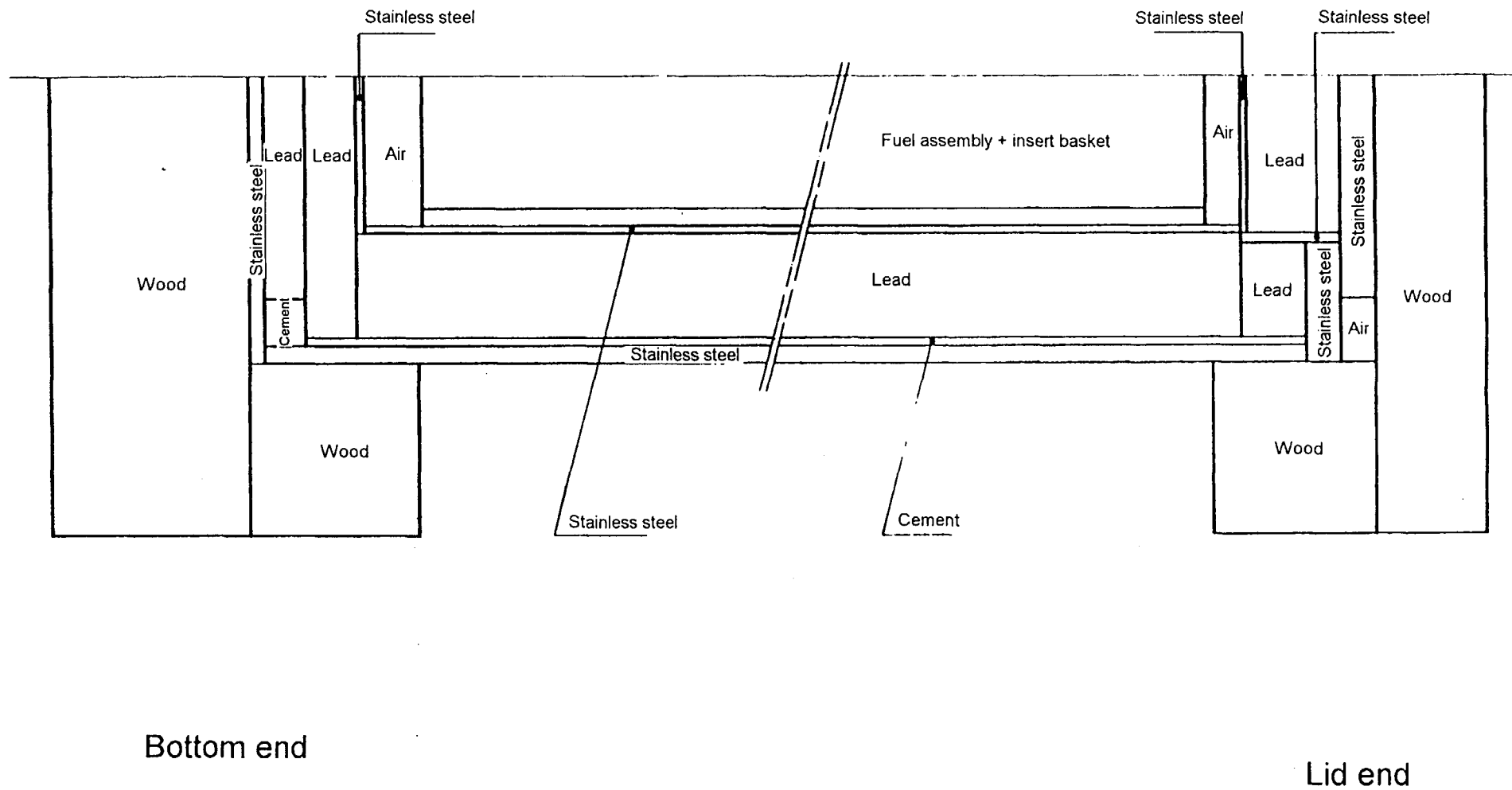
## 5.5 Literature

- /5-1/ Turner, Elrof, Siman-Tov  
HEATING 5  
Computer Sciences Division, Oak Ridge, Tennessee
- /5-2/ TN 7-2/MTR Package Design, Safety Report  
TN Report no. 7701
- /5-3/ Safety Analysis Report, Transport of two Irradiated RHF Fuel Assemblies  
in the TN 7 Cask,  
TN Report no. 8021
- /5-4/ VDI-Wärmeatlas, 3rd Edition, 1977
- /5-5/ IAEA Regulations for the Safe Transport of Radioactive Materials, 1973
- /5-6/ C.W. Wegst, Steel Codes  
Verlag Stahlschlüssel Wegst GmbH & Co., Marbach, 1980
- /5-7/ S. Aoki, H. Shimada, K. Tamura  
Assessments of the Heat Transfer Properties of Spent Fuel Shipping  
Casks (1976)
- /5-8/ Instrumented Drop and Fire Tests on a Model Spent Fuel Transport Cask  
of the TN 7-2 Type,  
Test Report no. 2041  
Federal Institute for Materials Testing Berlin  
May 19, 1982



Section through the central plane  
of the cask

Fig. 5-1



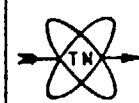
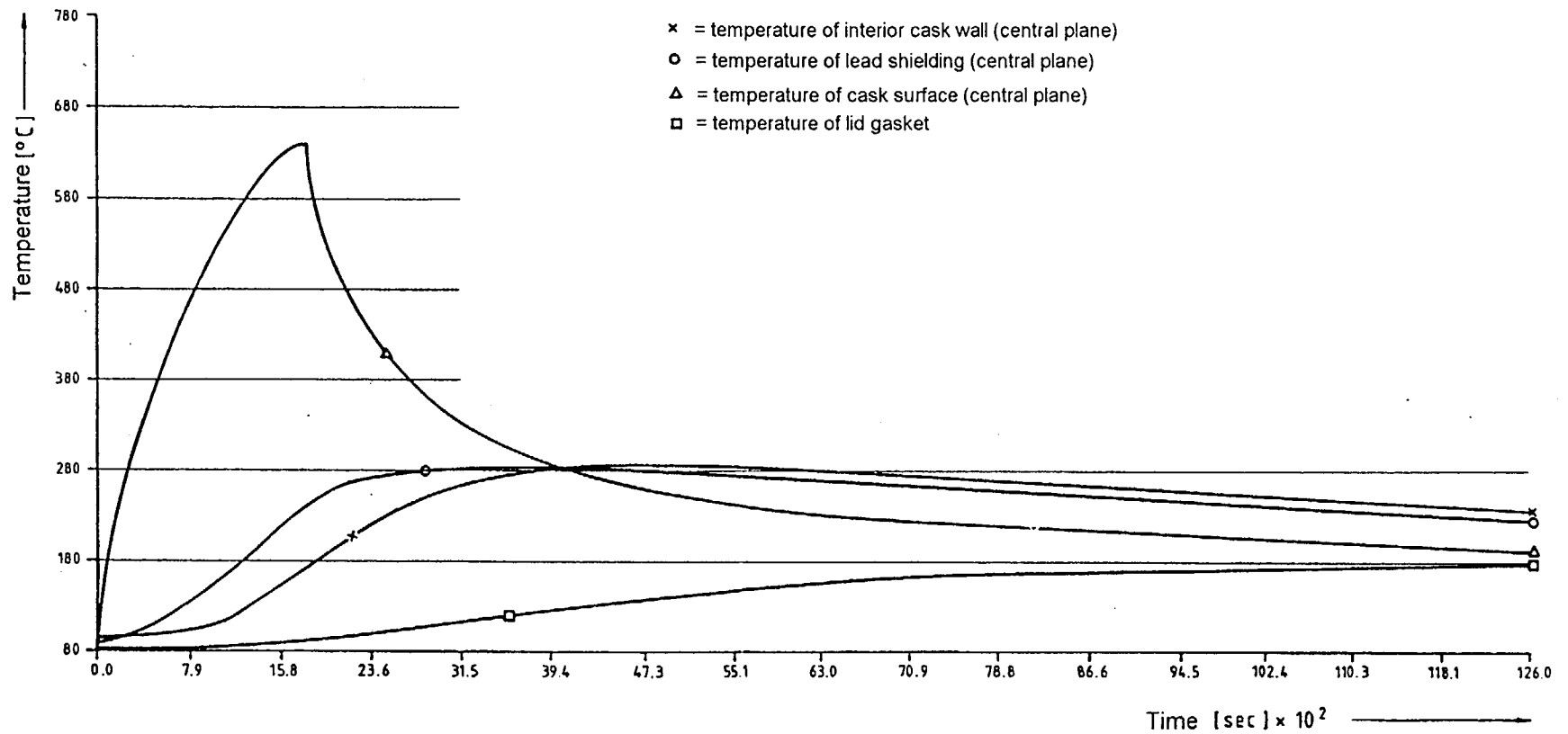
Calculation model of the TN 7-2 for  
non stationary thermal calculation

Fig. 5-2

### Calculation run 1

Fire phase:  $\lambda_{\text{cement}} = 1.6 \text{ W/mk}$

Cooling phase:  $\lambda_{\text{cement}} = 1.6 \text{ W/mk}$



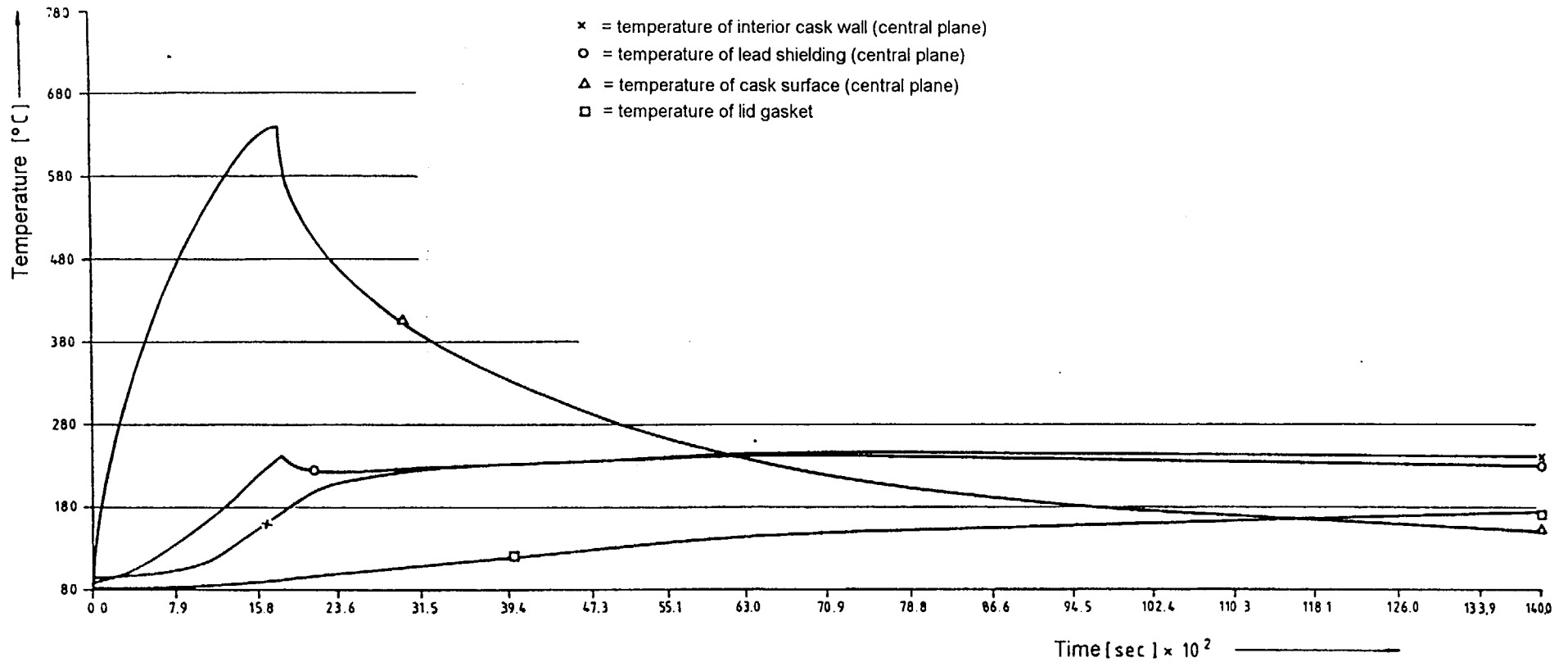
Time dependence of temperature for the  
TN 7-2 cask in an accidental fire

Fig. 5-3

## Calculation run 2

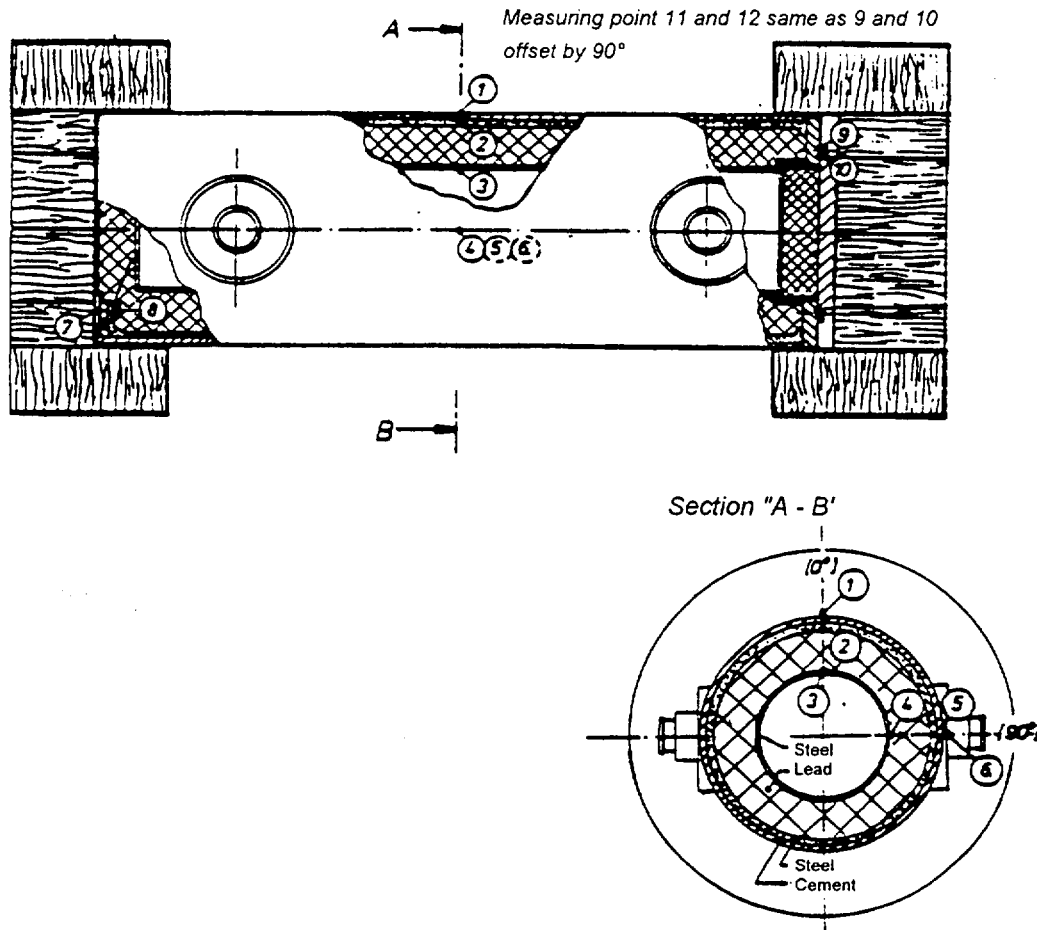
Fire phase:  $\lambda_{\text{cement}} = 1.6 \text{ W/mk}$

Cooling phase:  $\lambda_{\text{cement}} = 0.25 \text{ W/mk}$



Time dependence of temperature for the  
TN 7-2 cask in an accidental fire

Fig. 5-4



Meas. point	Situation or position of the measuring point
1	Exterior mantle, centre of cask [0°]
2	Lead shielding (exterior) centre of cask [0°]
3	Lead shielding (interior) centre of cask [0°]
4	Exterior mantle, centre of cask [90°]
5	Lead shielding (exterior) centre of cask [90°]
6	Lead shielding (interior) centre of cask [90°]
7	Bottom valve (upper area)
8	Bottom valve (lower area)
9	Lid gasket -1a- [0°]
10	Lid gasket -1b- [0°]
11	Lid gasket -1a- [90°]
12	Lid gasket -1b- [90°]

Fig. 5-5

